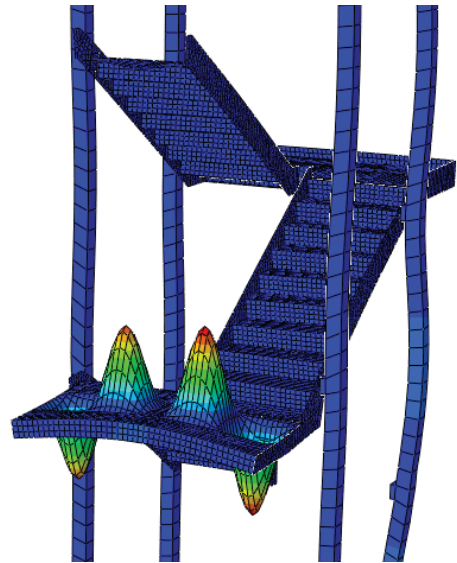
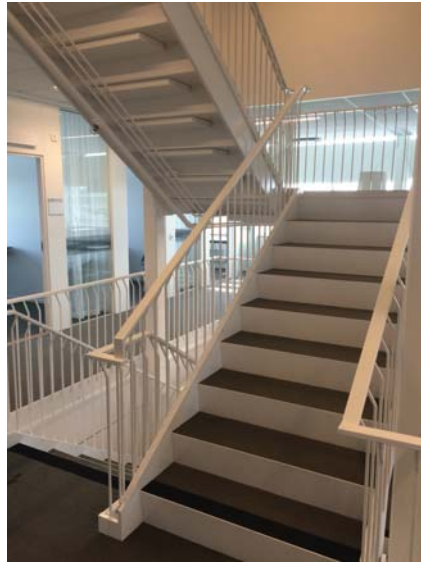




LUND
UNIVERSITY



DYNAMIC ANALYSIS OF VIBRATIONS IN STEEL STAIRCASES INDUCED BY WALKING

PATRIK GÖRANSSON and DAVID HANSSON

Engineering
Acoustics
Structural
Mechanics

Master's Dissertation

DEPARTMENT OF CONSTRUCTION SCIENCES

DIVISION OF ENGINEERING ACOUSTICS

ISRN LUTVDG/TVBA--14/5047--SE (1-136) | ISSN 0281-8477

DIVISION OF STRUCTURAL MECHANICS

ISRN LUTVDG/TVSM--15/5208--SE (1-136) | ISSN 0281-6679

MASTER'S DISSERTATION

DYNAMIC ANALYSIS OF VIBRATIONS IN STEEL STAIRCASES INDUCED BY WALKING

PATRIK GÖRANSSON and DAVID HANSSON

Supervisors: **DELPHINE BARD**, Associate Professor, Div. of Engineering Acoustics, LTH, Professor **KENT PERSSON** and **OLA FLODÉN**, Lic Eng, Div. of Structural Mechanics, LTH, together with **ANN-CHARLOTTE THYSELL**, PhD and **KENTH LINDELL**, Tyréns AB.

Examiner: Professor **ERIK SERRANO**, Div. of Structural Mechanics, LTH.

Copyright © 2015 by Div. of Engineering Acoustics and Div. of Structural Mechanics, Faculty of Engineering (LTH), Lund University, Sweden.

Printed by Media-Tryck LU, Lund, Sweden, December 2015 (*PI*).

For information, address:

Div. of Engineering Acoustics, LTH, Lund University, Box 118, SE-221 00 Lund, Sweden.

Homepage: <http://www.akustik.lth.se>

Div. of Structural Mechanics, LTH, Lund University, Box 118, SE-221 00 Lund, Sweden.

Homepage: <http://www.byggmek.lth.se>

Abstract

In today's architecture and construction there is an increasing demand for slender and lightweight structures. The possibility to use steel in slender and strong construction elements creates new ways of designing our buildings and their components. The increased use of slender steel structures leads to new and unexpected serviceability problems in structures, such as vibrations and noise. These dynamic issues pose new challenges to how we, as engineers, should or should not design our structural elements and acoustical conditions.

This thesis presents an investigation of the dynamic effects in steel staircases due to walking, from both a structural and acoustical point of view. A case study serves as a mean to reach a general understanding of the issues that lightweight structures can produce.

The case study consisted of a steel staircase in an office building where a noise related problem due to vibrations in the staircase had been identified. A number of analyses were conducted to map the dynamic response in the staircase leading up to conclusions regarding possible enhancements suitable for the specific structure.

After the presentation of the case study a general discussion regarding the studied issues is carried out. The overall suitability of the analyses used in the case study is discussed. Ultimately some recommendations regarding the approach structural and acoustical engineers should have in these matters are proposed.

Sammanfattning

I dagens arkitektur och konstruktion ökar ständigt efterfrågan på slanka och lätta strukturer. Möjligheten att använda stål i smala och starka byggelement skapar nya sätt för oss att konstruera våra byggnader och deras komponenter. Det ökade användandet av slanka stålstrukturer leder till nya och oväntade problem i bruksstadiet, som t.ex. vibrationer och buller. De här dynamiska svårigheterna utmanar oss, som ingenjörer, i hur vi borde eller inte borde utforma våra byggelement och akustiska förutsättningar.

I det här examensarbetet undersöktes dynamiska effekter i ståltrappor vid gång, i konstruktiva och akustiska avseenden. En fallstudie användes som ett medel för att få en generell förståelse kring de utmaningar som lätta strukturer kan skapa.

Fallstudien bestod av en ståltrappa i en kontorsbyggnad där ljudrelaterade problem från vibrationer i trappan identifierats. Ett antal analyser utfördes för att kartlägga trappans dynamiska respons vilket ledde till att slutsatser gällande möjliga och lämpliga förbättringar för det specifika fallet kunde dras.

Efter att fallstudien avslutats genomförs i rapporten en generell diskussion om de studerade problemen. Analyserna från fallstudiens allmänna lämplighet diskuteras. Slutligen föreslås några rekommendationer gällande konstruktörers och akustikers tillvägagångssätt i den här typen av fall.

Preface

This master dissertation was carried out as a joint project at the Division of Structural Engineering and the Division of Engineering Acoustics, Faculty of Engineering LTH at Lund University, and the departments of structural and acoustical engineering at Tyréns AB, Malmö. The work was carried out partly at Tyréns in Malmö and partly at LTH during the fall of 2015.

We would like to extend our gratitude to our supervisors, Kent Persson, Ola Flodén and Delphine Bard at LTH. Furthermore we would like to thank Juan Negreira, Anders Sjöström and Nikolas Vardaxis for sharing their expertise during the fall. We would also like to thank our colleagues at Tyréns for supporting us, especially our supervisors Kenth Lindell and Ann-Charlotte Thysell and Rickard Appelin for the assistance at MAX IV.

Last but not least we would like to thank each other for enduring and supporting one another throughout the thesis work.

Lund, 2015

Patrik Göransson and David Hansson

Contents

1. INTRODUCTION.....	1
1.1. BACKGROUND.....	1
1.2. PURPOSE AND AIM.....	1
1.3. CASE STUDY	1
1.4. SCOPE AND LIMITATIONS.....	2
1.5. THESIS OUTLINE	3
1.6. METHOD.....	3
1.6.1. Literature study.....	3
1.6.2. Case study.....	3
1.6.3. General conclusions	5
2. APPLIED THEORY.....	7
2.1. STRUCTURAL DYNAMICS.....	7
2.1.1. Operative standards.....	7
2.1.2. Natural frequencies.....	8
2.1.3. Comparison techniques	9
2.1.4. Propagation of vibrations in structures	10
2.1.5. Vibration control.....	10
2.2. ACOUSTICS	12
2.2.1. Operative standards.....	12
2.2.2. Noise perception.....	14
2.2.3. Noise control with absorbents	15
2.2.4. Reverberation	15
2.2.5. Reduction of sound due to distance.....	16
2.3. MEASUREMENT SYSTEMS	16
2.3.1. Pulse system	17
2.3.2. Signal treatment and Fourier transformation	17
3. CASE STUDY DESCRIPTION.....	19
3.1. INTRODUCTION.....	19
3.2. PROPERTIES OF THE STAIRCASE	20
3.3. PREVIOUS MEASUREMENTS	21
4. CASE STUDY MEASUREMENTS.....	23
4.1. SOUND PRESSURE LEVEL.....	23
4.1.1. Background noise and disturbances.....	25
4.1.2. Walking and running on landing and tread.....	25
4.2. NATURAL FREQUENCY MEASUREMENTS	28
4.3. VIBRATION ANALYSIS WITH WALKING AND RUNNING	32
4.4. VIBRATION ANALYSIS WITH IMPACT HAMMER.....	38
4.5. VIBRATION PROPAGATION ANALYSIS.....	41
4.6. REVERBERATION TIME MEASUREMENT	45
5. CASE STUDY MODELING.....	47
5.1. NATURAL FREQUENCY ANALYSIS	47
5.1.1. FE-Model	47
5.1.2. Natural frequencies from FE-model	49
5.2. REVERBERATION TIME ANALYSIS.....	50
5.3. VERIFICATION OF FE-MODEL	54

5.4.	VERIFICATION OF REVERBERATION SIMULATION.....	56
6.	CASE STUDY DISCUSSIONS AND CONCLUSIONS	57
6.1.	DISCUSSIONS.....	57
6.1.1.	<i>Sound pressure level analysis.....</i>	<i>57</i>
6.1.2.	<i>Natural frequency analysis</i>	<i>59</i>
6.1.3.	<i>Vibration analysis with walking and running.....</i>	<i>63</i>
6.1.4.	<i>Vibration analysis with impact hammer.....</i>	<i>64</i>
6.1.5.	<i>Vibration propagation analysis</i>	<i>65</i>
6.1.6.	<i>Reverberation time analysis.....</i>	<i>65</i>
6.2.	CONCLUSIONS	66
6.3.	POSSIBLE ADJUSTMENTS.....	67
6.3.1.	<i>Structural alterations.....</i>	<i>67</i>
6.3.2.	<i>Acoustical alterations</i>	<i>72</i>
7.	GENERAL CONCLUSIONS AND DISCUSSIONS	75
7.1.	GENERAL STRATEGIES IN DESIGN	75
7.1.1.	<i>Structural recommendations</i>	<i>75</i>
7.1.2.	<i>Acoustical recommendations</i>	<i>76</i>
7.2.	OVERALL PROS AND CONS OF THE ANALYSIS	76
7.3.	FURTHER STUDIES	77
8.	REFERENCES	79

- Appendix A1 - Visual identification of motion in natural frequencies from FE-model.
- Appendix A2 - Visual identification of motion in natural frequencies from measurements.
- Appendix A3 - Comparison initial decimated model and FE-model.
- Appendix B1 - Measurement data vibration from walking and running setup 1.
- Appendix B2 - Measurement data vibration from walking and running setup 2.
- Appendix C1 - Visual comparison for validation and AutoMAC of mode shapes in setup 1.
- Appendix C2 - Visual comparison for validation and AutoMAC of mode shapes in setup 2.
- Appendix C3 - Visual comparison for validation and AutoMAC of mode shapes in setup 3.
- Appendix D1 - Coherence data for vibration measurements with hammer impact
- Appendix D2 - Audibility investigation in different positions and adjustments.
- Appendix E1 - Theoretical background

List of figures

Figure 1.1.	Schematic appearance of the staircase.....	2
Figure 1.2.	Type of analyses performed.....	4
Figure 2.1.	SDOF system.	8
Figure 2.2.	Effect of TMD.....	12
Figure 2.3	Perception threshold for vibrations. (Swedish Standards Institute, 2004b).....	14
Figure 2.4.	Wisner curves and the four zones.....	15
Figure 2.5.	The LAN-XI module connecting accelerometers, impulse hammer and computer (Copyright © Brüel & Kjær).....	17
Figure 2.6.	An impulse hammer (left) used for exciting vibrations and an accelerometer (right) for collecting the vibration data (Copyright © Brüel & Kjær).....	17

Figure 3.1. Position of the staircase(marked with red box) with marking(arrow) of test floor.	19
Figure 3.2. Map over MAX IV facilities with red arrow marking the test area.....	20
Figure 3.3. Components of the staircase.....	20
Figure 3.4. Staircase with absorbents under each tread.	21
Figure 4.1. Microphone during sound pressure level measurements.	23
Figure 4.2. Schematic picture of microphone placement.	23
Figure 4.3. Sound pressure function in different frequencies during walking on landing.	24
Figure 4.4. Sound pressure function in different frequencies during walking on tread.....	24
Figure 4.5. Background noise and walking on slab.	25
Figure 4.6. Mean equivalent sound pressure level on impact for walking and running on landing.	26
Figure 4.7. Mean equivalent sound pressure level on impact for walking and running on tread. ...	26
Figure 4.8. Mean equivalent sound pressure level for entire measurement sequence.....	27
Figure 4.9. Initial decimated model.	29
Figure 4.10. Mode shape of natural frequency 122,65 Hz. Left: FE-model. Right: Second bending mode in the landing well recognized by the decimated model.	29
Figure 4.11. Mode shape of natural frequency 180,95 Hz. Left: FE-model. Right: The initial decimated model fails to recognize the third bending mode in the landing due to the dominant deflection in the first tread.	30
Figure 4.12. Reconstructed decimated model.	30
Figure 4.13. Setup during impact hammer test with marking for hitting points.....	31
Figure 4.14. Setups during impact hammer test. Blue marker for impact position and red for accelerometer.	31
Figure 4.15. Placements of accelerometers during experiments.....	32
Figure 4.16. Response in all three directions.....	33
Figure 4.17. Response in the vertical direction.	33
Figure 4.18. Frequency peaks in the lower landing in logarithmic scale.	34
Figure 4.19. Frequency peaks in the tread in logarithmic scale.	34
Figure 4.20. Mean FFT for walking, setup 1.	35
Figure 4.21. Normalized mean FFT for walking, setup 1.	35
Figure 4.22. Mean FFT for running, setup 1.....	36
Figure 4.23. Normalized mean FFT for running, setup 1.	36
Figure 4.24. RMS-values compared to the perception threshold according to ISO 2631-1 while walking in the staircase.	38
Figure 4.25. RMS-values compared to the perception threshold according to ISO 2631-1 while walking in the staircase.	38
Figure 4.26. Response in landing (blue) and tread (red) when hammer impact on tread.....	39
Figure 4.27. Response in landing (blue) and tread (red) when hammer impact on mid-span landing.....	39
Figure 4.28. Response in landing (blue) and tread (red) when hammer impact on beam landing.	40
Figure 4.29. Coherence for measurement in tread with impact on tread.....	40
Figure 4.30. Placement of accelerometer (red) with arrows showing measurement directions and hammer impact positions during propagation tests.	42
Figure 4.31. Placements of accelerometers. Left; accelerometer on column and slab. Right; accelerometers on stringer.	42

Figure 4.32. Impact and response from impact position H1.....	43
Figure 4.33. FFT for impact position H1.	43
Figure 4.34. FFT for impact position H2.	44
Figure 4.35. FFT for impact position H3.	44
Figure 4.36. FFT for impact position H4.	44
Figure 4.37. Positions from reverberation time measurements.....	46
Figure 4.38. Mean reverberation time from measurement.....	46
Figure 5.1. Floor plan describing the columns on the floor.	47
Figure 5.2. Flexibility in column and stiffness in the slab in the horizontal direction.	48
Figure 5.3. The stiffness of a column.	48
Figure 5.4. Pinned and rigid connections.	49
Figure 5.5. ABAQUS model.....	49
Figure 5.6. CATT-model.....	51
Figure 5.7. Effect of the voids.....	53
Figure 5.8. Source and receiver positions in reverberation time tests.	54
Figure 5.9. Mean reverberation time from CATT simulation.	54
Figure 5.10. Measured response in middle tread.	55
Figure 5.11. Determining suitable damping coefficients.	55
Figure 5.12. The final adjusted reverberation in the modeled compared to the measured.....	56
Figure 6.1. Possible installation causing background noise.....	57
Figure 6.2. Sound pressure level on impact compared to Wisner curves.	58
Figure 6.3. Forces from walking in different positions in the staircase.....	64
Figure 6.4. Reverberation time comparison between simulation and measurement.....	66
Figure 6.5. Summary of results. Dashed lines for treads and continuous lines for landings.....	67
Figure 6.6. Example of added steel stiffener to obstruct bending motion (dashed line).....	67
Figure 6.7. Sections with steel stiffeners obstructing probable plate motion.....	68
Figure 6.8. Stiffening plates under landing at Ubåtshallen in Malmö.....	68
Figure 6.9. Example of tuned mass dampers on treads.....	69
Figure 6.10. Example of added mass on treads.	70
Figure 6.11. Treads with infill at Ubåtshallen and Malmö Höghskola Orkanen in Malmö.....	70
Figure 6.12. Response from modeling of alteration on tread.	71
Figure 6.13. Bending moment corresponding to material placement.	71
Figure 6.14. Overview of the room with its alterations. The figure shows the source position (in staircase) and the receiver position (in the office area) marked with a red X. The screens placement and absorbents on wall (dark yellow area) are shown and the missing ceiling is where the extra bass was applied.	72
Figure 6.15. Comparison of the simulated reverberation time with different alterations.	73
Figure 6.16. Modeled sound pressure level in the office area with a sound source placed on the upper landing, see Appendix D2.....	73
Figure 6.17. The sound pressure loss in the receiver position compared to when no alteration have been done.	74

List of tables

Table 2.1. Reverberation time classification for office buildings.	13
Table 2.2. Installation noise classification for office buildings.	13
Table 3.1. Dimensions of components in the staircase.	21
Table 4.1. Identified peaks on impact in sound pressure level analysis.....	27
Table 4.2. A-weighted sound pressure levels.	28
Table 4.3. Chosen mode set.....	28
Table 4.4. General result of Setup 1.	32
Table 4.5. Identified frequency peaks from mean values of walking and running.	37
Table 4.6. Response peaks in vibrations due to hammer impact.	41
Table 4.7. Propagation results.	43
Table 4.8. Reverberation time for different measurements and frequencies.....	45
Table 5.1. Summary of type of motion in different natural frequency spans.....	50
Table 5.2. Materials and surfaces used in CATT.	52
Table 5.3. Absorption coefficients (α) of different materials in CATT.	53
Table 6.1. MAC-values for the three lowest modes from measurement in setup 3.	61
Table 6.2. Top three MAC-values for the second mode shape in setup 3.	61
Table 6.3. Modeling of measure on tread.	71

1. Introduction

This chapter describes the thesis report considering the scope and conditions at hand.

1.1. Background

In constructions today there is an increasing demand for lightweight structures. The properties of steel, and its possibilities for slender structures, meet many of these demands for slabs and columns but also for detail solutions like staircases. The increased use of slender steel structures leads to new and unexpected serviceability problems in structures, such as vibrations and noise. Designing a steel staircase often requires more than just checking the load bearing capacity. The dynamic effects must be considered as they can create discomfort for the user and the surrounding environment. How the vibrations spread in the structure depends on the staircase components and connections. This could create a problem in the interface between the structural engineers and the acoustical engineers work. This is something we will further investigate in this joint master thesis, with one part in the Department of Structural Mechanics and one part in the Department of Acoustical Engineering at Tyréns AB. The company provided us with a case study of special interest and suggested that we do further analysis on a steel staircase in MAX IV, Lund. Tyréns has identified a noise related problem originating from walking in the staircase, which is the starting point for this master thesis.

1.2. Purpose and aim

In this master thesis an investigation of the dynamic behavior of steel staircases and how it affects the surroundings will be performed. The influence of connections and structural components will be considered in the analysis. The main goal is to find general strategies for predicting and preventing certain vibrations in steel staircases leading to enhanced structural and acoustical behavior. The aim of the thesis is that these general strategies can be used in steel staircase design. A staircase at the MAX IV facility will serve as an example through a case study.

1.3. Case study

In previous work, loads induced by walking on slender staircases have been studied. Dynamic response approaching three times the static response has been measured and walking pattern under different conditions has been mapped. (Kerr, 1998) In other dissertations, such as *Modal Testing and Structural Identification* by Tobias Kristensson and *Vibration of Hollow Core Concrete Elements Induced by Walking* by Pia Johansson, vibrations and dynamic behavior in slender elements were evaluated in laboratory environment. (Kristensson, 2014) (Johansson, 2009) In this case study a structure in its actual intended location is studied where these previous findings can be applied and developed further.

The case study will serve as a mean to find general strategies for preventing unwanted vibrations and will be carried out at the MAX IV facility in Lund. The staircase is situated in an office building in connection to the laboratory area, see Figure 1.1. The MAX IV facility has been widely analyzed for vibrations due to the demanding laboratory facility which has posed a lot of challenges during the design phase. After the office building was constructed noise originating from the staircase was detected. Measurements were performed by the Department of Acoustics at Tyréns, which showed results above the allowed limit. This formed the basis for a discussion not only involving the

1. Introduction

contractor and Tyréns but also the Division of Structural Mechanics and the Division of Engineering Acoustics at Lund University.

1.4. Scope and limitations

This master thesis will investigate the dynamic response in slender steel staircases in order to be able to find a way to alter it to improve its vibration pattern. Disciplines considered in this thesis will be acoustical and structural engineering. The investigation is limited to a specific case study, general theory and interviews with engineers active in similar work processes. The scope for this dissertation is:

- Dynamic analyses containing noise and vibration measurements and finite element modeling are to be performed on the staircase in the presented case study.
- Acoustic simulation of the case study is to be performed where the reverberation effect of the surroundings is to be considered.
- Methods of handling noise and vibration issues in slender steel staircases are to be investigated.

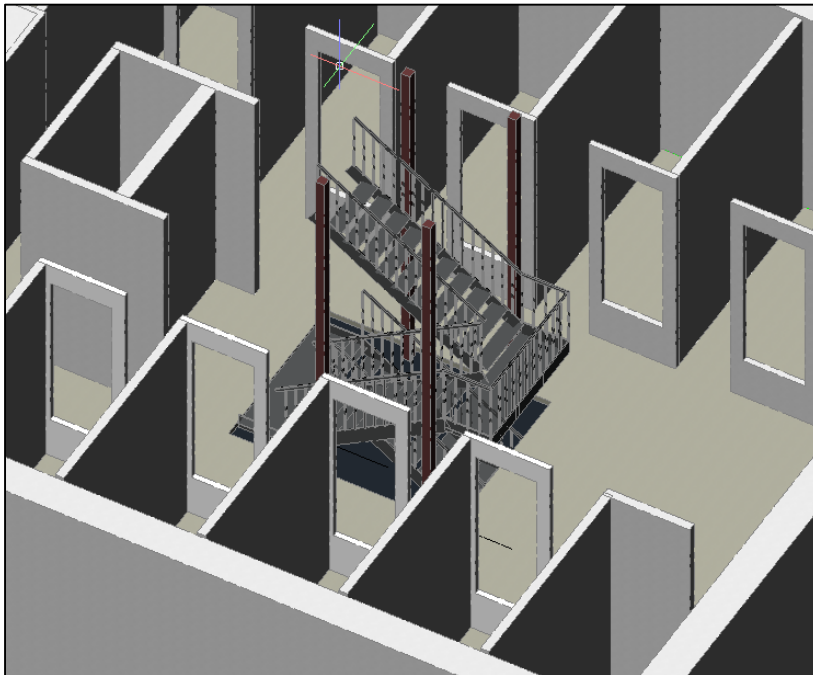


Figure 1.1. Schematic appearance of the staircase.

The limitations of the thesis is:

- Only one flight on the entry level is investigated in the case study.
- The railings of the staircase are disregarded.
- Only vibrations propagating to immediately adjacent structures are studied.
- The frequency range is determined from the sound measurements.

1.5. Thesis outline

The outline of this thesis is:

- Introduction – Introducing the purpose, aim and means of completing the thesis.
- Applied theory – The theory that will be used hands-on in the thesis.
- Case study description– An introduction to the case study that will serve as a mean to reach the aim of the thesis.
- Case study measurements – The measurements performed in the case study.
- Case study modeling – The modeling performed in the case study.
- Case study discussions and conclusions – The discussions and conclusions leading up to possible adjustments for the case study.
- General conclusions and discussions – The general conclusions fulfilling the purpose and aim of the thesis.
- References – The literature referenced in the report.
- Appendices

1.6. Method

In this part the methods to meet the purpose and aim in the thesis are declared.

1.6.1. Literature study

A literature study is performed both regarding theory of structural dynamics and acoustics and operative standards in the fields. The study will be carried out separately by the structural and acoustical engineering student for each field and form a common base of knowledge.

Applied theory

The first part of the master thesis is to study relevant literature and summarize it. This is to be done both from a structural and an acoustical point of view. The theory will form the basis for conclusions regarding which adjustments could be made on the staircase in the case study. The goal of the literature study is also to show the connection between the two sciences. The operative standards for each field are investigated.

Theoretical background

The theoretical background will serve as a general theory chapter covering some of the basic phenomena in structural and acoustical engineering. The theoretical background will be appended to the thesis.

1.6.2. Case study

A case study regarding a steel staircase in the MAX IV facility in Lund is carried out as a mean to find general conclusions in staircase design. The general layout of the investigation can be divided into four type of analyses. The first two analyses, *Natural frequency analysis* and *Room acoustic simulation*, can be performed in the design phase, or when there is no actual staircase to take measurements from. The second two analyses, which are performed as validation tests on the actual structure and its surroundings, see Figure 1.2. In the study both walking and running will be investigated to cover a larger possible load span, but keeping the main focus on walking.

1. Introduction

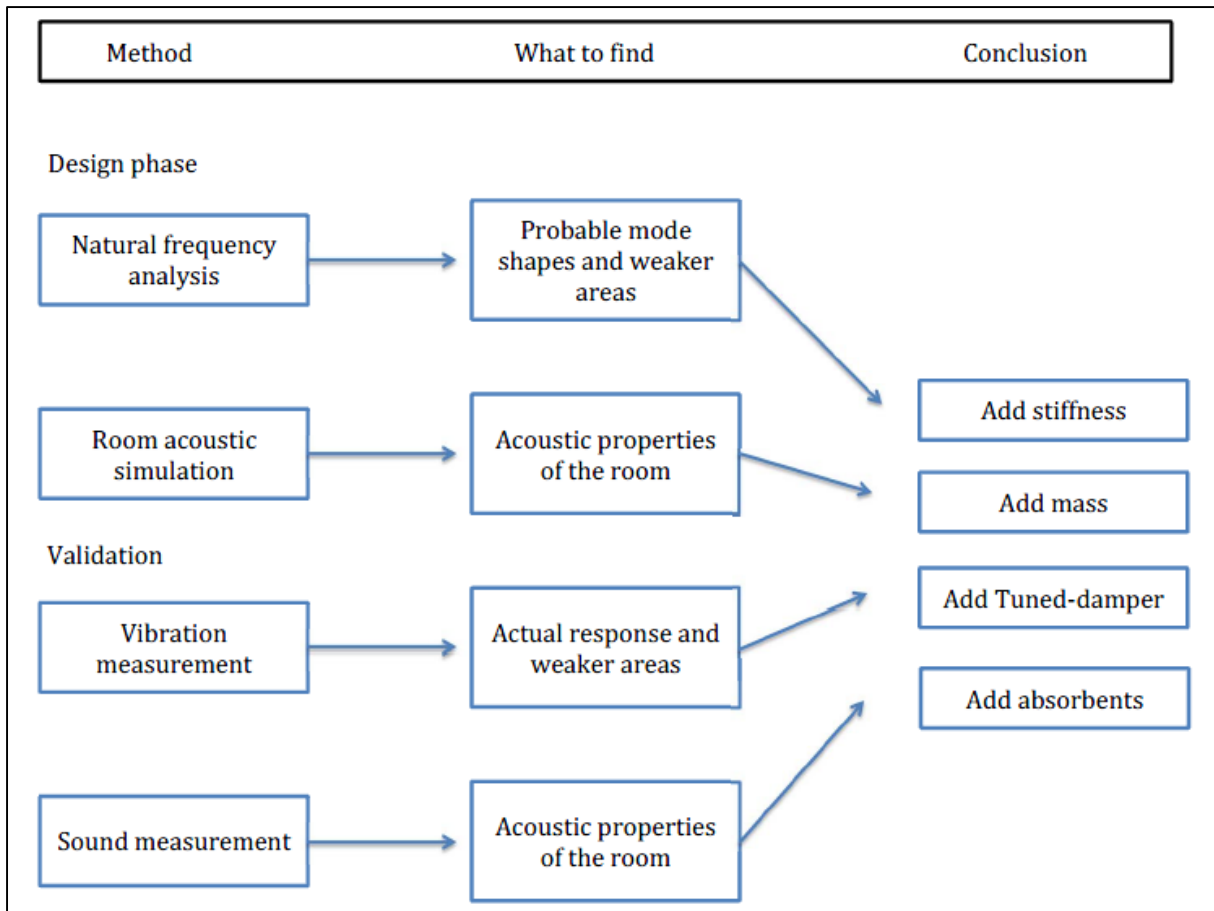


Figure 1.2. Type of analyses performed.

Properties of the staircases and old measurement data

First of all the actual geometry of the staircases are measured and compared to the drawings. Materiality and surroundings will also be investigated. Old measurement data is examined and presented.

Sound measurement

Airborne sound pressure and reverberation measurements are to be performed by the acoustical engineering student in the case study. This will be done by measuring the sound pressure level both when an impulse loading is being applied and when people are walking in the staircase. Since the definition of walking might be subjective running is also investigated. From these measurements the problematic frequencies causing noise can be determined. The reverberation is measured to investigate the absorption in the room.

Natural frequency analysis

A finite element model will be constructed by the structural engineering student according to the investigated geometry and properties. When the model has been constructed the natural frequencies can be determined and probable mode shapes and weaker areas can be found. The natural frequencies can also be compared to the problematic frequencies discovered during the experimental part.

A natural frequency analysis from measurement data will be performed using *Brüel & Kjaer's Pulse* system. By applying loads with an impact hammer at numerous positions on the staircase and measuring the motion in some positions the software can generate natural frequencies detected during the measurement. The application mainly is presented by *Brüel & Kjaer* as a mean of analyzing mechanical structures but in (Kristensson, 2014) it is used for analyzing a slender steel bridge in a laboratory setting.

Vibration measurement

Vibration measurements are to be made by the structural and acoustical engineering student. Suitable positions to place accelerometers during the measurements will be determined. This can be done by analyzing the natural frequencies of the structure. Vibration measurements can then be performed by the acoustical engineering student both by applying load with and impact hammer and by applying the load from actual walking. Further vibration measurements can be performed to investigate the propagation of vibrations to adjacent structural elements.

Acoustical simulation

An acoustical simulation will be performed by the acoustical engineering student. The simulation will consider the properties of the surroundings to assess the perception of the vibrations from the staircase in its setting, for example by looking at the reverberation time. The reverberation time will also be verified by reverberation time measurement in the room surrounding the staircase.

Conclusions from analyses

From the performed analyses conclusions regarding possible adjustments will be drawn. Strengths and weaknesses of the different analyses will be discussed. This part will conclude the learnings from the case study and form the basis for the general conclusions regarding dynamic analyses of any steel staircase. After verifying the models they can be used to adjust and improve the structure and its surroundings.

1.6.3. General conclusions

When a solution has been found some general conclusions will be drawn. These conclusions should be formulated so that they can be used when designing a lightweight structure. The conclusions are to complement the existing standards for both acoustics and structural dynamics.

2. Applied theory

In this chapter the main theory applied in the thesis is presented. Structural dynamics and acoustics are presented, respectively, and finally measurement systems used in the case study are presented. A theoretical background to the two fields is appended in Appendix E1.

2.1. Structural dynamics

In this chapter theory regarding structural dynamics, i.e. mainly vibrations, is presented.

2.1.1. Operative standards

Engineers working with dynamics and vibrations consider the theory by following applicable standards or guidelines for a structure. The regulations might differ from the theory in some senses and therefore it will be described separately in this chapter covering how engineers are regulated to work in these matters. For dimensioning structures in the European Union a set of rules, the Eurocodes, are applicable. It is necessary to study parts of the Eurocodes concerning different structures and structural elements to find requirements suitable for the structure at hand.

Regarding vibrations in buildings and structural members the Eurocode states that generally two aspects need to be considered, namely comfort of the user and functioning of the structure and its structural members. The criterion in serviceability state is not to be exceeded due to vibrations and the natural frequencies should be above appropriate values for the function in the building. If this cannot be fulfilled, a more accurate analysis of the dynamic response considering damping in the structure should be performed. (Swedish Standards Institute, 2002)

In the Eurocode it is stated that, for serviceability in footbridges and deck areas, a comfort criterion applies to any part of the structure. The criterion concerns maximum acceptable acceleration and is divided into three parts:

- 0,7 m/s² for vertical vibrations,
- 0,2 m/s² for horizontal vibrations due to normal use,
- 0,4 m/s² for exceptional crowd conditions.

Furthermore it is also stated that for structures with fundamental frequencies below 5 Hz for vertical vibrations and 2,5 Hz for lateral and torsional vibrations, a verification of the comfort criteria above should be performed. Additionally, it is stated that calculations for this type of criteria comes with high uncertainties and it is therefore necessary to fulfill the criterion with some margin and it may also be required to design the structure in a way that dampers can be installed after completion. (Swedish Standards Institute, 2002)

In Eurocode 5, Design of timber structures, there is a rule concerning timber slabs. It is stated that timber slabs should not have a fundamental natural frequency of less than 8 Hz. (Swedish Standards Institute, 2004a) According to Austrell¹ this rule applies to timber structures since they traditionally are light enough to be in danger of being excited by human activity. For lightweight steel slabs and staircases this rule also should be applicable. Austrell claims that the 8 Hz-limit is quite conservative

¹ Per-Erik Austrell. Prof. Department of Structural Mechanics, Faculty of Engineering LTH at Lund University. Email correspondence 11th August 2015.

2. Applied theory

but also says that it is possible to trigger the fundamental frequency through transient loading, such as the dominant heel strike from walking in staircases.

2.1.2. Natural frequencies

To find the natural frequencies of a system the equation of motion with free vibration can be studied. The simplest system to study is the SDOF system, a system with only one degree of freedom, see Figure 2.1.

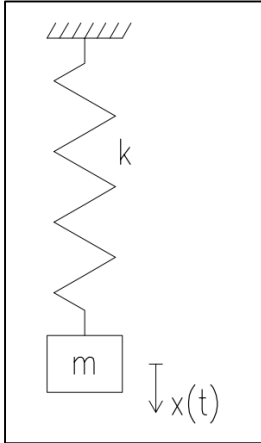


Figure 2.1. SDOF system.

The equation of motion for a SDOF system in free vibration can be expressed as

$$m \ddot{x} + kx = 0 \quad (\text{Eq. 2-1})$$

where

m is the mass

k is the spring stiffness

x is the deflection of the mass

\ddot{x} is the acceleration of the mass

A trial solution is introduced where

$$x = A \sin \omega t \quad (\text{Eq. 2-2})$$

$$\ddot{x} = -A\omega^2 \sin \omega t \quad (\text{Eq. 2-3})$$

Inserting these in Eq. 2-1 generates

$$(k - \omega^2 m)A \sin \omega t = 0 \quad (\text{Eq. 2-4})$$

To be fulfilled at all times with $A \neq 0$ the following must be fulfilled

$$(k - \omega^2 m) = 0 \rightarrow \omega = \sqrt{\frac{k}{m}} \quad (\text{Eq. 2-5})$$

Which is the natural frequency of a SDOF system. In the same manner an eigenvalue problem can be solved to generate the natural frequencies for systems with numerous DOFs.¹

2.1.3. Comparison techniques

When finding sets of modes from different models or measurements it could be useful to verify the mode sets by comparing them to one another. This can be done in various ways, either analytically or visually. In this thesis two different analytical comparisons will be accounted for besides the visual comparison, namely the modal assurance criterion and the cross orthogonality check.

Cross orthogonality check

Historically, the main technique for validation of mode shapes has been vector orthogonality. This is usually done by using the weighted mass or stiffness matrix and the mode shape vectors from the different mode sets. In theory, all mode vectors will be orthogonal to the other mode vectors in the same system, if weighted as described above. (Allemang, 2003) This means that all natural mode shapes are differentiable, which should hold theoretically since the natural frequencies describe the possible motions of the system. Experimentally this can rarely be achieved but it should be visible that comparing modes of the same mode set generates a low correlation. Cross orthogonality can be expressed as

$$Ortho(\phi_i^A, \phi_j^B) = \phi_i^{A^T} [M] \phi_j^B \quad (\text{Eq. 2-6})$$

where

ϕ_i^A is mode i in mode set A

ϕ_j^B is mode j in mode set B

$[M]$ is the analytical mass matrix of the system

(Allemang, 2003)

Modal assurance criterion

The modal assurance criterion, or MAC, is a technique used for quantitative comparison of the correlation between two sets of modes, often estimations of different nature, like measurement or FE-modeling. The correlation can differ between 0 and 1 where 1 means a perfect correlation between two modes. (Miller, 1993) Any correlation above 0,9 is commonly said to be acceptable for establishing an actual correlation between the modes. The MAC-values are set up in a matrix where the correlation between every mode in the two mode sets are calculated as

$$MAC(\phi_i^A, \phi_j^B) = \left(\frac{\phi_i^{A^T} \phi_j^B}{|\phi_i^A| |\phi_j^B|} \right)^2 \quad (\text{Eq. 2-7})$$

where

ϕ_i^A is mode i in mode set A

ϕ_j^B is mode j in mode set B

¹ Per-Erik Austrell. Prof. Department of Structural Mechanics, Faculty of Engineering LTH at Lund University. Lecture Spring 2015, Lund.

2. Applied theory

In the same manner as for cross orthogonality MAC-value for modes in a natural frequency mode set should be close to 0 for different modes and exactly 1 for the same mode shape. If the MAC-value is closer to 1 for different modes in the same set the differentiability between modes is low in the mode set. (Allemang, 2003)

The upside of using MAC-values is that there is no need to know the analytical mass matrix, making it fairly easy to test estimated mode shapes for correlation. A disadvantage however is that the MAC can return misleading results if there for instance is lack of information in measuring points. (Miller, 1993) Furthermore the MAC can only imply correlation but does not show validity or orthogonality, meaning that it does not reveal modes not being natural mode shapes as an orthogonality check would. The MAC is sensitive to large values and insensitive to small values which means that extreme values from measurements may result in inaccuracy in the MAC-values. (Allemang, 2003)

Visual comparison

Visual comparison between mode set, surely includes a risk of being subjective, but it is also a crucial part since the motion is studied directly. The visual comparison consists of a graphic assessment of the mode shapes and a comparison of natural frequency. Complex mode shapes and experimental modes that appear to match more than one natural mode shape can be problematic in this sort of comparison technique. (Imamovic, 1998)

2.1.4. Propagation of vibrations in structures

A vibrating structure can propagate its motion into adjacent structures causing them to start to vibrate. The phenomenon of spreading motion from a vibrating structure to an adjacent structure is known as transmission.¹ A vibrating structure's transmission to an adjacent structure can be quantified by analyzing the transmissibility ratio, defined as the ratio between the amplitude of the vibration in the structure and the adjacent structure. (Sciulli, 1997) If the transmissibility is too high the unwanted vibrations can be prevented from reaching the adjacent structure by introducing a dynamic absorber or an isolator. The dynamic absorber or tuned mass damper, see chapter 2.1.5, prevents the propagation by absorbing the vibration energy in its own deflection while the isolator work as a damper between the two structures. (Thorby, 2008) The isolator can, besides its damping effect, provide stiffness to the connection depending on the choice of isolator. A commonly used isolator is rubber which often is used for isolating vibrating machines or as a shock absorber. (Sciulli, 1997)

2.1.5. Vibration control

In this part theories that can be used as a mean to enhance structural behavior are presented.

Adding stiffness to the structure

One way to prevent certain vibration patterns is to change the stiffness in the structure. This will result in change in natural frequencies and dynamic response. For structures subjected to periodic loading it can be of great importance not having natural frequencies near the frequency of the periodic load due to the risk of resonance. It should also be considered that it is common for forcing frequencies to occasionally be lower than the given frequency. For example a spinning

¹ Per-Erik Austrell. Prof. Department of Structural Mechanics, Faculty of Engineering LTH at Lund University. Lecture Spring 2015, Lund.

laundry machine will work its way up to the forcing frequency, which is quite high. On its way up it will pass several natural frequencies which will have to be damped in order to keep the machine from entering resonance stage.¹

Adding mass to the structure

Adding mass to a structure will lower its natural frequency, according to the expression of the first natural frequency as

$$\omega = \sqrt{\frac{k}{m}} \quad (\text{Eq. 2-8})$$

This could be useful if there is a certain frequency that is to be avoided in the structure. Regardless of this, adding a mass element to a structure will also influence its acceleration. For an applied given load the acceleration in a structural element can be calculated using Newton's second law of motion as

$$f = m \cdot a \quad (\text{Eq. 2-9})$$

If the mass of the structural element would be increased and the force remains, the acceleration would have to be decreased in the element to fulfill the equation. By increasing the mass the kinetic energy applied to the element could be stored with decreased effort in terms of acceleration. (Rao, 2011)

Tuned mass damper

To reduce vibrations that can create resonance in the structure a so called tuned mass damper, TMD, can be added to the system. A TMD consists of a mass which is connected to the system with a spring and a damper. By choosing appropriate values for the added mass and spring stiffness the resonance top can be prevented. Appropriate values in the TMD are chosen so that the natural frequency of the added damper system corresponds to the original system i.e.

$$\omega_{td} = \sqrt{\frac{k_{td}}{m_{td}}} = \omega_S \quad (\text{Eq. 2-10})$$

where

ω_{td} is the natural frequency of the tuned mass damper

k_{td} is the stiffness of the connection between the added mass and the original structure

m_{td} is the added mass

ω_S is the natural frequency of the system

(Brandt, 2011)

¹ Per-Erik Austrell. Prof. Department of Structural Mechanics, Faculty of Engineering LTH at Lund University. Lecture Spring 2015, Lund.

2. Applied theory

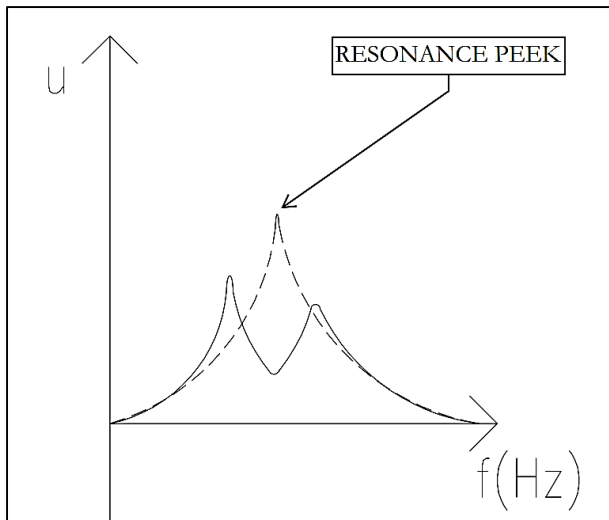


Figure 2.2. Effect of TMD.

By introducing a TMD the resonance peak will be reduced creating two smaller peaks instead of one bigger resonance peak, see Figure 2.2. The movement that will take place in the TMD will create a faster damping in the entire structure since the energy consumption from movements will increase. (Brandt, 2011)

2.2. Acoustics

In this chapter pertaining standards and theory regarding vibration and noise perception and control are presented.

2.2.1. Operative standards

The main Swedish regulations are covered in Boverkets byggregler (BBR). For acoustical engineering a set of Swedish standards exists covering different types of buildings.

In SS 25268:2007 concerning office buildings a classification system is used with ratings from A to D, where A is the highest. Reverberation time and installation noise are two subjects that are applicable in this report. Installation noise is the sound created from all the installations in the building, for example ventilation. The criteria for the different classifications are described in Table 2.1 and Table 2.2 (Swedish Standards Institute, 2007).

Table 2.1. Reverberation time classification for office buildings.

Reverberation time Type of space	T_{20} [s]			
	A	B	C	D
Big area for personal work (>20 people) Example open offices	0,4	0,4	0,4	0,8
Space for working in groups (20> people) Example big offices, project rooms	0,4	0,5	0,5	0,8
Meeting, conference and conversation room	0,6	0,6	0,6	0,8
Dining room, cafeteria (>100 m ²)	0,5	0,6	0,6	0,8
Areas in use more than temporarily. Example closed offices, reception, resting room.	0,6	0,6	0,6	-
Areas in use only temporary. Example corridor, entry, hall, copy room	0,6	0,8	0,8	-
Stairwell	1,0	1,2	-	-

Table 2.2. Installation noise classification for office buildings.

Installation noise Type of space	L_{pA} [dB] A-weighted			
	A	B	C	D
Area for presentations, video conference (>20 people)	30	30	30	35
Area for personal work, conversations or resting. Example closed offices, meeting room, reception, resting room	30	35	35	40
Big open areas for personal work Example open offices, big offices	35	35	35	40
Areas in use more than temporary. Example restaurants, dining area	35	35	40	40
Areas in use only temporary. Example corridor, entry, hall, copy room, WC	35	40	40	-

In Figure 2.3 the expected experienced disturbances of given sources of vibrations are displayed, their frequencies and RMS-values are shown. (Swedish Standards Institute, 2004b) The RMS-values are also frequency weighted and summarized to get a more perception based result that takes into consideration how the given vibrations effect humans according to ISO 2631-1:1997. The standard also states that the frequency weighting is done in the 1/3-octavebands.

Weighted RMS-value, a_w

2. Applied theory

$$a_w = \sqrt{\frac{1}{T} \int_0^T a_w^2(t) dt} \quad (\text{Eq. 2-11})$$

$$a_w(t) = a_i(t) \cdot W_i \quad (\text{Eq. 2-12})$$

Where

$a_i(t)$ is the frequency based acceleration in each time step

W_i is the weighting factor for each frequency

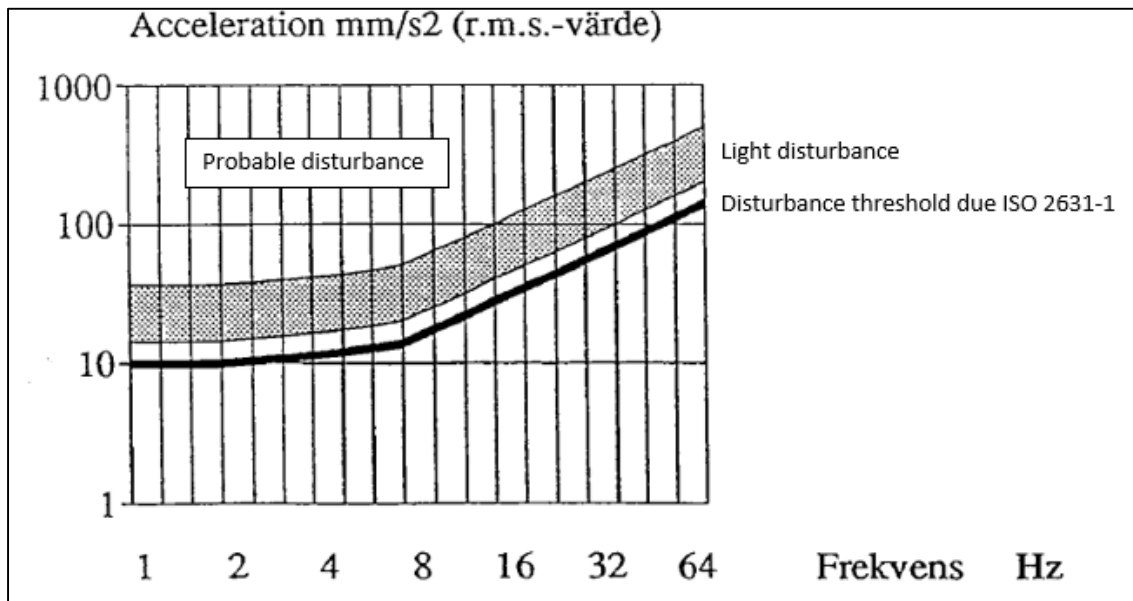


Figure 2.3 Perception threshold for vibrations. (Swedish Standards Institute, 2004b)

2.2.2. Noise perception

Noise perception in open offices depends on a variety of variables such as stress, health, task at hand for naming a couple of them. This makes the perception very personal and it can even vary from day to day. Although these variables are personal there are some factors that have been proven more likely to affect people similarly. These are the physical factors such as overall noise level, frequency specific noise levels and what type of noise it is. To measure or validate these, reference curves have been developed. For example the Wisner curves are widely used in France to evaluate ambient noise. These curves divide the frequency spectrum into four zones which take into consideration how different tasks can be performed during exposure of certain sound pressure levels, see Figure 2.4.

- Zone 1: No discomfort or disturbance while performing tasks that requires a high level of thinking.
- Zone 2: Routine work is not disturbed but tasks that requires a high level of thinking might be hard.
- Zone 3: Very hard to complete tasks that requires a high level of thinking and routine tasks starts to get difficult.
- Zone 4: Leads to deafness or hearing impairing if exposed for a too long time.

(Chevret & Chatillon, 2015)

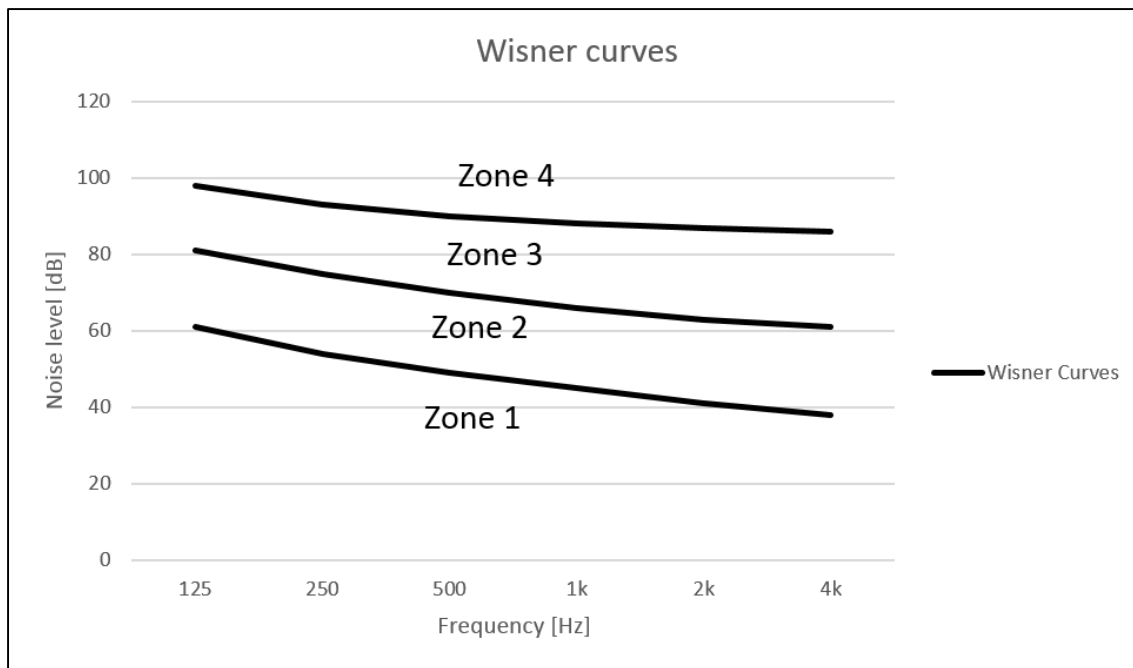


Figure 2.4. Wisner curves and the four zones.

These types of curves are not conclusive since many of the variables are subjective and further investigations have to be made to be able to predict with certainty what level of disturbance the noise creates. This can be done by performing surveys involving the affected users. (Chevret & Chatillon, 2015)

2.2.3. Noise control with absorbents

The main function of absorbents is to prevent radiated sound from a specific sound source to reach a recipient. This is done by absorbing the sound which means that the energy that the sound contains is decreased after either reflecting or penetrating the material. (Howard & Angus, 2009) Different porous materials, membrane absorbents and perforated plates are common types of absorbents. Porous materials contain a high quantity of open pores and are usually manufactured from different fibers. Membrane absorbents consist of a thin layer of some material, for example a plastic sheet, with low stiffness. The effectiveness is achieved when placed on a surface with a cavity between the membrane and the surface. Perforated plates work as a Helmholtz's resonator which means that the air, or other material, in the holes of the perforated areas work as dampers of incoming sound waves. These types of absorbents can also be combined to alter their performance. A combined damper and absorbent consists of a material similar to a damper with high density or stiffness but at the same time have the possibility to absorb sound. (Vigran, 2008)

2.2.4. Reverberation

To determine a room's acoustic properties analysis of the reverberation time (T) is a very powerful tool. The reverberation time measures the time it takes for an excited sound to decrease 60 dB when shutting the source. When looking at an impulse of a single sound wave it will propagate throughout the room until it hits something and it will then reflect of its surface. But this comes with a cost of energy which means that a wave's energy will decrease every time it hits a surface. When looking at global perspective of a room with an infinite amount of sound waves radiating from an impulse source, the sound pressure level will decrease after time. Different surfaces will

2. Applied theory

absorb different amount of energy. This is dealt with by defining an absorption coefficient for each material's surface and its frequencies. This phenomenon has a big impact on the loudness of the sound in a room. (Cremer & Müller, 1982)

Sabine's formula gives the theoretical reverberation time for a room with given surfaces with their respective absorption coefficients:

$$T = 0,163 \cdot \frac{V}{A} \quad (\text{Eq. 2-13})$$

$$A = \sum S_x \cdot \alpha_x \quad (\text{Eq. 2-14})$$

where

V is the volume of the room

A is the absorption area in the room

S_x is the surface area of the material

α_x is the absorption coefficient for the material

The absorption coefficient (α) is defined as the ratio between incoming and reflected sound energy at a surface.

$$\frac{\Pi_a}{\Pi_i} = \alpha \quad (\text{Eq. 2-15})$$

Where

Π_a is the absorbed energy

Π_i is the incoming energy

(Nilsson, Johansson, Brunskog, Sjökvist, & Holmberg, 2002)

2.2.5. Reduction of sound due to distance

When describing the propagation and reduction of sound from one point to another there are many variables to consider, e.g. weather, wind and temperature. But also what kind of source it is that emits the sound. In a controlled environment the difference in sound pressure level can be described with a simple formula

$$\Delta L = 20 \cdot \log\left(\frac{r_1}{r}\right) \quad (\text{Eq. 2-16})$$

Where

r_1 is the distance to the position closest to the sound source

r is a position further away from the sound source

(Nilsson, Johansson, Brunskog, Sjökvist, & Holmberg, 2002)

2.3. Measurement systems

In this chapter theory on data and signal treatment as well as the system used for measuring and collecting data are presented.

2.3.1. Pulse system

In the case study a system from *Brüel & Kjær* called *Pulse* was used. *Pulse* is a platform for noise and vibration analysis with both hardware and software. Frontends, called *LAN-XI*, are used to connect transducers and exciters to a computer. In this thesis measurements were performed using the *Pulse Labshop* software. Later on the captured data was reviewed and treated in the *Pulse Reflex* software.



Figure 2.5. The LAN-XI module connecting accelerometers, impulse hammer and computer (Copyright © Brüel & Kjær).



Figure 2.6. An impulse hammer (left) used for exciting vibrations and an accelerometer (right) for collecting the vibration data (Copyright © Brüel & Kjær).

Before measurements, a model can be made of the structure in *Pulse Labshop* and *Pulse Reflex*. This is used to pre-set the measurement with all its components and measurement locations.

2.3.2. Signal treatment and Fourier transformation

When measuring vibrations the pure signal from the vibration event is very complex. Thus, corrections have to be made so that the results can be overviewed more easily. The recorded frequency spectrum has to be transformed so that, for example, separate frequencies can be analyzed. This transformation is called Fourier transformation which is a mathematical procedure used to transform complex signals without any loss of valuable information. (Howard & Angus, 2009)

The Fourier Transformation comes from Fourier's theorem which states:

“Any periodic function can be expressed as an infinite sum of sinusoids multiplied by appropriate coefficients”

2. Applied theory

and is described mathematically

$$f(t) = a_0 + \sum_{n=1}^{\infty} (a_n \cdot \cos(n\omega_0 t) + b_n \sin(n\omega_0 t)) \quad (\text{Eq. 2-17})$$

with the time period T_0 such as

$$\omega_0 = 2\pi/T_0 \quad (\text{Eq. 2-18})$$

Where

$f(t)$ = periodic time function

ω_0 = angular frequency ($2\pi f_0$) of the periodic function

a_0 = content of the periodic function

a_n = level of the n th cosine harmonic of the periodic function

b_n = level of the n th sine harmonic of the periodic function

For transforming digital audio signals Discrete Fourier Transformation is used. With the equation below it is possible to transform the complex time spectrum to the signal's frequency spectrum. (Howard & Angus, 2009)

$$F_k = \sum_{n=0}^{N-1} f_n \cdot e^{-\frac{j2\pi nk}{N}} \quad (\text{Eq. 2-19})$$

where

k is the frequency index with the values $0, 1, 2 \dots N - 1$

N is the length of the signal sequence

For transforming the frequency spectrum back to the time signal the following equation is used:

$$X_k = \frac{1}{N} \sum_{n=0}^{N-1} X_m \cdot e^{-\frac{j2\pi nk}{N}} \quad (\text{Eq. 2-20})$$

These two equations are the basic way to handle complicated signals. Nowadays the Discrete Fourier Transformation has been optimized to the Fast Fourier Transform by J.W Cooley and J.W Tukey which in principle works in the same way. (Howard & Angus, 2009)

3. Case study description

In this case study six measurement analyses and two modeling analyses were performed on a staircase. These analyses could have been performed dependent or independent of each other but in this case study the first analysis, Sound pressure level, formed the basis for the remaining analyses. The case study was carried out as a mean to reach the aim of the thesis and it is described in three separate chapters covering measurements, modeling and conclusions (chapter 4-6).

3.1. Introduction

The case study took place at the MAX IV facility in northeast Lund. MAX IV is a synchrotron light source facility and is to be used as a laboratory. The facility consists of a main building for the storage, a linear accelerator, and a couple of office buildings attached to it. Vibration control has been a big issue during planning and construction of the facility due to the strict requirements of the laboratory work. The case study took place in one of the attached office buildings, called the E-building. The E-building spans over the ring with one foundation on each side and contains office space for scientists. The staircase studied is situated in the outer part of the E-building, see Figure 3.1 and Figure 3.2. The part of the staircase that was studied was on the entry level, due to accessibility and minimum disturbance from office activity. Previous investigations were also performed at this part, see chapter 3.3. The room surrounding the staircase is used as an office space with closed offices on the entry level and open office landscape on the floor above.



Figure 3.1. Position of the staircase(marked with red box) with marking(arrow) of test floor.

3. Case study description

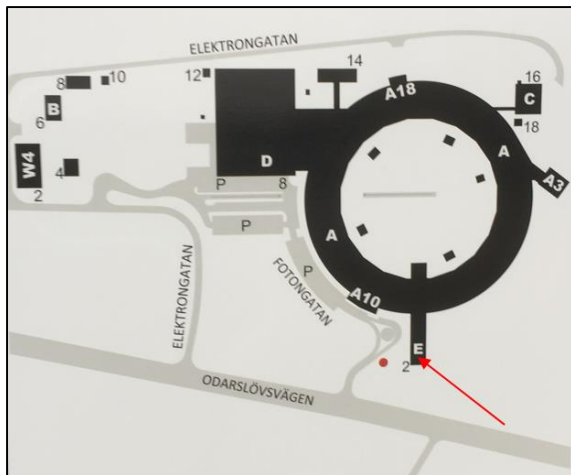


Figure 3.2. Map over MAX IV facilities with red arrow marking the test area.

3.2. Properties of the staircase

In this chapter the properties of the staircase in the case study are described. The properties were obtained either by measurements on the actual staircase or by information from the manufacturer. First of all, the components of the staircase were defined to avoid any confusion. In Figure 3.3 the components of the staircase are displayed. In the case study the handrails were not regarded or studied and any effects from these were not discussed. The reason for this was that they are not load bearing and could thus be considered a separate structure regarding vibrations due to the pinned bolt connection to the flight.

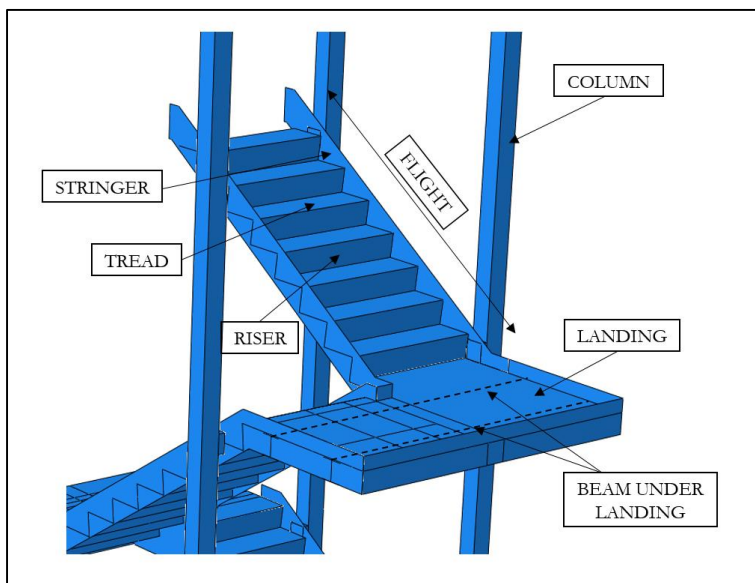


Figure 3.3. Components of the staircase.

The steel staircase was evaluated both from a structural and an acoustical standpoint. The staircase was prefabricated by Häfla Bruks AB in welded sections that were put together on-site. Each section consists of steel plates that are welded together, building up the staircase. The connections are made with bolt plates to the columns that provide the overall bearing capacity of the structure. In each connection, steel distance plates were used when needed, maximum two per connection. On each floor there are landings, shown in Figure 3.3, incorporated in the concrete slabs by a

carpet covering up the landings. Otherwise the structural connections are made through the columns and into the slabs. Railings were mounted on the staircase separate from the flights.

After the construction a problem with noise due to vibrations in the staircase was identified which led to additional measures to prevent disturbance. Therefore absorbents made from glass wool insulation, *Ecophon Master B*, were mounted under each tread and landing to decrease the noise problem.

The staircase drawings have been studied and an assessment was done at Max IV which verified that information from the manufacture was accurate.



Figure 3.4. Staircase with absorbents under each tread.

The dimensions of the steel components are described in Table 3.1.

Table 3.1. Dimensions of components in the staircase.

Component	Dimensions
Treads	295x1060x5 mm ³
Risers	180x1060x5 mm ³
Stringers	20mm plate
Landings	5 mm plate
Columns	VKR 150x150x10
The density of steel is assumed to be 7850 kg/m ³	

3.3. Previous measurements

After the construction of the staircase, problems with noise from the staircase were identified. Therefore measurements were made, by engineers from Tyréns AB, to investigate the vibrations in the staircase. The data was used in an evaluation leading to examples of possible adjustments to the staircase. These measurements were carried out with the *Pulse* system with two accelerometers, a sound level meter and an impact hammer. The measurements showed that most of the sound originated from vibration frequencies of about 100 and 200 Hz. In the landings, resonance

3. Case study description

frequencies at about 100 Hz were dominating while at the treads resonance was found around 200 Hz. From the measurements it was proposed that actions to stiffen the landings should be taken.¹ These actions were not taken, instead the absorbent mentioned in chapter 3.2 was used.

¹ Ann-Charlotte Thysell, Acoustical Engineer, Tyréns AB

4. Case study measurements

In this chapter the results from measurements are presented.

4.1. Sound pressure level

Sound pressure level measurements were performed during excitation of the staircase through walking and running. The measurements were performed using sound level meter of the type *Norsonic 140* with fixed microphone position in the room surrounding the staircase, see Figure 4.1.



Figure 4.1. Microphone during sound pressure level measurements.

This test was performed to evaluate how much sound and in what frequencies the staircase radiates in normal use. The results are strongly dependent on the person using the staircase due to walking style, mass, type of shoes etc. Also the definition of running and walking can differ from person to person. Therefore the conditions were kept the same throughout the tests.

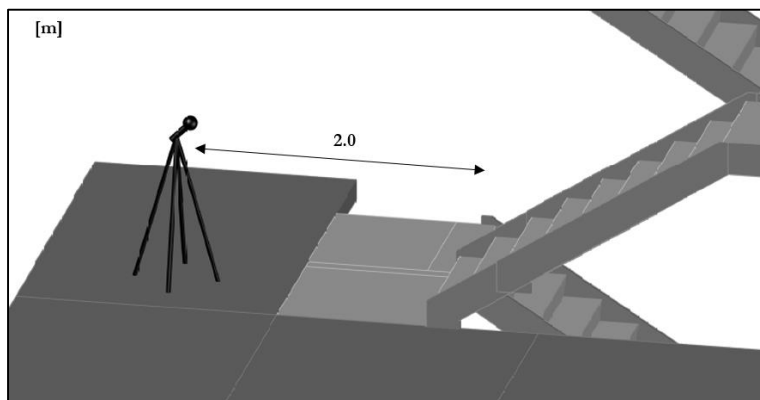


Figure 4.2. Schematic picture of microphone placement.

4. Case study measurements

The sound pressure level in the room during walking and running was measured in a single position, about two meters from the staircase flight, see Figure 4.2. Walking and running from the bottom to the top and back again were applied to the staircase and the sound pressure level was recorded during the entire test. Both measurements during walking and running were duplicated five times each. The sound pressure level for different frequencies was analyzed in *Audacity*. In Figure 4.3 the sound pressure function in different frequencies during walking on the landing is displayed.

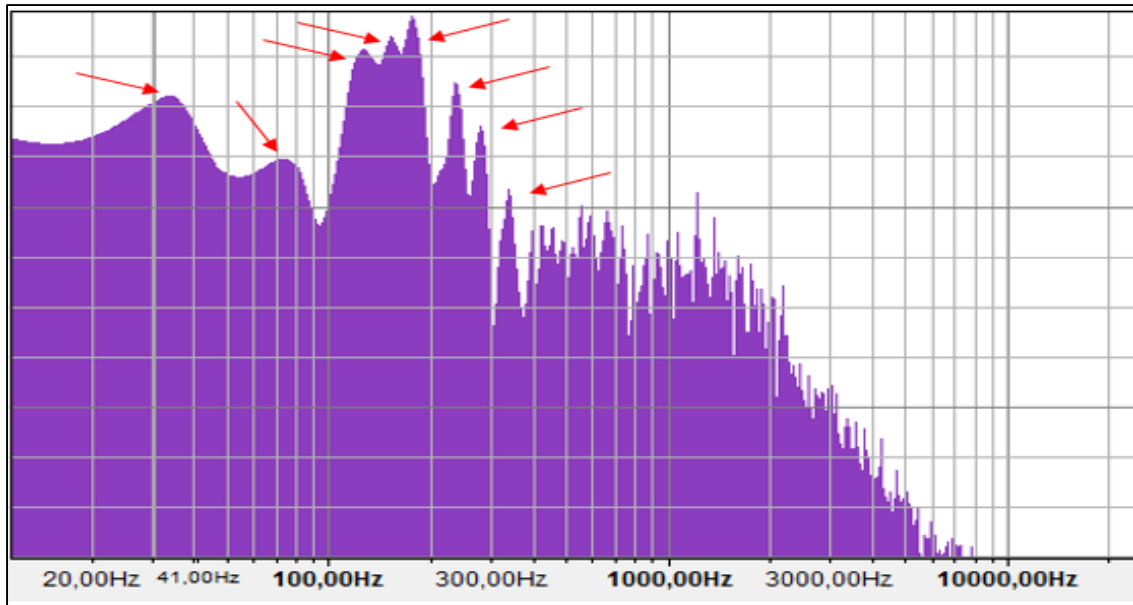


Figure 4.3. Sound pressure function in different frequencies during walking on landing.

A few resonance peaks are marked in the figure, the lowest one occurring around 40 Hz and the highest one around 340 Hz. In Figure 4.4 the sound pressure function in different frequencies during walking on a tread is displayed. The sound pressure level is displayed later on as an averaged value from the measurements.

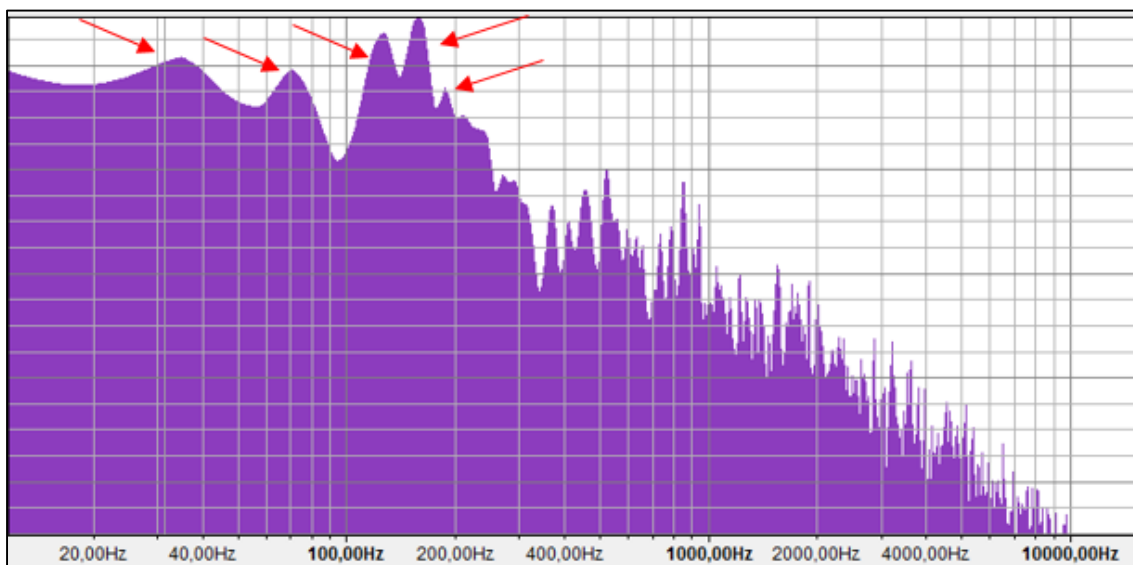


Figure 4.4. Sound pressure function in different frequencies during walking on tread.

A few frequency peaks are marked in the figure above, the lowest one at about 40 Hz and the highest one just under 200 Hz.

4.1.1. Background noise and disturbances

To investigate possible noise and sound originating elsewhere than from the staircase, the background noise in the room was measured. Beside the background noise the sound of the footstep against the carpet also can disrupt the measurements. Since sound originating from vibrations of the staircase was of interest other possible noise had to be identified. This was done by measuring the sound pressure level during walking on the slab, with the same carpet as in the staircase. The sound pressure level of the noise and disturbances for different frequencies are displayed in Figure 4.5. It is visible that frequencies below 50 Hz dominate the background noise and footstep.

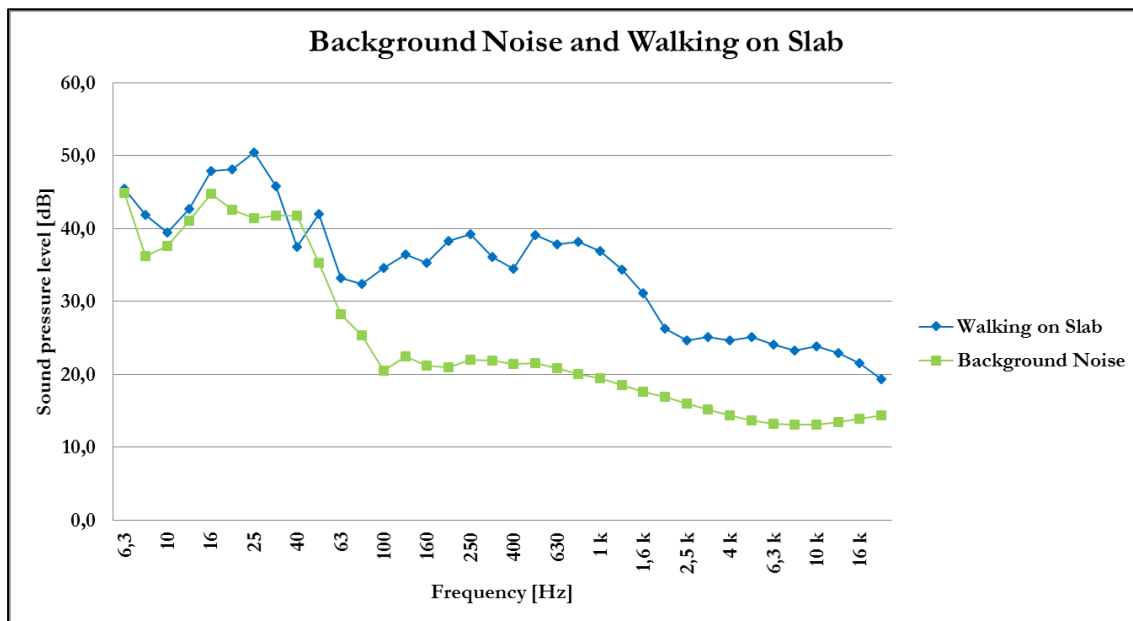


Figure 4.5. Background noise and walking on slab.

4.1.2. Walking and running on landing and tread

The mean equivalent sound pressure levels on impact for all measurements were calculated for the different frequencies and are displayed for impact on the landing for walking and running in Figure 4.6. The background noise is shown as a reference.

4. Case study measurements

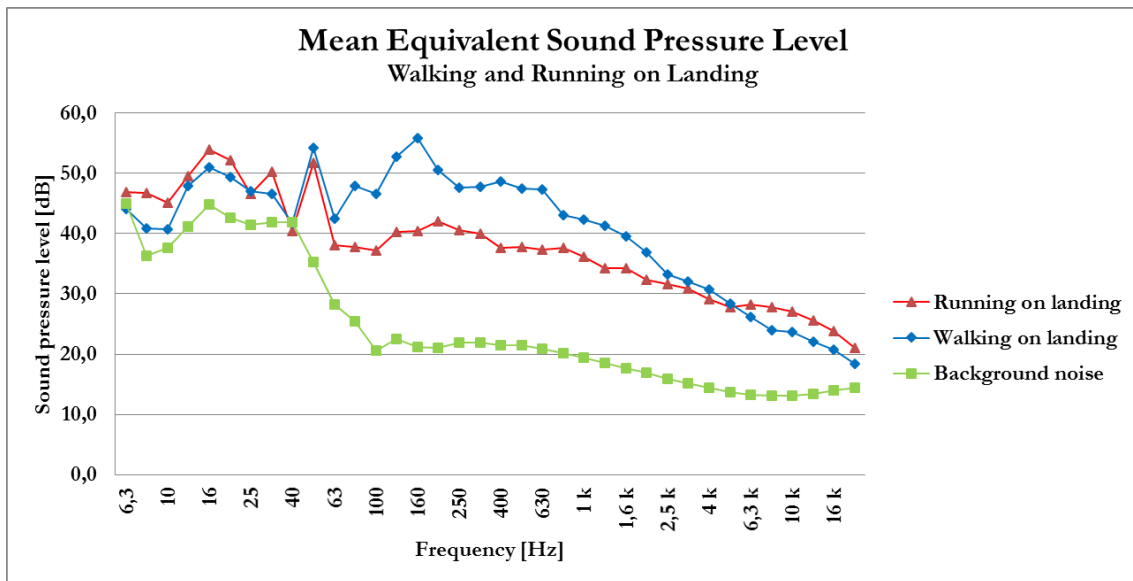


Figure 4.6. Mean equivalent sound pressure level on impact for walking and running on landing.

The mean equivalent sound pressure levels on impact for all measurements were calculated for the different frequencies and are displayed for the tread for walking and running in Figure 4.7.

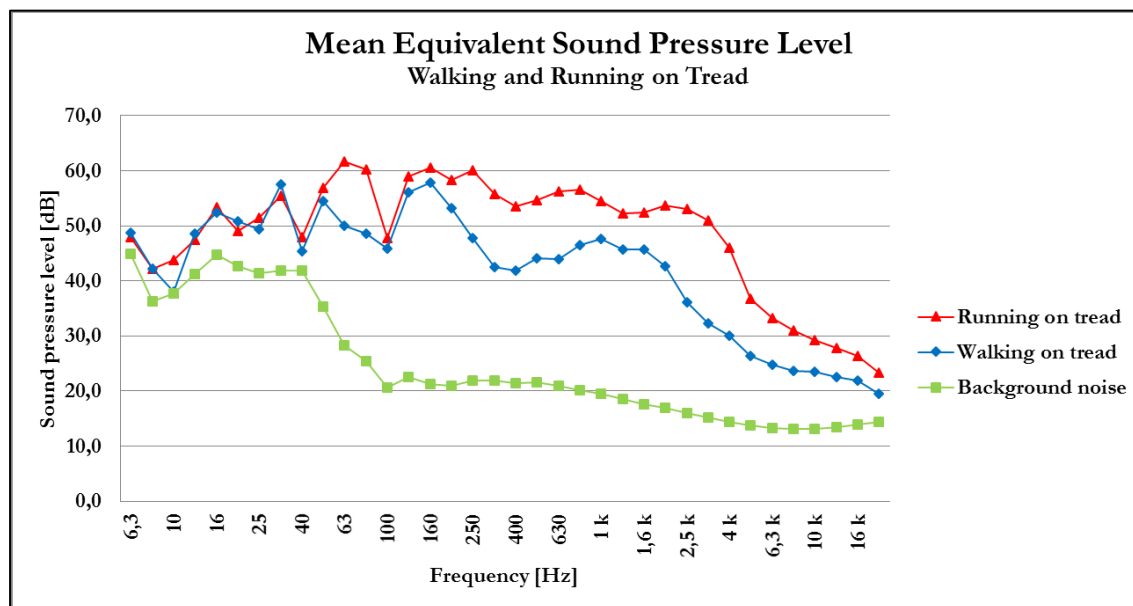


Figure 4.7. Mean equivalent sound pressure level on impact for walking and running on tread.

The values of the identified peaks in the figures above are presented in Table 4.1.

Table 4.1. Identified peaks on impact in sound pressure level analysis.

[dB] [Hz]	Walking on slab	Background Noise	Running on landing	Walking on landing	Running on tread	Walking on tread
16		44,7	54	50,9	53,4	52,4
25	50,4					
31,5			50,3	46,6	55,5	57,6
40		41,8				
50	42,1		51,7	54,2		54,4
63					61,6	
80				47,9		
125	36,4		40,2	52,7	59,0	56,1
160			40,4	55,8	60,6	57,9
200			42,1	50,5	58,3	53,1
250	39,2		40,6	47,6	60,0	47,7
315			40,0	47,7	55,8	
400				48,6	53,4	

Furthermore, the mean sound pressure level from the whole measurement sequence, i.e. not on impact but from walking or running from one floor to the next and back, was calculated. The sound pressure level is presented in Figure 4.8.

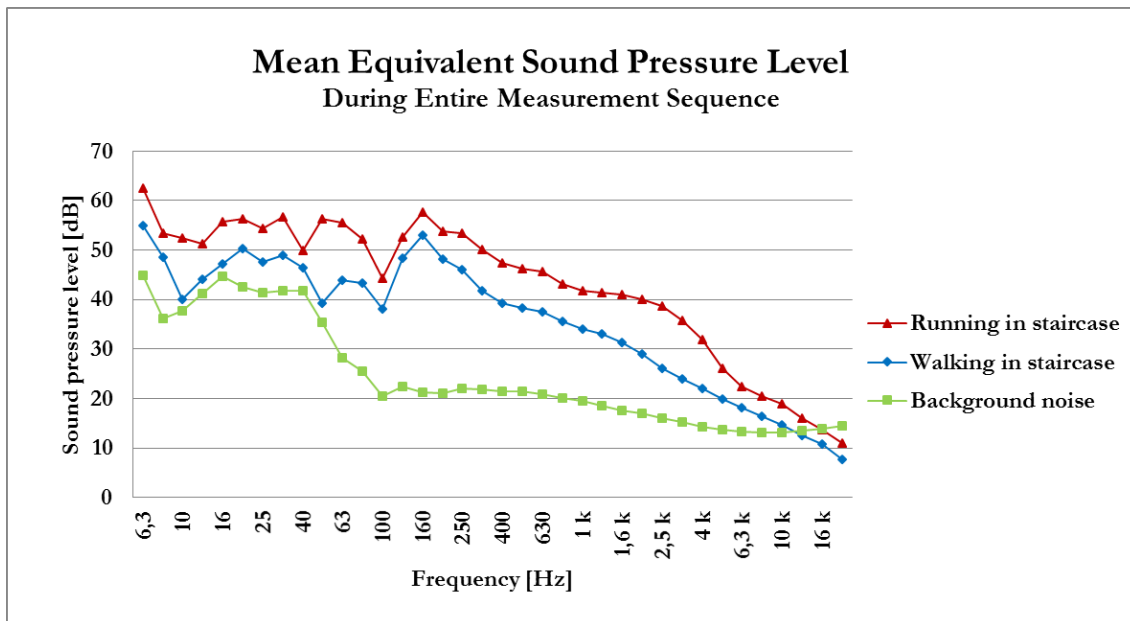


Figure 4.8. Mean equivalent sound pressure level for entire measurement sequence.

In Table 4.2 the A-weighted values are shown as mean equivalent sound pressure levels both during the whole measurement sequence and for impacts while running and walking.

4. Case study measurements

Table 4.2. A-weighted sound pressure levels.

The whole sequence	$L_{eq,A}$ [dB]	Standard deviation [dB]
Walking	46,8	0,74
Running	55,0	0,96
On impacts		
Walking on landing	55,3	5,14
Running on landing	45,9	1,59
Walking on tread	55,1	2,28
Running on tread	64,3	2,24

4.2. Natural frequency measurements

Vibration measurements were performed using *Briuel & Kjaer's Pulse* system. From the finite element modeling of the staircase, see chapter 5.1, natural frequencies and corresponding mode shapes had been calculated using a model with many degrees of freedom. The natural frequencies found in the FE-model were studied. The natural frequencies and their corresponding mode shapes gave an idea of in which points the vibration measurements should be done. A set of mode shapes, see Table 4.3, with different type of motions which the measurements should be able to mirror, was selected.

Table 4.3. Chosen mode set.

Natural frequency [Hz]	Type of motion
88,49	First bending mode in lower landing plate.
92,821	First bending mode in lower landing plate and torsion in flight.
122,65	Second bending mode in lower landing plate.
133,16	First bending mode in upper landing plate.
134,54	Second bending mode in lower landing plate, first bending mode in lower landing beam, torsion in flight.
140,35	Second bending mode in lower landing plate, first bending mode in lower landing beam, torsion in flight, first bending mode in treads.
160,26	Third bending mode in lower landing plate, torsion in flight, first bending mode in treads.
172,82	Third bending mode in lower landing plate, first bending mode in tread.
180,95	Third bending mode in landing and first bending mode in tread.
183,59	Second and third bending mode in landing, first bending mode in tread.
190,93	Third bending mode in lower landing plate, first bending mode in treads, second bending mode in upper landing.
194,85	Third bending mode in lower landing plate, first bending mode in treads, second bending mode in upper landing.
206,34	Third bending mode in lower landing plate, first and third bending mode in treads.
216,41	Third bending mode in lower landing plate, first bending mode in treads.

Applying more measurement points will give a more accurate analysis. By decimating the FE-model an initial measurement model was created, see Figure 4.9.

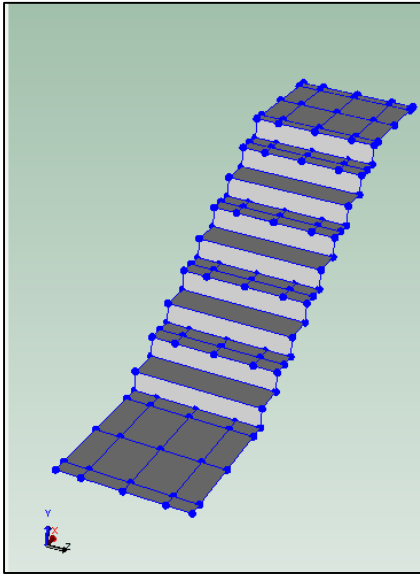


Figure 4.9. Initial decimated model.

The decimation of the model was checked against the selected set of mode shapes using a modal analysis feature in *Pulse Reflex*. The initial decimated measurement model was able to describe most of the mode shapes, but was lacking in detailing to describe more complex mode shapes at higher frequencies. In Figure 4.10 and Figure 4.11 examples of good and bad recognition in the decimated model are shown. The full comparison is displayed in Appendix A1.

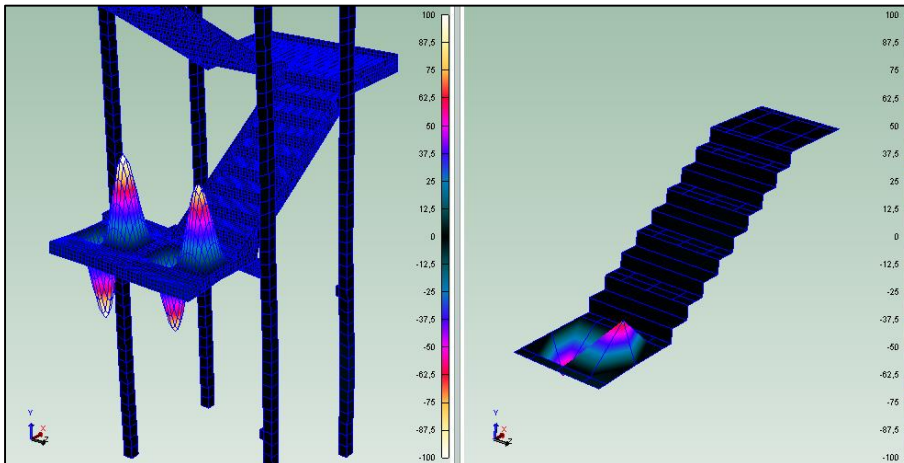


Figure 4.10. Mode shape of natural frequency 122,65 Hz. Left: FE-model. Right: Second bending mode in the landing well recognized by the decimated model.

4. Case study measurements

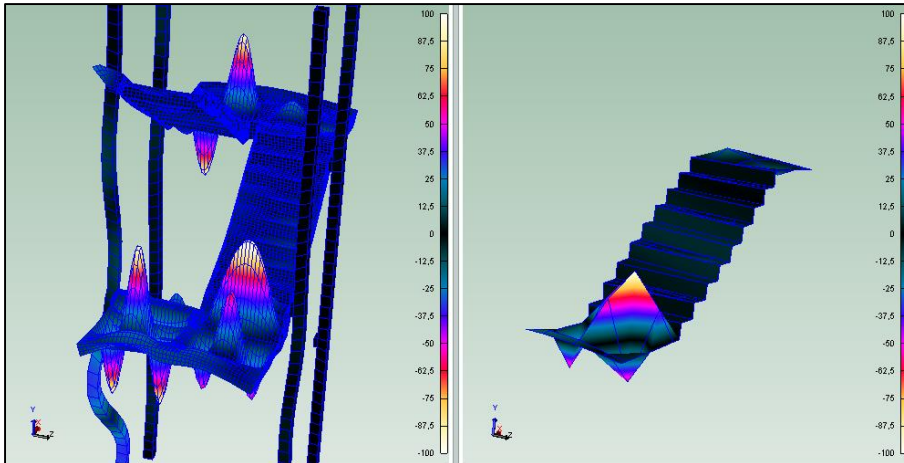


Figure 4.11. Mode shape of natural frequency 180,95 Hz. Left: FE-model. Right: The initial decimated model fails to recognize the third bending mode in the landing due to the dominant deflection in the first tread.

After the comparison was made the decimated model was reconstructed to better recognize the mode shapes of the natural frequencies, see Figure 4.12. Measurement points were added in the lower landing and one of the risers to manage the more complex mode shapes.

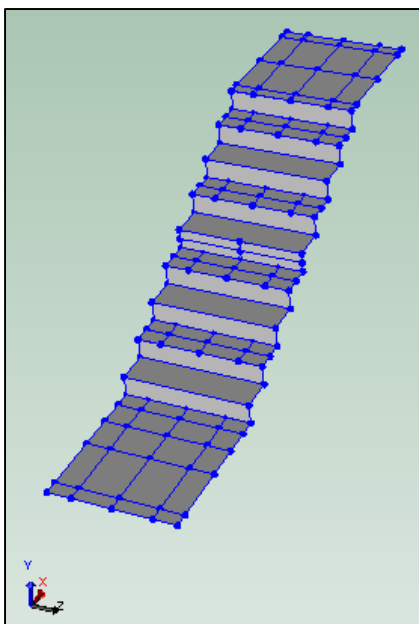


Figure 4.12. Reconstructed decimated model.

The model now contained 37 degrees of freedom, DOFs, and was put into *Pulse Labshop* where the data was recorded during the measurement. Two accelerometer positions were used according to Figure 4.14. The red arrows show impact directions when they are not vertical. In all the DOFs an impulse loading was applied through an impact hammer, see Figure 4.13. By recording the loading in the impact hammer and responses in the accelerometers from each hit, the natural frequencies triggered during the measurement could be found.



Figure 4.13. Setup during impact hammer test with marking for hitting points.

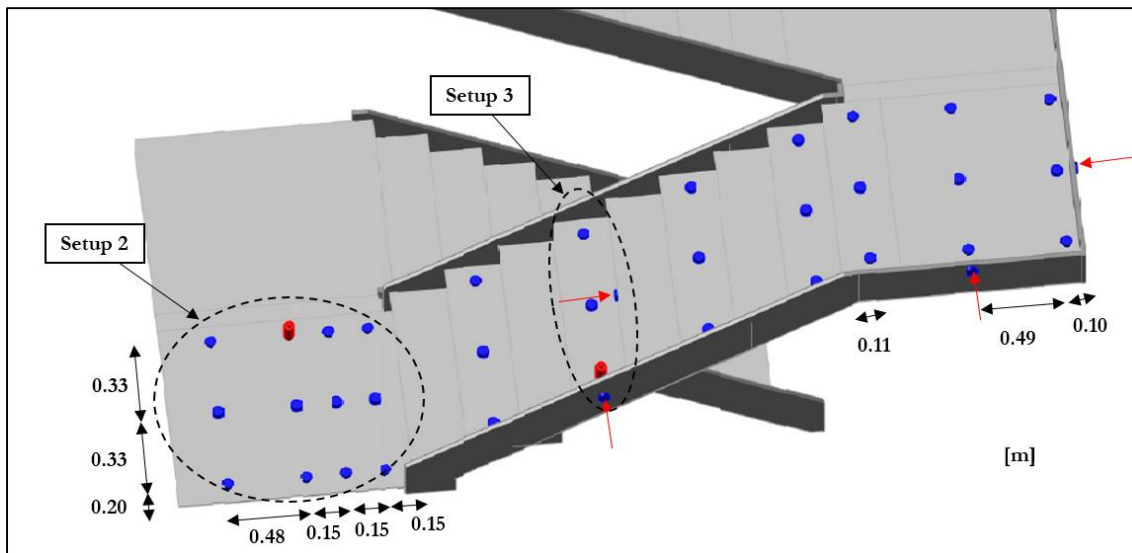


Figure 4.14. Setups during impact hammer test. Blue marker for impact position and red for accelerometer.

Three test setups were performed. The first one was a global test containing all 37 DOFs from the decimated model. The second and third setups were performed locally, one on the lower landing and one on the middle tread. The local tests were added to get more data in areas that the natural frequencies implied were probable to vibrate rather easily. It was established that the coherence in the measurements generally was close to one between 50 and 400 Hz, meaning that the measurement should be rather good in this interval.

Once the measurements were performed the data was exported from *LabsHop* to *Reflex* where the software detected natural frequencies and corresponding mode shapes that occurred during the measurements. The natural frequencies, divided into the frequency intervals: 0-30, 30-100, 100-170, 170-240, 240-330 and 330-400 Hz, were detected using a polynomial curve fit with 40 iterations per frequency interval.

4. Case study measurements

The mode shapes were identified visually and are presented in Appendix A2. The general result of Setup 1 is presented in Table 4.4. The results from the local setups, Setup 2 and 3, confirm the mode shapes in Table 4.4, but were too coarse to give any additional information.

Table 4.4. General result of Setup 1.

Setup 1	
Frequency span [Hz]	Type of motion
47,333-86,523	Global motion in landings and treads. Mainly motion in landings depending on mode.
91,911-189,461	Mainly plate motion in landing, some motion in treads.
190,887-229,034	Plate motion in landings and treads.
231,107-320,861	Plate motion in landings and treads. Possibly second or third bending mode in treads.
338,387-374,531	Complex plate motion in landings and treads.

4.3. Vibration analysis with walking and running

Vibration measurements were performed using *Brüel & Kjær's Pulse* system. Measurements were performed both with excitation due to walking and running. As for the sound pressure level analysis the results are strongly dependent on the person using the staircase due to walking style, mass, type of shoes etc. Also the definition of running and walking can differ from person to person. Therefore the conditions were kept unchanged throughout the tests.

The *Pulse Labshop* software was used combined with mounted accelerometers spread out on the staircase surfaces for collecting the data from each excitation event. During the measurement two tri-axial accelerometers, in two different setups, were mounted on the surfaces, as shown in Figure 4.15. The measurement positions were chosen to be able to detect motion in both landing and tread, since these were the most commonly found points of motion in chapter 5.1. The accelerometers had to be placed outside the normal walking path to maintain natural usage of the staircase. For each setup five measurements for walking and five measurements for running were performed.

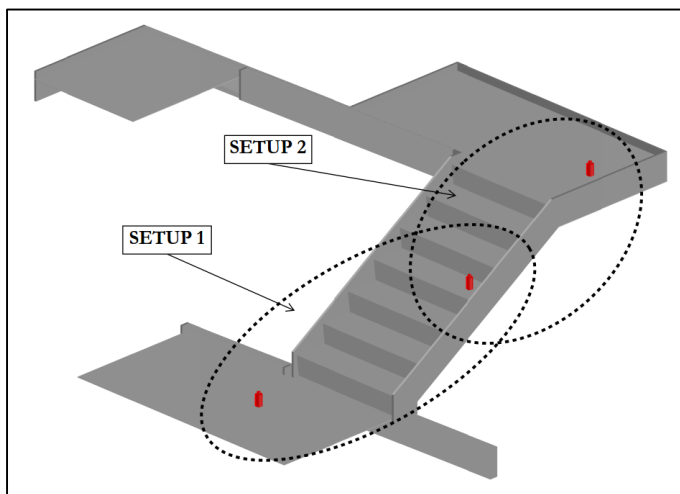


Figure 4.15. Placements of accelerometers during experiments.

Running and walking were tested in the two setups to give an idea of the actual forces that can be applied to the staircase on a regular basis and their respective responses. The setups generated information of the actual response in the staircase in the lower landing, the middle tread and the upper landing. In Figure 4.16 the responses in all three directions are displayed, and it is clear that the response is significantly larger in the vertical direction (y-axis) than the in-plane directions. Therefore only the vertical direction was considered during the analysis.

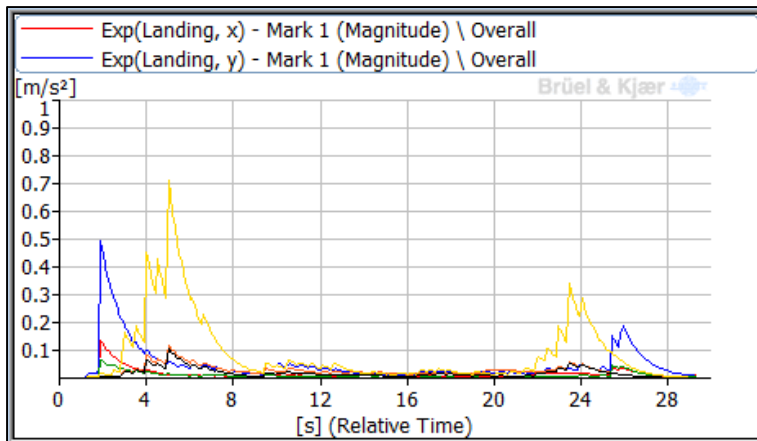


Figure 4.16. Response in all three directions.

In Figure 4.17 the response in the vertical direction during one of the walking measurements is displayed. In the figure it is visible that the maximum response, when walking occurred close to the accelerometers on the way up, reached about $0,7 \text{ m/s}^2$ in the tread and $0,5 \text{ m/s}^2$ in the landing.

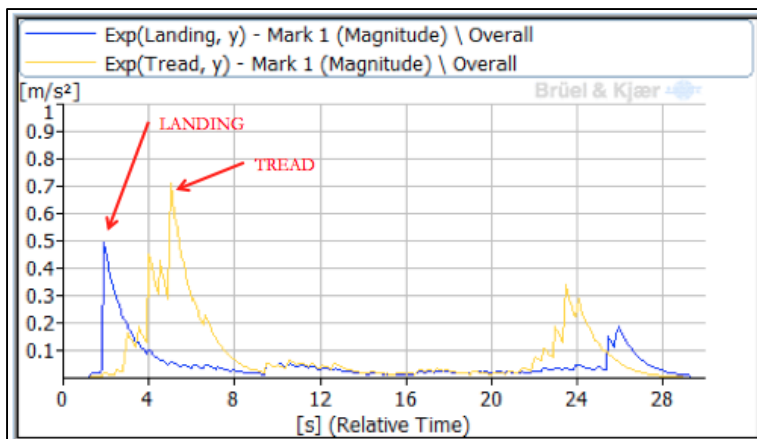


Figure 4.17. Response in the vertical direction.

By performing a Fourier Transformation, the frequency of the response at different times can be observed. From the maximum response in the lower landing, four major frequency peaks lower than 400 Hz are visible, see Figure 4.18. 400 Hz is the limit for detected sound during the sound measurement in chapter 4.1. Strong vibrations occurred in the frequencies: 124, 186, 266 and 366 Hz.

4. Case study measurements

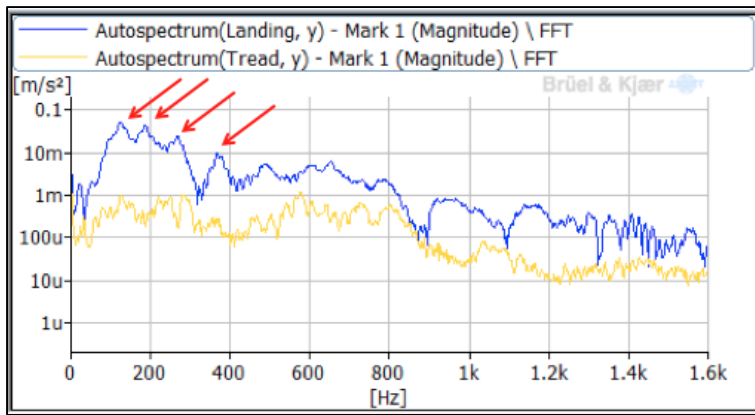


Figure 4.18. Frequency peaks in the lower landing in logarithmic scale.

In the same manner a FFT was performed at the maximum response in the tread, see Figure 4.17. Once again the response peaks in the FFT lower than 400 Hz were identified, see Figure 4.19. The Frequency peaks marked in the figure are: 234, 284 and 354 Hz.

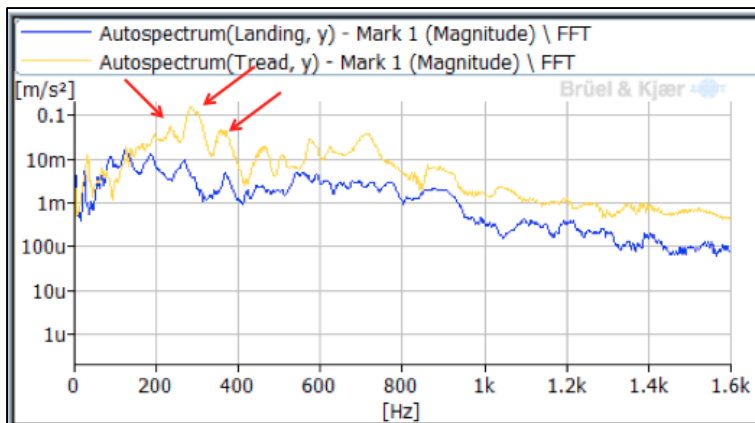


Figure 4.19. Frequency peaks in the tread in logarithmic scale.

This procedure was performed for all the measurements of both test setups. The mean response in the FFT functions were calculated and normalized for comparability for the different measurement positions and are displayed in Figure 4.21 for walking and Figure 4.23 for running in Setup 1. Note that the acceleration in landing after impact was lower in amplitude compared to the acceleration on impact. The normalized function makes it possible to see at which frequencies the structure continues to vibrate after impact.

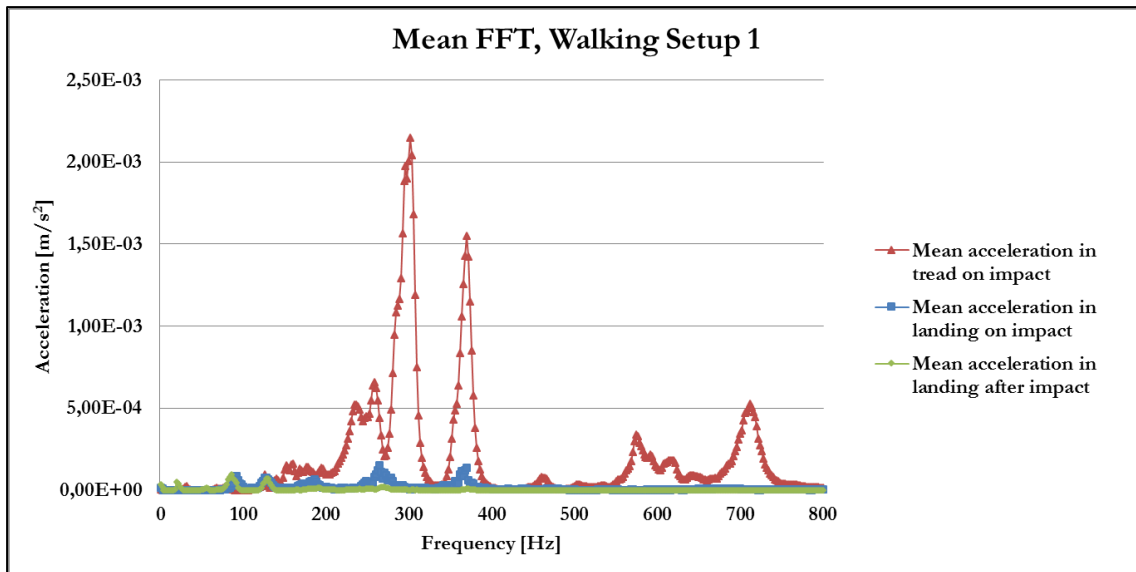


Figure 4.20. Mean FFT for walking, setup 1.

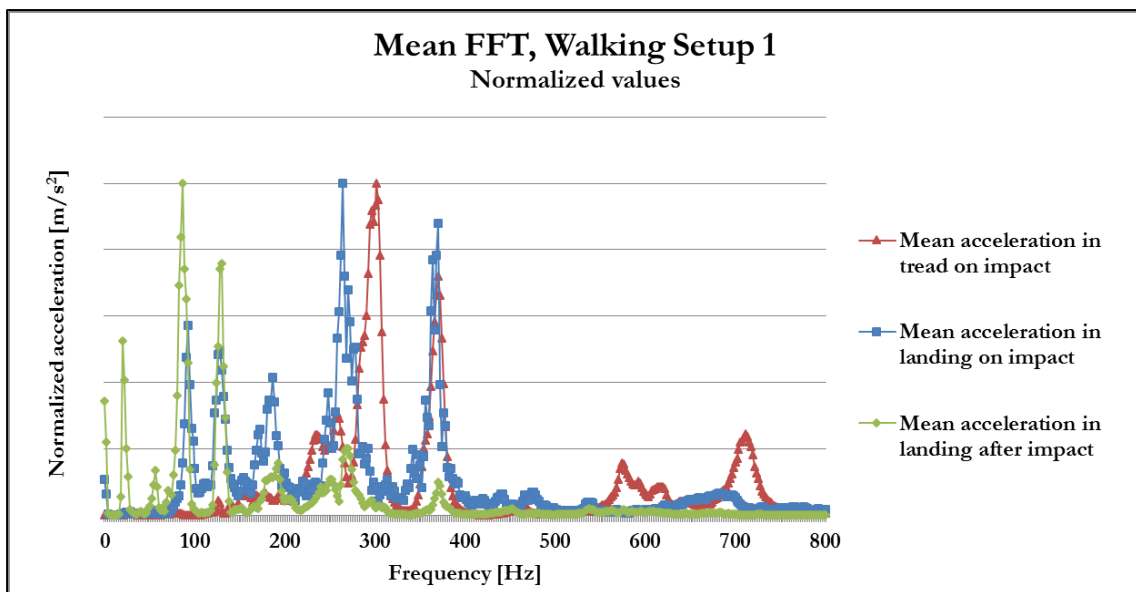


Figure 4.21. Normalized mean FFT for walking, setup 1.

4. Case study measurements

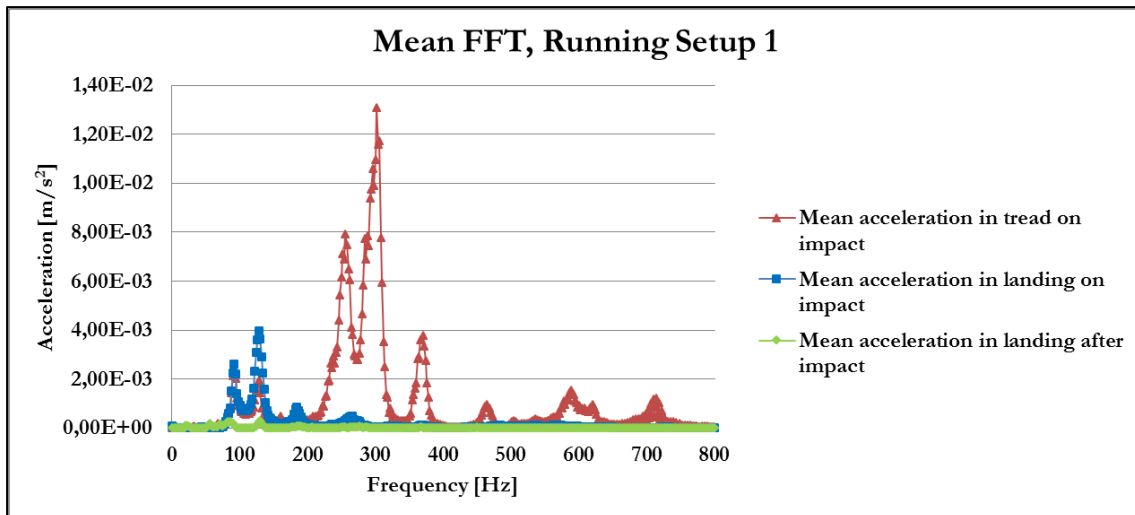


Figure 4.22. Mean FFT for running, setup 1.

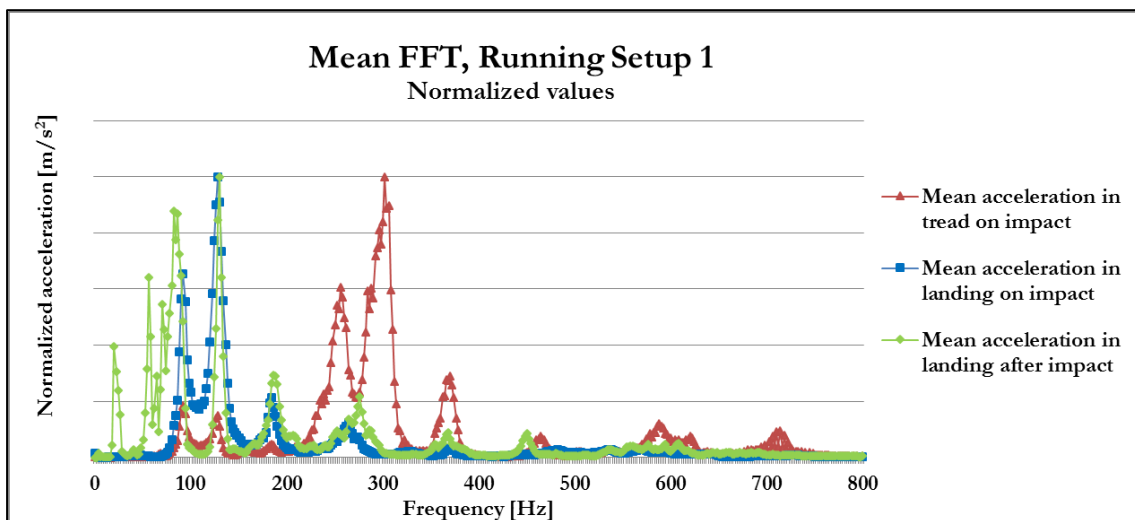


Figure 4.23. Normalized mean FFT for running, setup 1.

In the same manner the data from Setup 2 was investigated. The mean values and summaries with normalized response are shown in Appendix B2. Numerous peaks were identified in the different measurements and through the mean value the strongest frequency peaks could be identified. These are shown in Table 4.5 and resembling frequency peaks in different measurements and measurement points are marked with same color in the table.

Table 4.5. Identified frequency peaks from mean values of walking and running.

[Hz]	Walking			Running			
Point Setup	Tread (on impact)	Landing (on impact)	Landing (after impact)	Tread (on impact)	Landing (on impact)	Landing (after impact)	
Setup 1			20			20	
			56			56	
						70	
						82	
			92	86	92	92	86
			128	130	128	128	130
			186	192		184	186
	236						
	256	264	270	256	264	276	
	302			302			
370	370		370	370	368		
			464			452	
Setup 2			18			24	
			32	32		32	
						42	
			90			88	
			126	132		128	132
	160						
	192				188		
		202			206	196	
					238		
	278	286				284	
300			302	300			
368	368		368		360		
		384			380	388	
		450		464	446		

To compare perceived with measured values while walking and running, RMS-values were calculated according to chapter 2.2.1. This is shown in Figure 4.24 and Figure 4.25 for Setup 1 in the frequency span 1-80 Hz. This was done for one measurement in each case.

4. Case study measurements

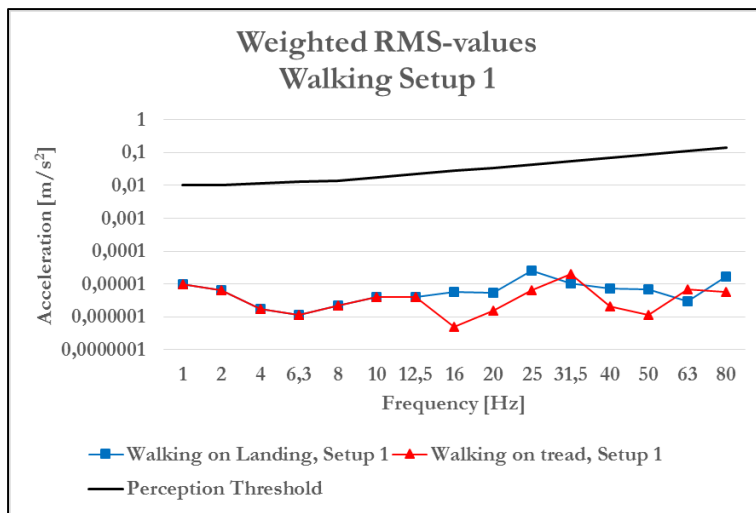


Figure 4.24. RMS-values compared to the perception threshold according to ISO 2631-1 while walking in the staircase.

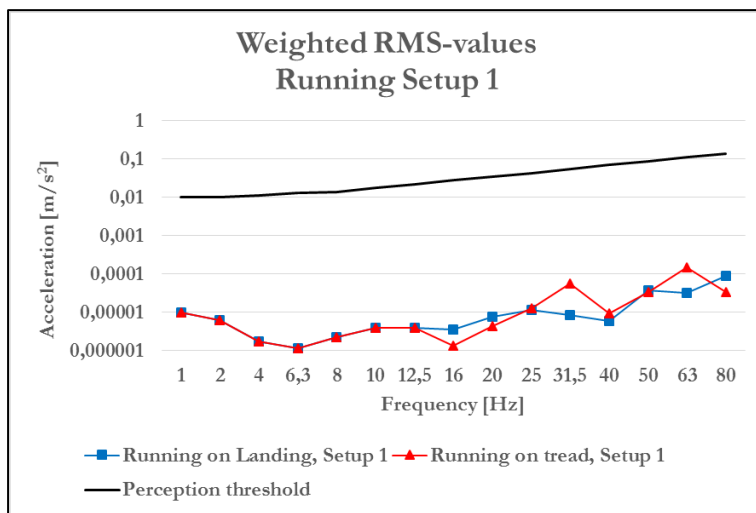


Figure 4.25. RMS-values compared to the perception threshold according to ISO 2631-1 while walking in the staircase.

4.4. Vibration analysis with impact hammer

The response in the staircase due to hammer impact was investigated by performing a number of hits with an impact hammer and recording its force and the response in some points of the staircase. This was done by using the *Pulse Labshop* software. Frequency responses in landing and tread from three different impact positions were investigated.

The responses in the lower landing and the middle tread were checked for three different impact positions, namely: center of the middle tread, center of the largest free-spanning plate in the lower landing and above one of the beams in the lower landing. These positions were chosen after performing the impact hammer test in chapter 5.1 and were identified as impact positions creating different sounds and giving sufficient response in the accelerometers. These points also define some typical walking parts of the staircase. As shown in chapter 4.3 the main accelerations occurred in the vertical direction which is why this was the only direction investigated.

The results from the first response checked, center of the middle tread, are visualized in Figure 4.26.

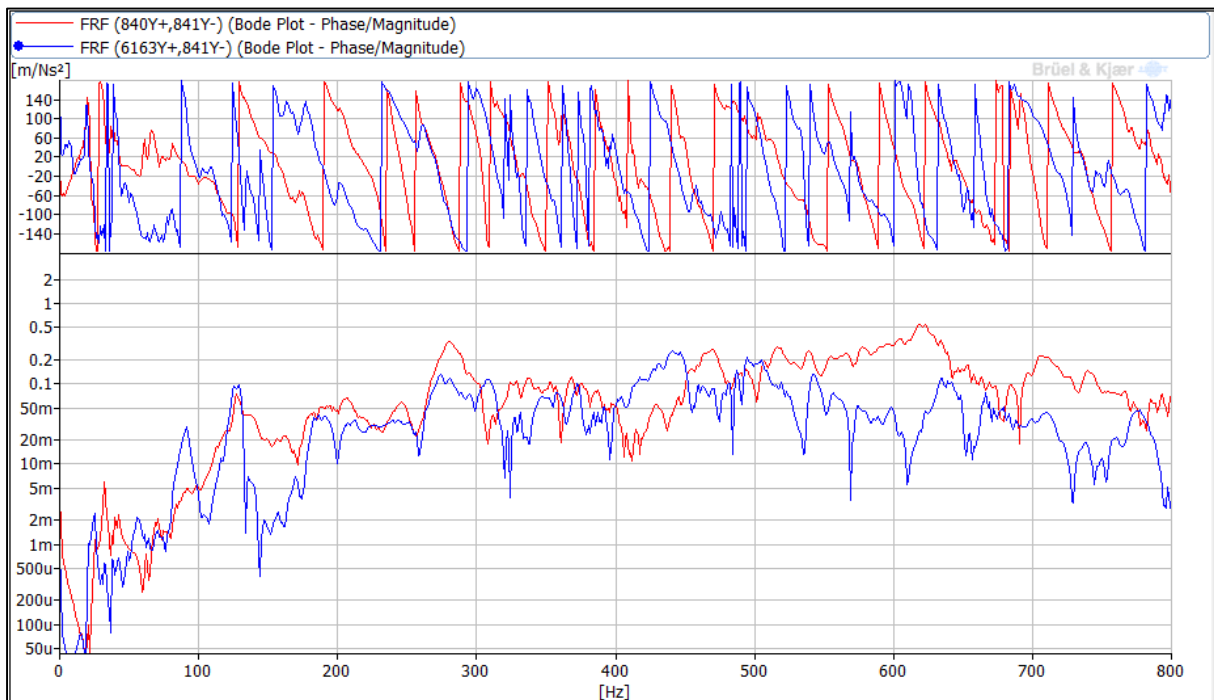


Figure 4.26. Response in landing (blue) and tread (red) when hammer impact on tread.

The results from the second response checked, center of the largest free-spanning plate in the lower landing, are shown in Figure 4.27.

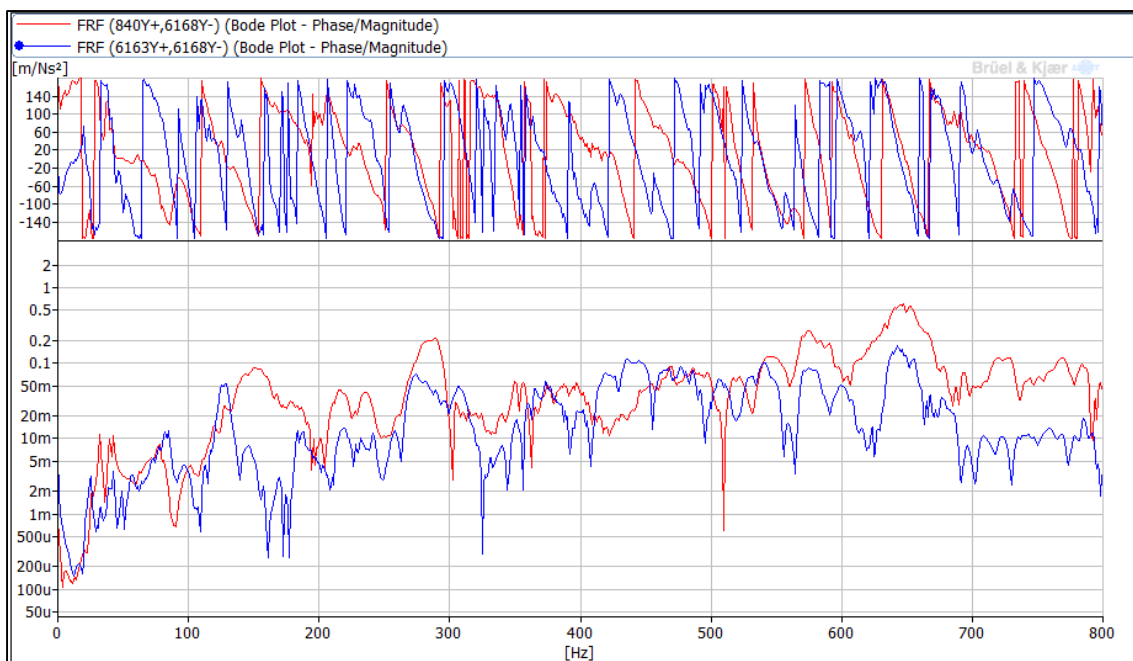


Figure 4.27. Response in landing (blue) and tread (red) when hammer impact on mid-span landing.

The third response that was investigated was with impact above one of the beams in the lower landing and the results are shown in Figure 4.28.

4. Case study measurements

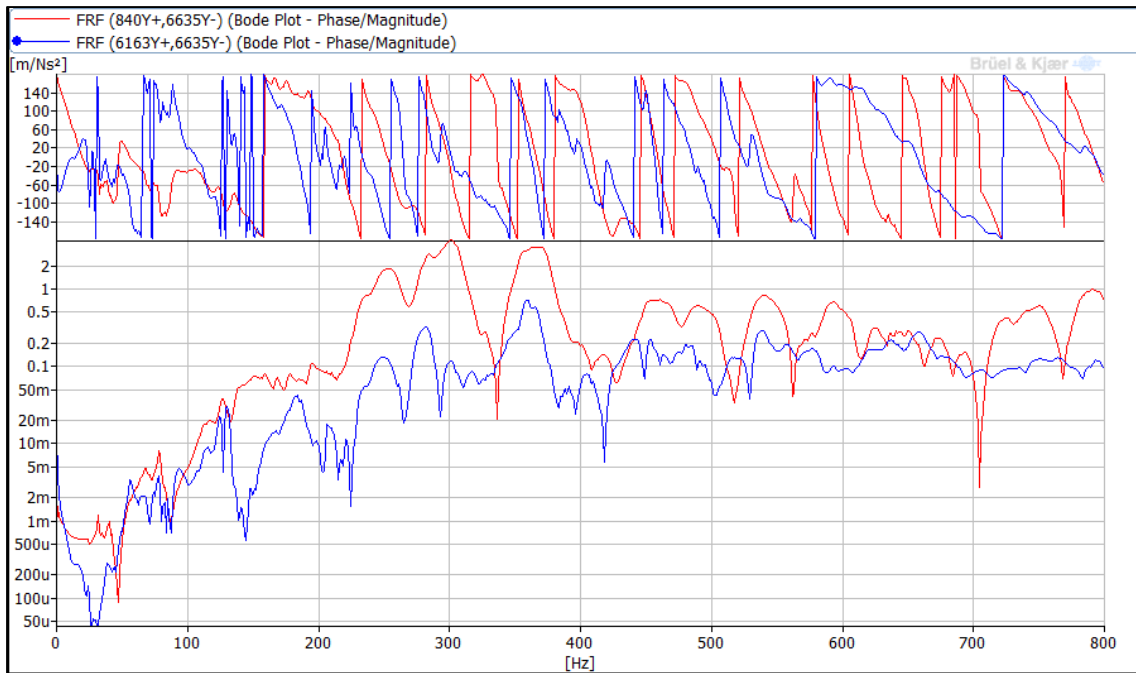


Figure 4.28. Response in landing (blue) and tread (red) when hammer impact on beam landing.

To validate the results from the measurements the coherence for each measurement was studied. The coherence gives a value between zero and one for each frequency where one means full coherence and a valid measurement and zero means uncertain measurement data due to some sort of disturbance. The coherence for each measurement are shown in Appendix D1. In Figure 4.29 an example of the coherence for measurement in tread with impact on the tread is presented. According to the figure the coherence was low for frequencies below 24 Hz. There were also some disturbances around 360 and 410 Hz.

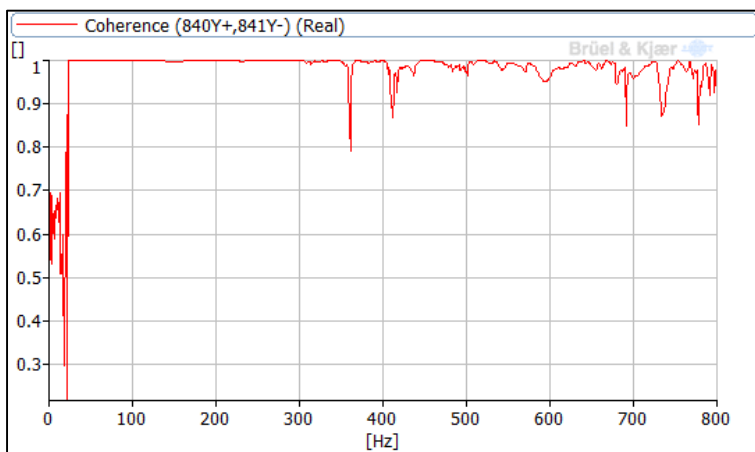


Figure 4.29. Coherence for measurement in tread with impact on tread.

The response peaks found in the figures are displayed in Table 4.6 below and resembling frequency peaks in different measurements and measurement points are marked with same color in the table.

Table 4.6. Response peaks in vibrations due to hammer impact.

[Hz]			
Impact on	Tread	Landing (Mid-span)	Landing (Beam)
Response In			
Tread	32	32	
		78	78
	128		
		151	160
	204	217	
	245		252
	281	290	
			302
	368	350-400	364
469	469	459	
Landing	25	25	
	56	42	57
	91	82	
	129	128	129
	187	184	183
		219	249
	273	274	281
	307		
	373	374	360
441	436	453	

4.5. Vibration propagation analysis

Propagation to adjacent elements can be of interest in dynamic analyses. To investigate how much the vibrations in the staircase spread to the connected slab a simple response test was conducted. By placing one accelerometer on the stringer of the staircase, one on the column and one on the slab the different responses due to hammer impacts were measured. In this case the slab and the columns were the only adjacent elements connected to the staircase. If the staircase would have been situated closer to the laboratory facilities a more detailed propagation analysis would be necessary.

One accelerometer was positioned on the stringer of the staircase to measure the motion of the whole flight (not only local motion in the tread), another was placed on one of the columns and the last one was placed approximately 30 cm into the adjacent slab, according to Figure 4.30 and Figure 4.31. The accelerometers were set to measure the vertical direction.

4. Case study measurements

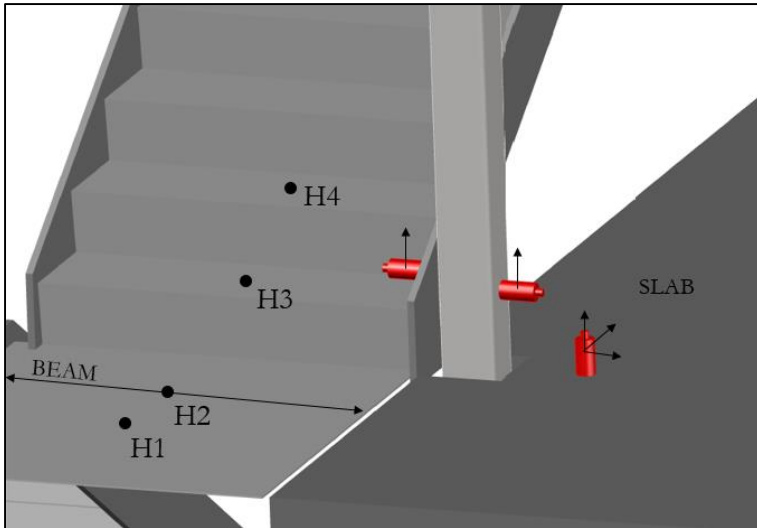


Figure 4.30. Placement of accelerometer (red) with arrows showing measurement directions and hammer impact positions during propagation tests.



Figure 4.31. Placements of accelerometers. Left; accelerometer on column and slab. Right; accelerometers on stringer.

Four different hammer impact positions were used during the test and the responses in the accelerometers were registered using the *Pulse Labshop* system. The hammer positions, called H1-H4 are shown in Figure 4.30.

From the measurements made in this analysis two types of result can be investigated. The first one was rather straight forward and showed the response in the different accelerometers for a certain hammer impact. This analysis showed how much of the vibration propagated from one point to another. In Figure 4.32 the impact and response from impact position H1 is presented.

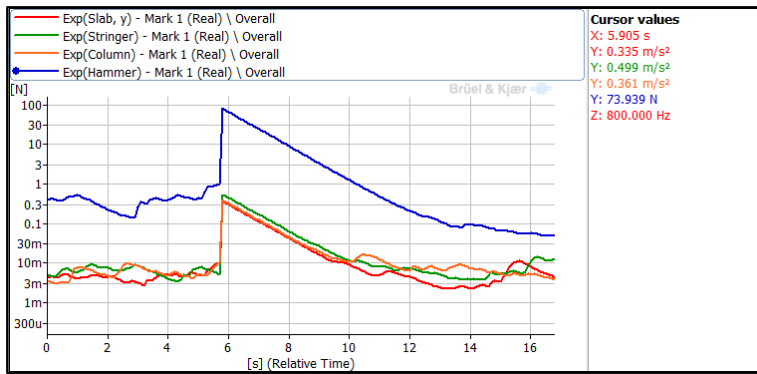


Figure 4.32. Impact and response from impact position H1.

The results of this analysis from all the impact positions are presented in Table 4.7. The amplitude of the hammer impact is also presented as a reference. In the last column of the table the transmissibility ratio between the response in the slab and the stringer is calculated showing what percentage of the response that spreads to the slab from the stringer.

Table 4.7. Propagation results.

Measurement pos. / Impact pos.	Stringer [m/s ²]	Column [m/s ²]	Slab [m/s ²]	Hammer [N]	Slab/Stringer [%]
H1	0,499	0,361	0,335	73,939	67
H2	0,714	0,469	0,297	106,758	42
H3	0,705	0,461	0,385	87,394	55
H4	0,883	0,612	0,364	80,180	41

The second analysis consisted of a FFT analysis of the response in the stringer and the slab. In this analysis the frequency peaks could indicate what frequencies the slab was extra sensitive to. The result from the different impact positions are presented in Figure 4.33, Figure 4.34, Figure 4.35 and Figure 4.36.

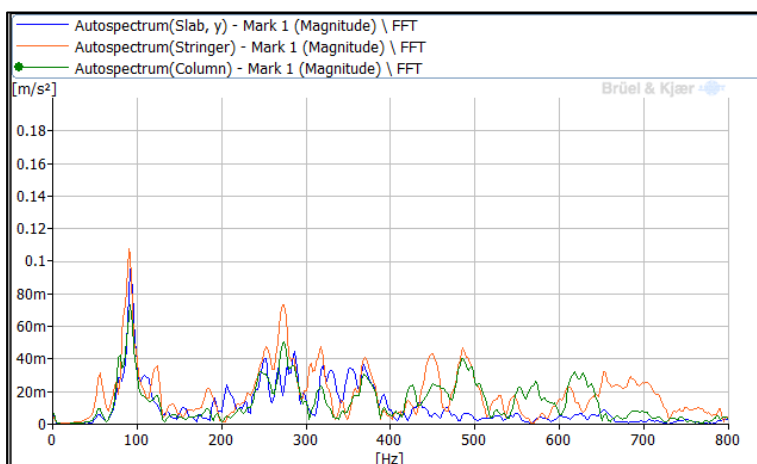


Figure 4.33. FFT for impact position H1.

The largest peaks in the slab with impact position H1 occurred at about 90, 250 and 280 Hz.

4. Case study measurements

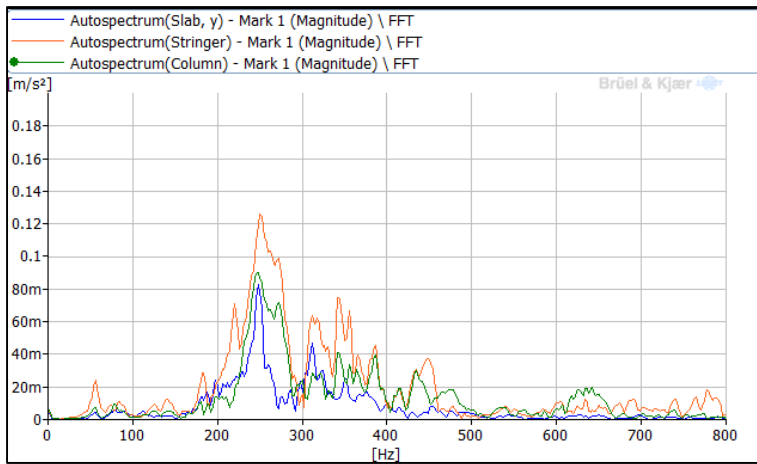


Figure 4.34. FFT for impact position H2.

The largest peaks in the slab with impact position H2 occurred at about 250 and 310 Hz.

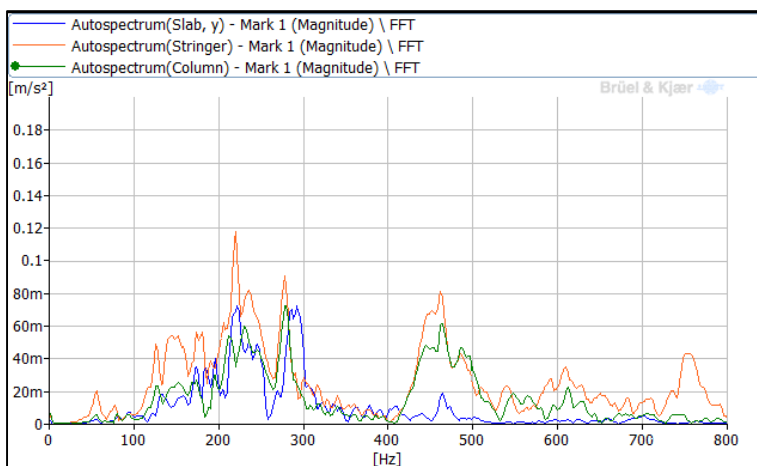


Figure 4.35. FFT for impact position H3.

The largest peaks in the slab with impact position H3 occurred at about 230 and 280 Hz.

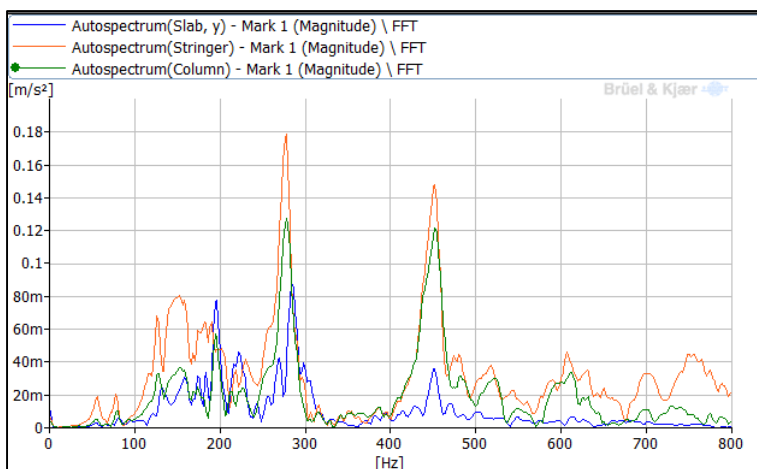


Figure 4.36. FFT for impact position H4.

The largest peaks in the slab with impact position H4 occurred at about 200 and 280 Hz.

4.6. Reverberation time measurement

The reverberation time in the surrounding room was measured using noise excitation with loudspeakers. The measurement was performed in octave band. The loudspeakers emitted a constant pink noise, i.e. noise with a wide frequency spectrum, until the response reached steady state. The loudspeakers then were shut off and the reverberation time was registered. Measurements were performed in seven different combinations of speaker and microphone positions. The different positions are shown in Figure 4.37. During the test two measurements were made for each position to improve the collected data. In Table 4.8 the measurement data is displayed and in the bottom the mean value for each octave band is calculated, which also is visualized in Figure 4.38. The measurement positions were constructed so that measurement 1.2 means loudspeaker position 1 and microphone position 2 and so on. The standard deviation shows how certain the mean value was in each octave band.

Table 4.8. Reverberation time for different measurements and frequencies.

Measurement [s]	Frequency [Hz]						
	63	125	250	500	1k	2k	4k
1.1	0,87	0,69	0,51	0,45	0,35	0,48	0,52
1.1	0,81	0,58	0,61	0,44	0,34	0,44	0,53
1.2	1,10	0,44	0,59	0,32	0,46	0,54	0,56
1.2	0,86	0,58	0,39	0,42	0,44	0,49	0,60
1.3	0,87	0,43	0,50	0,52	0,39	0,47	0,49
1.3	0,72	0,62	0,53	0,49	0,37	0,49	0,52
2.4	0,80	0,67	0,46	0,42	0,43	0,42	0,49
2.4	0,87	0,65	0,53	0,51	0,45	0,42	0,44
3.5	0,62	0,51	0,57	0,44	0,38	0,46	0,49
3.5	0,73	0,52	0,44	0,49	0,38	0,45	0,51
3.6	0,87	0,72	0,60	0,46	0,45	0,46	0,50
3.6	0,90	0,65	0,55	0,36	0,50	0,49	0,52
3.7	0,58	0,66	0,58	0,53	0,40	0,45	0,46
3.7	0,88	0,68	0,64	0,51	0,37	0,44	0,48
Mean	0,83	0,59	0,52	0,44	0,41	0,47	0,51
Standard deviation	0,12	0,09	0,07	0,06	0,05	0,03	0,04

4. Case study measurements

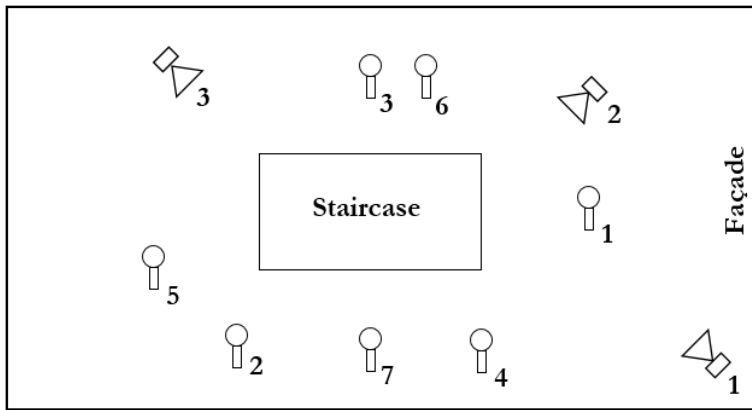


Figure 4.37. Positions from reverberation time measurements.

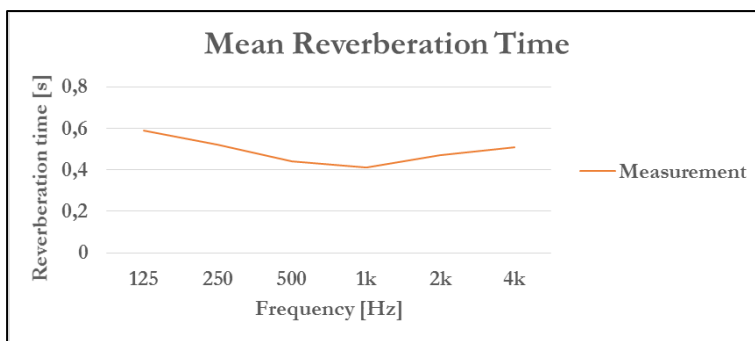


Figure 4.38. Mean reverberation time from measurement.

The mean value for reverberation time through measurements was 0,5 s.

5. Case study modeling

In this chapter the results from modeling are presented.

5.1. Natural frequency analysis

In this part the FE-modeling, aimed at analyzing the structure and its probable behavior, is presented.

5.1.1. FE-Model

Some choices regarding the scope of the models were first made. A model is always a simplification of the reality and it was therefore necessary not to make too big simplifications and risking that crucial information regarding the results is lost in the model. In this part the delimitation of the modeled structure and its boundary conditions are discussed.

Connection to slab

The steel columns surrounding the staircase are connected to the slab on each floor. The floors are generally hollow core concrete elements placed on steel beams around the staircase and along the façade. The connections from the columns to the slab are made through steel plates welded onto the steel beams, making it reasonable to consider them as fixed together. However the building itself can be flexible in the horizontal direction since there are no stabilizing walls in connection to the staircase in the office space, see Figure 5.1.

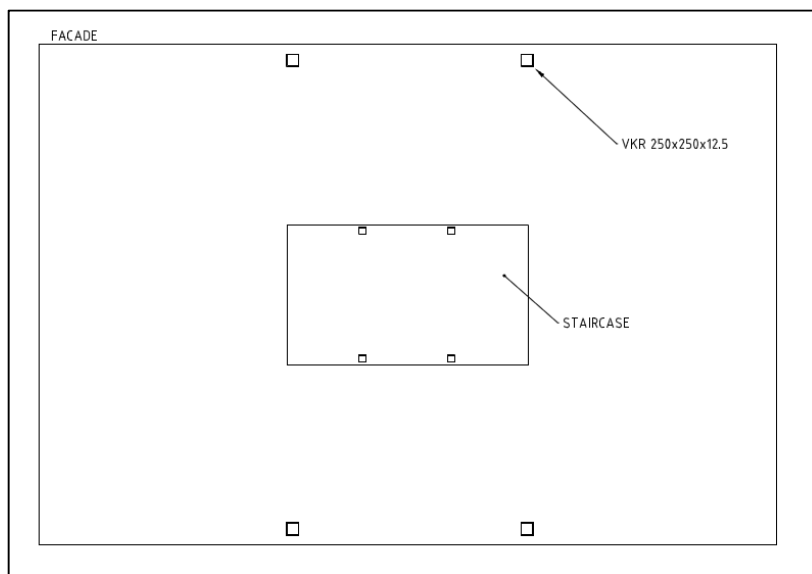


Figure 5.1. Floor plan describing the columns on the floor.

By considering the slab as stiff but the columns, VKR 250x250x12.5, as flexible in bending the stiffness in the horizontal direction could be calculated. By studying the column as in Figure 5.2 the bending stiffness could be approximated as a spring stiffness, k , to be put in the model.

5. Case study modeling

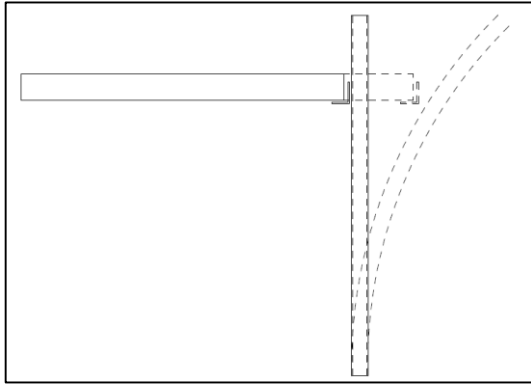


Figure 5.2. Flexibility in column and stiffness in the slab in the horizontal direction.

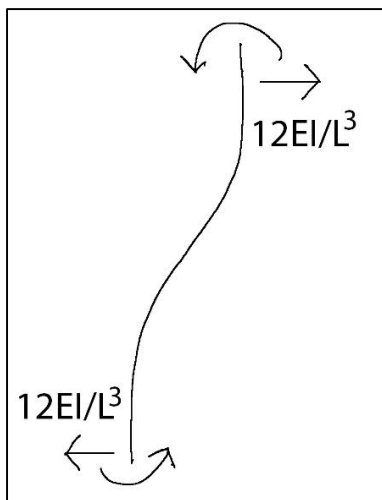


Figure 5.3. The stiffness of a column.

The bending stiffness in a column can be described as in Figure 5.3 i.e. the added stiffness to every column is $24EI/L^3$. By inserting the properties of the VKR 250x250x12.5 the bending stiffness could be calculated as

$$\frac{12EI}{L^3} = 3,1 \frac{MN}{m}$$

where

$E = 210GPa$ is Young's modulus.

$I = 10915 \cdot 10^4 mm^4$ is the moment of inertia.

$L = 4,5 m$ is the height between slabs in the building.

By putting the bending stiffness of the columns equal to a spring stiffness, and applying it to the columns surrounding the staircase, the boundary condition towards the connecting slabs could be modeled more properly.

Steel connections

When deciding which type of connection should be used between the different objects in the modeling programs it is important to understand what the chosen connections imply. When connecting two plate elements, for example the tread and the stringer, a pinned connection implies

that the stringer will not rotate when applying a load to the tread as opposed to the rigid connection that would make the stringer rotate with the tread, as displayed in Figure 5.4.

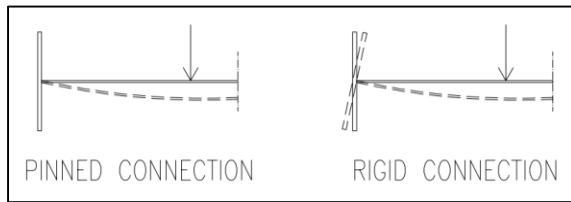


Figure 5.4. Pinned and rigid connections.

Since the parts of the staircase either were welded together or put together with large bolt plates the connections between elements were considered as rigid connections in the models.

Scope of model

Only one flight of the staircase was analyzed. To make the behavior of the investigated flight as accurate as possible, without modeling the entire staircase, the model was limited to two landings and three flights where the landings and the middle flight should be able to imitate the response of the considered part of the staircase. By using an expanded model, i.e. not just modeling the studied area, many of the boundary issues will be resolved in the studied area.

5.1.2. Natural frequencies from FE-model

FE-modeling was carried out in *Abaqus* and the model was analyzed to extract natural frequencies and vibration modes.

A model was composed in *Abaqus* using *Quad-dominated* shell elements. All the components were put together using rigid ties to imitate the welded connections. The natural frequencies from zero to 400 Hz were requested in the output, according to the frequencies of interest in chapter 4.1. Since walking can set the structure into motion in many different directions a triaxle analysis of natural frequencies was performed. The natural frequencies and their mode shapes were visually studied and commented, see Appendix A1. In Table 5.1 a summary of the type of motions in different frequency spans are presented.

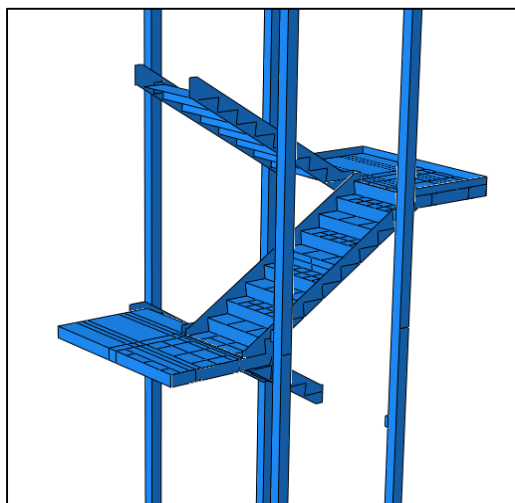


Figure 5.5. ABAQUS model.

5. Case study modeling

Table 5.1. Summary of type of motion in different natural frequency spans.

Natural frequency [Hz]	Type of motion in landings	Type of motion in flight
23,449-71,329	Global motion in landings as cantilevered from flight.	Some bending.
83,012-89,684	First bending mode in lower landing plate.	-
92,821-105,57	First bending mode in lower landing plate.	Torsion in flight.
110,68-129,24	Second bending mode in landing plate.	Some bending/torsion
131,30-134,54	First bending mode in upper landing plate.	-
138,74-167,58	First or second bending mode in landing plate.	First bending mode in treads
172,06-201,34	Second or third bending mode in lower landing plate.	First bending mode in treads
203,54-219,63	Second or third bending mode in lower landing plate.	First or second bending mode in treads.
220,81-254,47	Bending short direction landing plate. Third bending mode landing plate.	First or second bending mode in treads.
255,57-265,89	Bending short direction landing plate.	Second bending mode in treads and risers.
267,07-296,54	Third or fourth bending mode or bending short direction in landing plate.	First or second bending mode in treads. Second or third bending mode in risers.
298,91-318,43	Third or fourth bending mode or bending short direction in landing plate.	Third bending mode in treads.
318,95-390,46	Third or fourth bending mode or bending short direction in landing plate. Torsion in beams under landing.	Third bending mode in treads and/or risers.
391,18-399,48	Third or fourth bending mode or bending short direction in landing plate. Torsion in beams under landing.	Twisting of stringers. Third bending mode in treads and/or risers.

5.2. Reverberation time analysis

Acoustical simulation was carried out to investigate the environment around the staircases with respect to reverberation time. From the reverberation time a lot can be said about sound absorption in the room from a global standpoint. For the room acoustic simulation the software *CATT* (demo version) was chosen. For the room acoustic simulation the different surfaces in the room were investigated and the acoustic properties of materials were determined. The model was constructed by defining all the different surfaces in the room with a sketching program, *Google Sketchup 3D*, and then importing it to *CATT*. The demo version of *CATT* comes with a limitation of maximum 50 surfaces, which means that the number of surfaces used in the model must be fewer than 50. Thus a couple of simplifications were made to satisfy this limitation:

- The staircase was modeled without treads and risers i.e. a singular surface between landings.
- The layout of the office doors, inner windows and walls were connected in such a way that fewer single surfaces were used. The doors were assumed to be closed.
- No furniture was put in the model.
- Since the staircase runs through all levels in the building it connects the level above and the level below with the room evaluated. Therefore two surfaces were placed above and below the staircase to limit the model, see green surface in Figure 5.6.

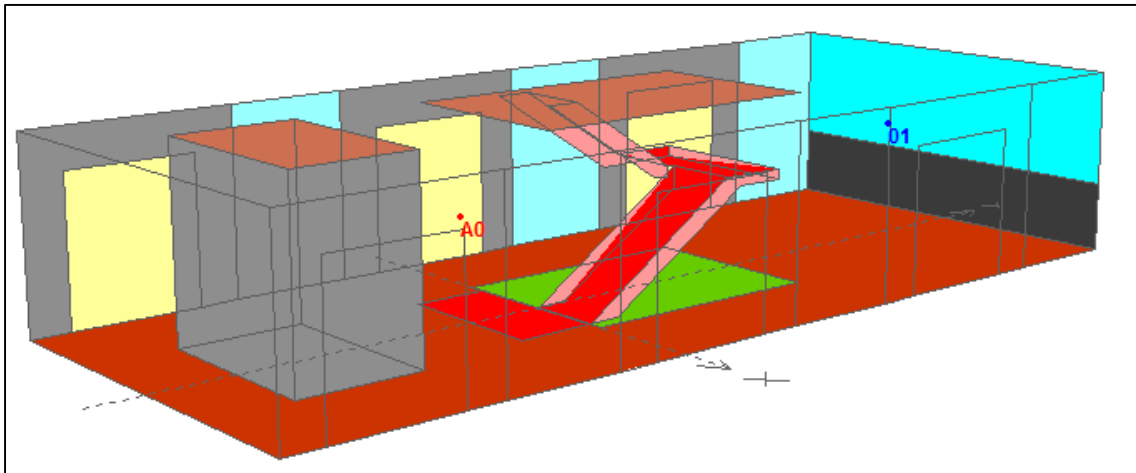


Figure 5.6. CATT-model.

The different materials used in the simulation and their sound absorption properties are shown in Table 5.2 and Table 5.3.

5. Case study modeling

Table 5.2. Materials and surfaces used in CATT.

Location	Color (+CATT label)	Material name
Windows (offices)	Light blue (H04)	Closed double glass
Windows (facade)	Blue (H01)	Windows with 3-4 mm "thermo" glass
Wall (facade)	Medium grey (007)	2 layers 5/8" <i>CertainTeed</i> gypsum board both sides 2 layers 2½" <i>CertainTeed AcoustaTherm</i> batts
Walls (offices)	Light grey (004)	1x13 mm gypsum, with mineral wool (100 mm from <i>Danogips</i>)
Doors (offices)	Yellow (E04)	Solid timber door
Floor	Brown (B06)	Carpet, thin, cemented to concrete
Ceiling	Light Brown (B08)	50 mm thick, 200 mm from ceiling
Kitchen area	Dark grey (D25)	1x13 mm gypsum, with mineral wool (100 mm from <i>Danogips</i>)
Staircase (bare)	Pink (A04)	Steel decking
Staircase (w. carpet)	Red (A01)	Carpet, thin, cemented to concrete
Above Staircase*	Light Green (F03)	Approximated absorption area for the empty void and the office level above
Below staircase**	Green (F06)	Approximated absorption area for the empty void and the cellar below
Absorbent	Brown (B12)	<i>Ecophon Master B</i>
* The office area above investigated room ** The cellar space below the investigated room		

Two tests were carried out in the reverberation time simulation. The first test was carried out to evaluate how the empty voids above and below the staircase influence the reverberation time. This test was performed assuming the volumes to behave as surfaces and testing different properties of these surfaces. To enclose the possible outcomes and investigate how the voids affect the properties of the entire room the absorption coefficients were set to either the lowest (1 %) or the highest (99 %) over the complete frequency span. This test was performed for random receiver and source positions in the simulation to visualize the effect of the voids. The results are shown in Figure 5.7. Since the simulation was performed regardless of furniture and other objects in the room and the difference between maximum and minimum absorbents as voids was small the maximum value was used henceforth. This was later verified through comparison with measurements and more extensive simulation, see discussion in chapter 6.1.6.

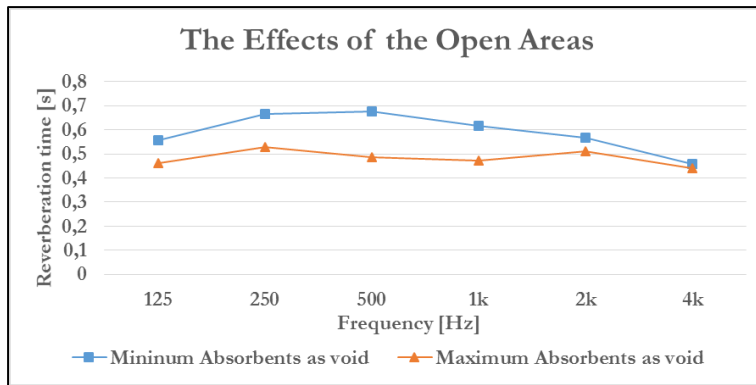


Figure 5.7. Effect of the voids.

Table 5.3. Absorption coefficients (α) of different materials in CATT.

Abs. coefficients	Frequency [Hz]					
	125	250	500	1k	2k	4k
Location						
Windows (offices)	0,10	0,04	0,03	0,02	0,02	0,02
Windows (facade)	0,10	0,07	0,05	0,05	0,02	0,02
Wall (facade)	0,4	0,55	0,63	0,73	0,67	0,74
Walls (offices)	0,30	0,12	0,08	0,06	0,06	0,05
Doors (offices)	0,14	0,10	0,06	0,08	0,10	0,1
Floor	0,02	0,04	0,08	0,20	0,35	0,40
Ceiling	0,49	0,63	0,83	0,97	0,99	0,96
Kitchen area	0,30	0,12	0,08	0,06	0,06	0,05
Staircase (bare)	0,13	0,09	0,08	0,09	0,11	0,11
Staircase (w. carpet)	0,02	0,04	0,08	0,20	0,35	0,40
Above Staircase*	0,99	0,99	0,99	0,99	0,99	0,99
Below staircase**	0,99	0,99	0,99	0,99	0,99	0,99
Absorbent	0,2	0,75	1,00	1,00	0,95	0,95

* The office area above investigated room
** The cellar space below the investigated room

Further simulations were done by calculating the reverberation time in two cases, before and after the extra absorbents were placed to prevent the existing sound problem, as described in chapter 3.2. This was done by using different receiver and source positions throughout the room to get a reliable result of how the sound will behave in reality. Six variations of receiver and source positions was used as shown in Figure 5.8 below and the mean reverberation times is shown in Figure 5.9. Receiver position 1-3 corresponds to source position 1 and 4-6 to source position 2.

5. Case study modeling

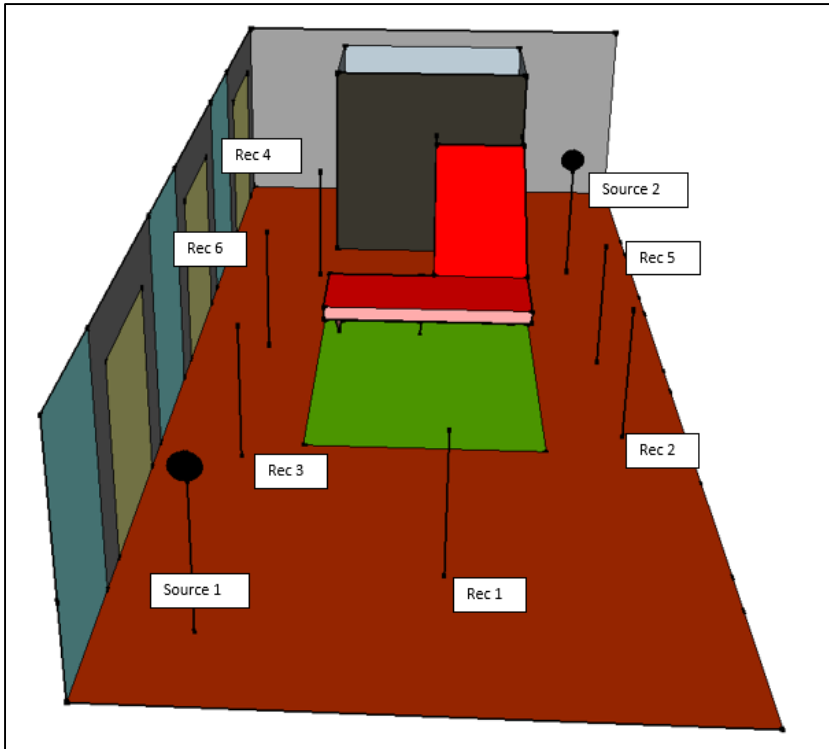


Figure 5.8. Source and receiver positions in reverberation time tests.

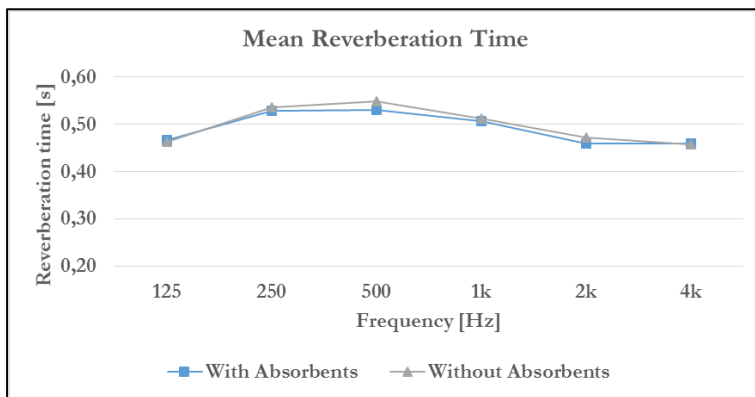


Figure 5.9. Mean reverberation time from CATT simulation.

The mean value for reverberation time calculated through simulations was around 0,5 s.

5.3. Verification of FE-model

To assure that the model was accurate enough the response in the model was tested and compared to the experiments. This led to an adjusted model that was used when modeling possible adjustments in chapter 6.3.1. The same impulse loading as in the experiment was applied, using the recorded data of the impulse. The damping could be varied to achieve a response similar to the one in the experiments. The measured response from a specific impact hammer hit on the middle tread is shown in Figure 5.10.

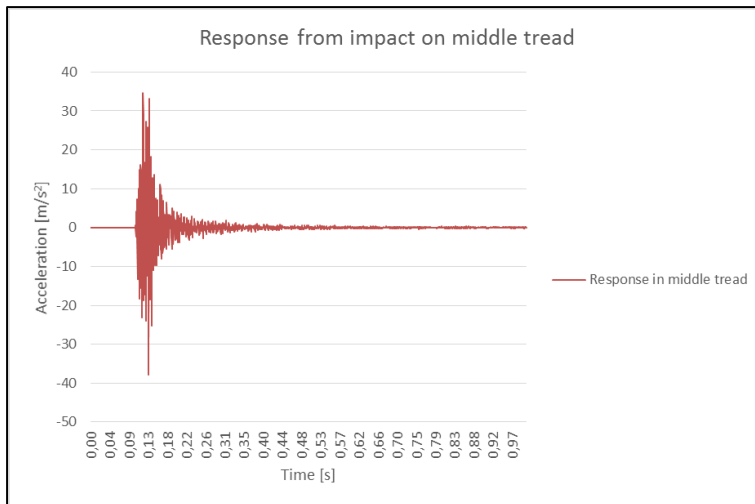


Figure 5.10. Measured response in middle tread.

In the natural frequency measurement, chapter 4.2, a damping ratio was recorded with the *Pulse* system. To find a suitable value for damping this damping ratio is plotted, see also Appendix A2. A curve was fitted to the plot by choosing values for the Rayleigh damping coefficients, α and β . After suitable coefficients had been chosen a reference force with a known response from measurements were tested in *Abaqus*. A response check could validate the chosen damping coefficients by regarding amplitude and decay in the measured acceleration.

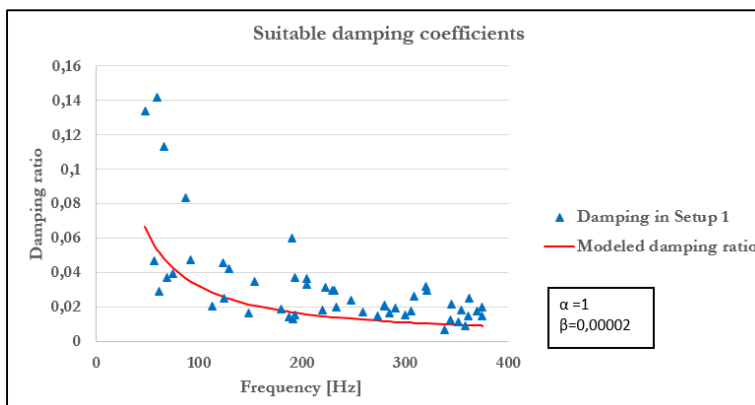


Figure 5.11. Determining suitable damping coefficients.

The measured damping coefficients are typically around 2-3 %, see Figure 5.11, which corresponds well with the theory in Appendix E1. Some of the lower frequencies had damping ratios above 10 % which for a welded structure seem quite high. Therefore it was reasonable to model the damping lower than the measured ratio in the lower frequencies.

As shown in the response graph in Figure 5.10 the amplitude of the response initially was about 30-35 m/s^2 . By applying Rayleigh damping with the chosen damping ratio according to Figure 5.11 the response in the same point reached an amplitude of 32 m/s^2 .

Having a model that responded with the same amplitude as the real staircase now produced a possibility to model the result of any alterations made on the staircase. These possible adjustments are further discussed and modeled in chapter 6.3.1.

5.4. Verification of reverberation simulation

To improve the acoustic model the absorptions coefficients were altered until the reverberation in the model matched the measured. This was done to get more accurate results in the investigation of possible measures to improve the room, see chapter 6.3.2. The ceiling was chosen to be altered since it is evenly spread throughout the room and had high enough absorption coefficients to alter. This was done by first calculating the total absorption area in the model and then subtract the old modeled absorption area for the ceiling using Sabine’s formula in each octave band. Then the measured reverberation was used to calculate the ceilings new absorption area.

Sabine’s formula (see also chapter 2.2.4)

$$T = 0,163 \cdot \frac{V}{A} \quad (\text{Eq. 2-13})$$

$$A = \sum S_x \cdot \alpha_x \quad (\text{Eq. 2-14})$$

This was used in the model and new simulations were made to check the reverberation time. Small adjustments were made in addition so that the modeled reverberation corresponded even better to reality. The final reverberation is shown below in Figure 5.12 below.

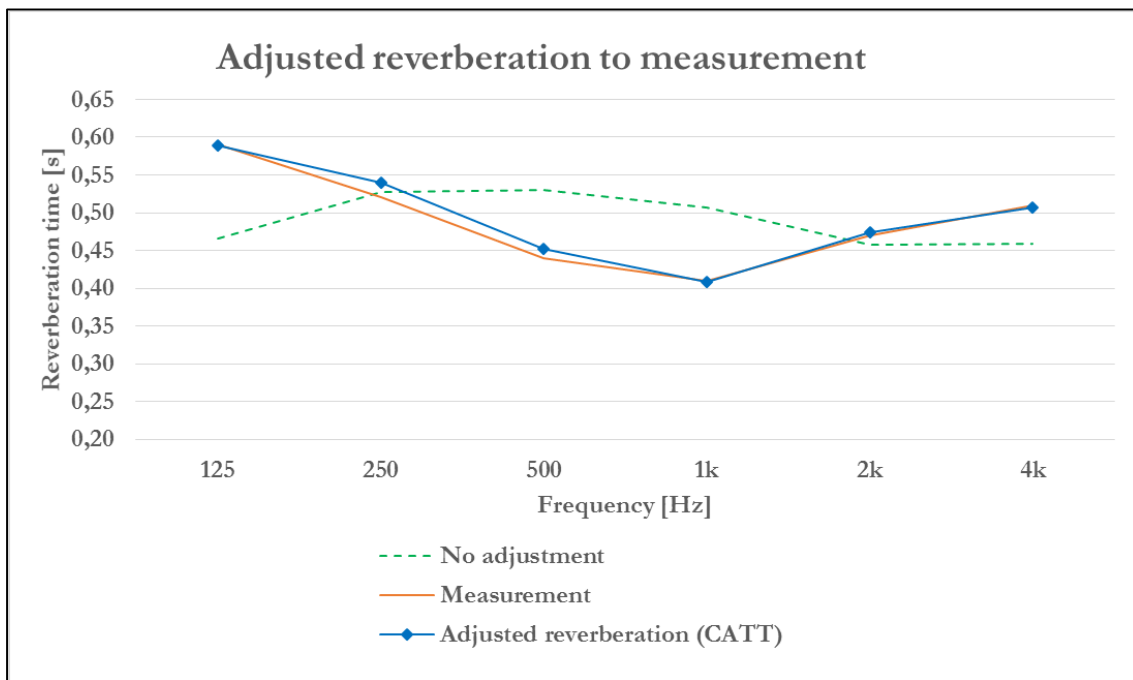


Figure 5.12. The final adjusted reverberation in the modeled compared to the measured.

6. Case study discussions and conclusions

In this chapter the discussions and conclusions ultimately leading to a proposal of suitable adjustments for the staircase are carried out.

6.1. Discussions

In this chapter the results from each analysis will be discussed and compared to lead to conclusions regarding the case study.

6.1.1. Sound pressure level analysis

During the measurements it was observed that when walking and running in the staircase all hearable sound either came from the footstep or the staircase, i.e. no other adjacent structure created sound that was detectable. The background noise measurement revealed a peak in the background noise around and below 50 Hz, possibly caused by some sort of installation, see Figure 6.1. Since the background noise and walking on slab were loud below 50 Hz these frequencies were not considered problematic in the staircase. The background noise was identified during the measurements from various installation in the room. Apart from the installations, background noise could originate from other activities in the building, since the measurement were performed during regular office hours.



Figure 6.1. Possible installation causing background noise.

It is visible in the graphs that the sound pressure levels during walking were similar for both treads and landings. During running on the other hand the sound pressure level from the treads were higher than during walking. This probably was caused by a harder impact in each step while running upwards on the treads as compared to running forward on the landings. From Figure 4.6 showing the sound from walking and running on the landing it is visible that walking gives a louder sound than running, especially in the higher frequencies.

The sound pressure level measurement during walking and running on the landing showed three clear frequency span peaks: 15-30, 40-60 and 100-250 Hz, see Figure 4.6. The first span also could be seen in the background noise, although not as loud. In Figure 4.5 it is visible that the first and the second span occurred during walking on the slab as well. The second span was notably louder

6. Case study discussions and conclusions

during walking and running in the staircase than on the slab. Therefore these frequency spans probably did not originate from the staircase vibration but rather from the sound of footsteps on the surface. The maximum sound pressure level on the landing was 55,8 dB and occurred at 160 Hz, this was achieved through walking.

In the same manner as for the landing the sound measurements from walking and running on the tread could be divided into frequency span peaks: 15-40, 50-80 and 125-250 Hz. As for the landing case the first frequency span could be explained by comparing to walking on slab in Figure 4.5. In the second span the lower part also could be explained by the same comparison, but it also contained higher frequencies that possibly originated from staircase vibrations rather than the sound of walking. The measurements showed that the sound from walking and running on the treads mainly occurred in the highest frequency span, 125-250 Hz. The maximum sound pressure level on the tread was 61,6 dB and occurred at 63 Hz, this was achieved through running. The peak while walking on slab occurred at around 50 Hz and it is possible that these frequencies were enhanced due to harder walking impact on the tread. Other loud frequencies were 160 and 250 Hz which might be more interesting since these did not occur during walking on slab. The maximum sound pressure level achieved through walking was 57,6 dB and occurred at 160 Hz.

Comparing the sound pressure level from walking and running with the Wisner curves, see chapter 2.2.2, gives an idea of the disturbance level from the sound source. The comparison in Figure 6.2 shows the sound pressure level on impact and it is visible that sound from impact on landing was in Zone 1, i.e. minimal disturbance to the environment. Impact from running on tread and the higher frequencies in walking on tread were in Zone 2, meaning that they caused more disturbance to the environment. According to the Wisner curves sound in Zone 1 will not cause more disturbance than for intellectual work to be carried out. In Zone 2 routine work will not be disturbed but tasks that require a high level of thinking might be difficult.

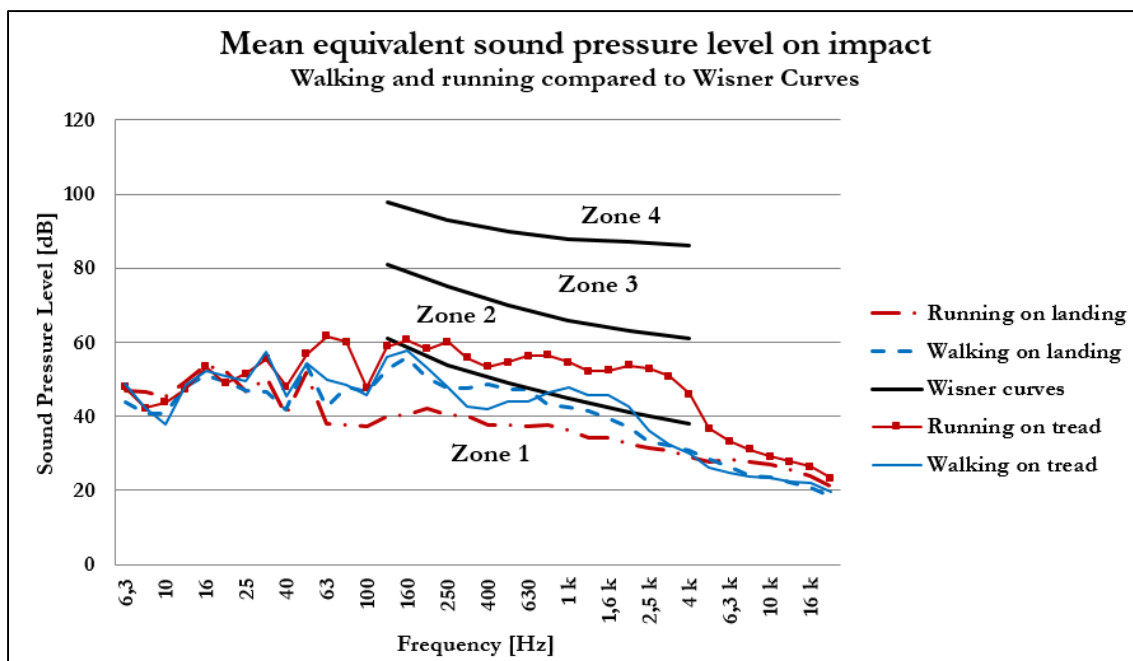


Figure 6.2. Sound pressure level on impact compared to Wisner curves.

Overall this analysis showed that frequencies most likely to originate from staircase vibrations should be between 100 and 250 Hz. This further confirmed the results from the previous measurement in chapter 3.3. To avoid missing possible important frequencies further analyses in this case studied frequencies below 400 Hz.

6.1.2. Natural frequency analysis

In this part discussions regarding natural frequency modeling and measurements are carried out.

Comparison and assessment of mode shapes

Depending on the size of the setup an analytical comparison, orthogonality check or modal assurance criterion, were performed. From the correlation found in the analytical comparison a visual assessment was performed to further compare the mode shapes.

In Appendix A2 the frequencies below 400 Hz found in the local setup for the tread and the corresponding damping are shown. These mode shapes were then compared to the calculated mode shapes of the natural frequencies in the FE-model.

An application called *CrossMac* was used to investigate the correlation between the mode shapes from the FE-model and the measurements. The MAC-values for the first three modes presented in chapter 4.2 compared to the frequency span from 100 to 170 Hz are shown in

6. Case study discussions and conclusions

Table 6.1. Modes correlating more than 90 % are marked red in the table, these were the best matches. Modes matching between 70 and 90 % are marked green, these were good but not ideal. The yellow ones have some resemblance and the white ones have no resemblance. In the table it is visible that the first mode did not have any good correlating mode shapes in the calculated mode set. It is also evident that the remaining two modes had more than one of the natural frequencies from the FE-model correlate rather well with the measured mode.

Table 6.1. MAC-values for the three lowest modes from measurement in setup 3.

Modes from FE-model [Hz]	Modes from measurements [Hz]		
	50,048	68,419	78,599
30,018	0,231	0,026	0,008
34,626	0,239	0	0,011
38,354	0,022	0,6	0,443
42,12	0,028	0,796	0,67
46,007	0,077	0,779	0,693
46,507	0,117	0,586	0,481
51,687	0,063	0,845	0,826
54,75	0,049	0,925	0,902
54,813	0,06	0,897	0,865
55,791	0,049	0,205	0,09
57,729	0,237	0,258	0,35
62,952	0,063	0,916	0,923
71,329	0,047	0,92	0,917
83,012	0,173	0,444	0,39
86,538	0,017	0,634	0,481
87,709	0,051	0,892	0,895
88,495	0,081	0,682	0,628

For every mode shape found during the measurements the closest frequency match and the top three correlation matches within 20 Hz from the measured frequency were checked for possible resembling modes. Any correlating mode shape further from the measured mode shape than 20 Hz was considered non-matching. To further investigate which mode was detected in the measurement the shapes were compared visually. The second mode shape in the measurement at 68,419 Hz was compared to its three strongest matches in the modes from the FE-model, see Table 6.2.

Table 6.2. Top three MAC-values for the second mode shape in setup 3.

Modes from FE-model	68,419 Hz
54,75 Hz	0,925
71,329 Hz	0,92
62,952 Hz	0,916

The matches found through visual comparison for each mode shape are presented in Appendix C1, Appendix C2 and Appendix C3 for the three setups. For the different setups AutoMAC tests, i.e. MAC-values within the mode set, were performed to give an idea of the precision in the measurement. This is presented in the appendix for each setup.

Discussion of natural frequency analysis

From the natural frequency analysis of the FE-model it can be established that larger global motions such as bending and torsion of entire landings or flight occurred in frequencies below 70

6. Case study discussions and conclusions

Hz. First bending mode in the landing plate was the first local bending mode to occur, from 80 Hz. Bending modes in treads were not excited below 160 Hz but both treads and risers were in motion in frequencies higher than 200 Hz. More complex bending modes in landing plates and combinations of such occurred throughout frequencies above 220 Hz. Frequencies above 320 Hz excited motion in the beams underneath the landings.

During the impact hammer test there were some difficulties with the sensitivity of the equipment. It proved to be rather difficult to both fulfill the trigger level of the impact hammer and simultaneously not overloading the measurements in the tri-axial accelerometer. Problems of this sort was hard to avoid especially in the hitting positions on the largest spanning landing plate, probably both due to the plate vibrations and the tri-axial accelerometer being situated on the plate. This problem was observed in Setup 1 where tri-axial accelerometers were used on the lower landing plate. This may have resulted in some disturbances in measurement data. We were unable to collect complete data for all positions, which results in incomplete averaging from the hits. With incomplete averaging a disturbance in a single impact or response will generate immediate improper data for that impact position. In Setup 2, covering the lower landing, this problem was avoided by using three uniaxial accelerometers, since their sensitivity was lower.

For some of the hitting positions it could not be avoided to stand in the staircase while hitting to reach all positions, so the flight above or below were used as standing positions. This may have caused some disturbances in the response.

In the AutoMAC in the appendices for each test setup the precision in the measurements are visible. Each natural frequency had the MAC-value 1,0 compared to itself, which obviously was correct. Some adjacent natural frequencies had MAC-values close to 1, between 0,9 and 1, which means that they were similar, see for example natural frequencies around 60 Hz in Setup 1 in Appendix C1. In this case the software identified the natural frequencies as different from each other, i.e. their MAC-values differ from 1, but because of their resemblance it is possible that some of them actually were the same or a combination of the same natural frequency.

Concerning visual comparison, CrossMAC and CrossOrthogonality in the appendices for each test setup some conclusions could be made. We chose to compare the three best calculated resemblance values (CrossMAC or CrossOrthogonality) and the closest frequency match from the FE-model and measured natural frequencies. An observation from the visual comparison was that good resemblance was most often found in the closest frequency rather than from the calculated resemblance values. Since the calculated resemblance values did not seem to be of much use in these test setups we believe that an increased number of DOFs would be necessary for this application. With the limited DOFs used in the setups there was lack of many directions and detailing in the more complex mode shapes. Therefore visual comparison will give a better result in setups of this sort. The use of calculated resemblance values might be more suitable for smaller structures where all mode shapes are excitable with an impact hammer.

In this thesis EMA, Experimental Modal Analysis, has been used meaning that both load and response has been measured to determine modal behavior. An alternative way to perform this analysis could be by applying OMA techniques, Operational Modal Analysis. OMA could be used to extract natural frequencies and mode shapes from measurements during a longer time period from random actual walking loads. It is possible that this type of analysis would be a suitable option

for this kind of structure. OMA techniques would better consider variations in impacts than a hammer test, but are more time consuming and require high accessibility.

In the modeling phase, different boundary conditions were used, starting out with fully fixed in the top and bottom of the modeled staircase and also at the slabs. After applying the more elaborated boundaries as springs, implying that the resistance in the slabs and following staircase are limited, the natural frequencies only shifted slightly in value but the typical mode shapes were unchanged. At the boundaries of the staircase, the upper and lower flights, some local bending modes at the boundaries emerged. These bending modes could later on be disregarded by stating that there was no motion in the studied areas. By using the springs as boundary conditions instead of fully fixed boundaries the behavior should be more realistic, even though the typical mode shapes were the same as for the simpler boundaries. This implies that by expanding the models from the studied parts, i.e. the middle flight and the adjacent landings, realistic boundaries are achieved even with simpler boundary conditions such as fully fixed boundaries. By using the expanded model probable motion and sufficient detailing were fulfilled in the analysis.

6.1.3. **Vibration analysis with walking and running**

A limitation in this analysis was that only vibrations occurring in the chosen measurement points could be detected. Vibrations exciting other parts of the staircase or having a node point in the measurement position would not be detected with this analysis.

The accelerometers were attached to the carpet on the staircase using wax which potentially causes disturbances in the measurements. The carpet might dampen the movement in the staircase preventing the accelerometer from measuring the actual response in the staircase.

In Table 4.5 it is visible that frequency peaks around 90 and 130 Hz (marked in green and blue) always occurred in the landings. Vibrations around 190 Hz (marked in orange) were also regularly found in the landings. Higher frequencies of around 260 and 370 Hz (marked in light orange and purple) could be found, especially for setup 1 measuring the lower landing. After impact lower frequencies tended to seem strong in amplitude compared to the same frequencies on impact. The overall amplitude was much lower after impact and the higher frequencies tend to be damped faster than lower frequencies due to energy consuming motions.

For the treads a clear pattern of vibration frequencies around 260, 300 and 370 Hz (marked in light orange, red and purple) is visible in the table. In Figure 4.20 and Figure 4.22 it is evident that the amplitudes in the treads were much higher than in the landing.

We believe that the difference in amplitude between landings and treads originates from the impact from walking. When walking on a landing you walk horizontally, as on a slab, so in that case the heel-toe strike in Figure E1. 5 is applicable. In the tread on the other hand you walk both vertically and with only one toe impact in each step. Since the entire force is put into the toe strike the impact force is more concentrated. By studying the forces when walking on the landing and on the tread it is easier to understand why the vertical forces are larger during walking on the tread. A schematic picture of the motion of a body with mass in different positions in the staircase is shown in Figure 6.3. The red arrows show the resulting force and how its direction varies between the two cases.

6. Case study discussions and conclusions

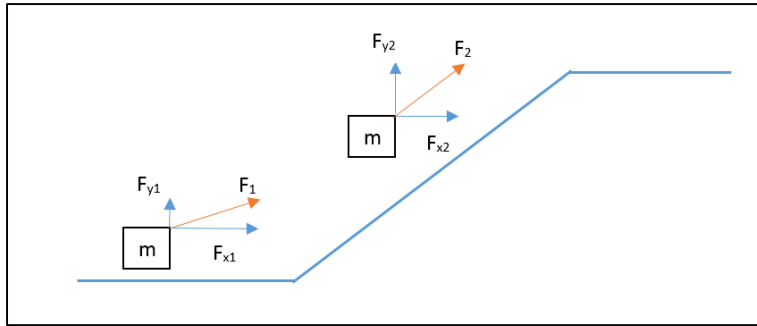


Figure 6.3. Forces from walking in different positions in the staircase.

Compared to the comfort criteria for footbridges and decks stated in the Eurocode, see chapter 2.1.1, the vertical acceleration was on the verge of being exceeded in the tread according to Figure 4.17. The criterion of $0,7 \text{ m/s}^2$ was reached in the test when stepping on the tread, this indicates that discomfort from vibrations also could be a problem in the structure. In the landing, $0,5 \text{ m/s}^2$ was reached which is below the criterion for footbridges and decks. This indicates that the landing should not be discomforting to use. In the lateral direction $0,15 \text{ m/s}^2$ was reached in the landing, marked red in Figure 4.16. The criterion in chapter 2.1.1 states that for normal use $0,2 \text{ m/s}^2$ should not be exceeded, which was fulfilled. The Eurocode states that some margin is preferable in this situations which could imply that also the vertical direction was too close to exceeding the requirements.

When investigating the RMS-values in the frequency range between 1-80 Hz it was seen that they were well below the perception threshold according to (Swedish Standards Institute, 2004b), see Figure 4.24, Figure 4.25 and Appendix B2. The probable cause of this is that the main part of the high values occurred above this frequency range. This is strengthened by the fact that no vibrations or discomfort was noticeable during walking or running in the staircase by the test person.

Alternative ways of checking vibrations from walking could be performed using accelerometers on the structure for a longer time period measuring the actual response from usage. In that way vibrations from different users could be identified giving a more accurate loading than that of one individual, as in the performed analysis. This would also show the spread between different walking patterns and loads, but might for that matter not give a quite as clear peaks for different frequencies as in this case study.

6.1.4. Vibration analysis with impact hammer

One of the biggest limitation in this analysis was that only a few measurement points in the normal walking path were analyzed. To improve measurement results a larger variety of points could have been checked. Since the analysis was performed with an impact hammer the load differs from actual walking both in magnitude and shape.

In Table 4.6 it visible that the landing vibrated at frequencies around 130, 185, 275 and 370 Hz (marked blue, orange, red and purple) independent from impact position. With impact on tread and mid-span landing a frequency at about 80 Hz (marked green) was triggered.

For the tread, a vibration frequency of around 370 Hz (marked purple) was triggered independent from impact position. Frequencies around 80 and 155 Hz (marked green and brown) were triggered

in the tread from impact on the landing but not on the tread itself. This implies that the vibration measured rather propagated from the landing than occurred in the tread.

The frequencies marked yellow in Table 4.6 are uncertain due to low coherence in the measurements, see Appendix D1. Low coherence means that there were large disturbances between the response and impact functions around these frequencies.

In Figure 4.26 and Figure 4.27 it is visible that the tread vibrated in frequencies of 580 and 650 Hz, but since these were not identified in the sound pressure measurements for walking they were not further investigated.

During the impact hammer test a ringing sound was observed that did not occur as much through walking or running. The sound needed long time to be dampened.

6.1.5. Vibration propagation analysis

In Table 4.7 the transmissibility for each measurement is presented. Typically transmissibility ratios of 40-70 % were measured from the stringer to the slab. Since there are no special requirements for the slab the propagation is not a limiting factor for the vibrations. If, on the other hand, sensitive equipment is to be used close to the staircase, propagation has to be taken into consideration. In the MAX IV facility there are similar staircases closer to the main laboratory building that potentially could cause vibrations exceeding the criterion for disturbances during use.

The second part of the propagation analysis showed certain frequencies that the slab was sensitive to. From measurements with impact in H1 it was visible that 90 Hz was causing most propagation to the slab. For all measurements frequencies around 250 and 300 Hz stood for almost all of the propagation. To prevent propagation from the staircase to the slab, actions to decrease these frequencies should be taken.

It would have been interesting to check the reversed propagation, i.e. from the slab to the staircase, but since propagation was not the main issue in the case study this was not further investigated.

6.1.6. Reverberation time analysis

Two different ways of determining the reverberation time have been used. A comparison is presented in Figure 6.4. The comparison showed good resemblance between the measurement and the simulation, though the simulation gave a slightly higher reverberation time. Absorptions in some frequencies, especially from 500 to 1000 Hz, were underestimated in the simulation. This is likely to depend on the simulation's inaccurate material properties, empty room and many simplifications in the structure. The mean value for reverberation time was 0,5 s both in the simulation and the measurement which shows that the simulation tool was a good way to predict properties in the room. The demand according to the operative standards is 0,5-0,6 s depending on classification, see chapter 2.2.1, which is the same as the measured value.

6. Case study discussions and conclusions

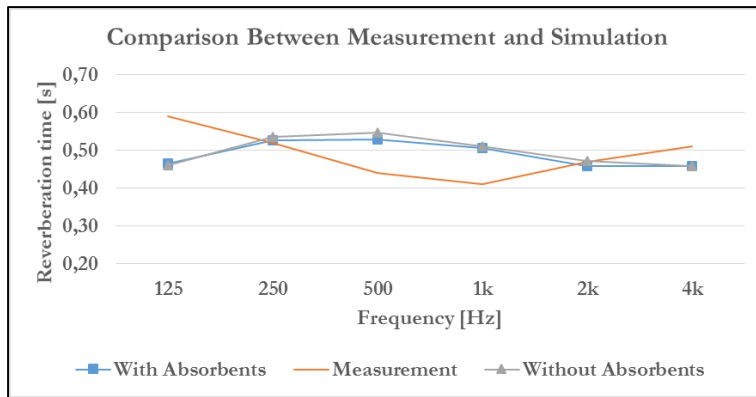


Figure 6.4. Reverberation time comparison between simulation and measurement.

The results from the measurements showed that frequencies below 250 Hz and around 4000 Hz could be causing problems due to lack of absorbers. Therefore these frequencies should be taken action against using absorbers if they are causing acoustical problems. Frequencies between 500 and 1000 Hz were already absorbed rather well but there is still room for enhancement.

The standard deviations in the measurements showed that the largest uncertainties lie in the lower frequencies, 125 Hz and below. This means that there is a risk these values are misleading for some areas in the room.

6.2. Conclusions

In this chapter the results were interpreted and conclusions leading up to a proposal of proper possible adjustments for the staircase in the case study are presented.

- The sound pressure analysis showed that high sound pressure levels occur between 100 and 250 Hz. More specifically frequencies around 125 and 160 Hz were highest in the landing and frequencies around 160 and 200 Hz were highest in the tread.
- The natural frequency measurements and simulations showed global bending modes below 80 Hz, bending modes in landing plates from about 80 Hz and bending modes in tread plates from about 160 Hz.
- The vibration analysis with walking showed response peaks in landings at 90, 130 and 260 Hz. In the treads the response peaks from walking occurred at 270, 300 and 370 Hz. The maximum acceleration occurred in the tread on impact and reached $0,7 \text{ m/s}^2$, note that this only occurred instantaneously on impact.
- The vibration analysis with impact hammer showed response peaks in landings at 90, 130, 190, 270 and 370 Hz regardless of impact position. In the tread response peaks occurred at 290 and 370 Hz.
- The propagation analysis between staircase and slab showed largest sensitivity around 90 and 250-300 Hz. Since there were no specified requirements on the adjacent structures no measures needed to be taken to prevent the propagation.
- The reverberation time measurements and simulations show good reverberation properties, around 0,5 s, in the room, with some enhancement potential below 250 Hz.

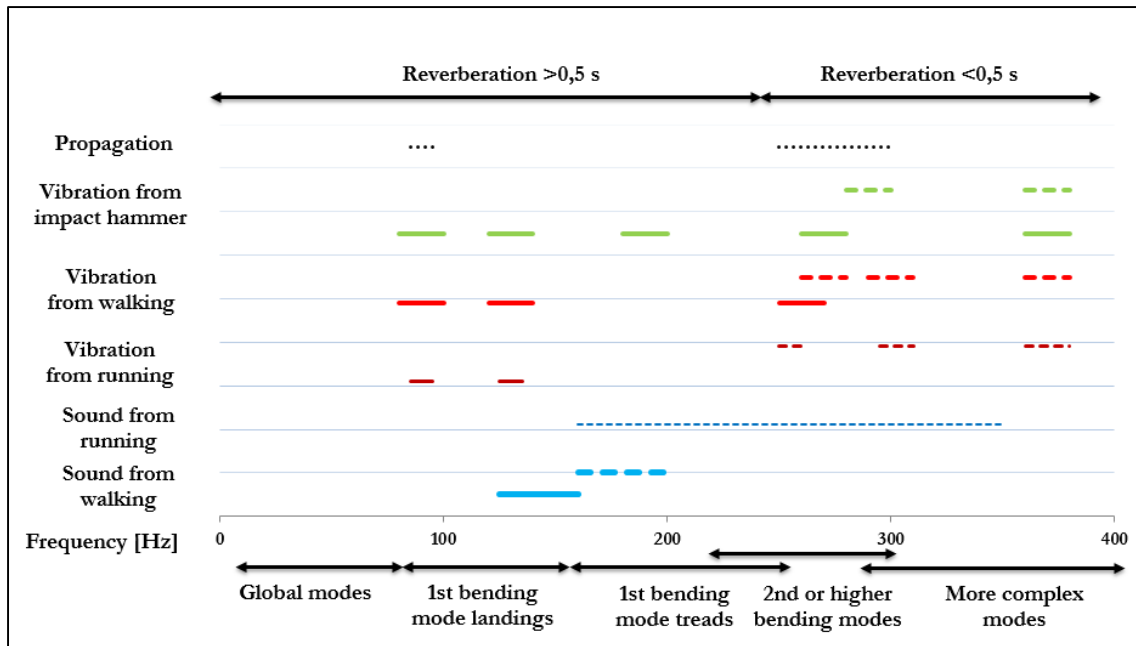


Figure 6.5. Summary of results. Dashed lines for treads and continuous lines for landings.

In Figure 6.5 the results are summarized to present the results graphically. The y-axis presents the measurements and the x-axis the frequencies. Below the graph the natural motion pattern from the natural frequency analysis and measurements are shown and above the graph, the reverberation time in the surrounding room is presented.

6.3. Possible adjustments

In this chapter possible adjustments and their suitability for the staircase in the case study will be discussed.

6.3.1. Structural alterations

The conclusions showed that it could be of interest to perform some structural alterations to control the vibrations in the landings and treads of the staircase. By applying the vibration control measures discussed in chapter 2.1.5 some different solutions are suggested here.

Since there mainly has been observed issues with plate motions a structural solution for the plate in the landing with the largest span is proposed. To reduce the bending motion of the plate a stiffening profile could be added to the structure, see Figure 6.6.

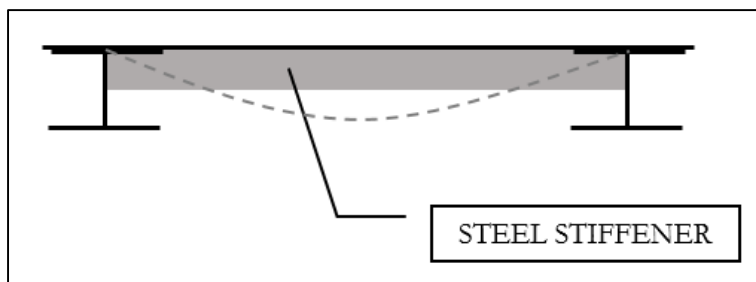


Figure 6.6. Example of added steel stiffener to obstruct bending motion (dashed line).

6. Case study discussions and conclusions

These steel stiffeners could for example consist of either an L- or T-section welded onto the plate, see sections with stiffeners placed to reduce motion in Figure 6.7. In Figure 6.8 an example of stiffening plates under a landing is displayed.

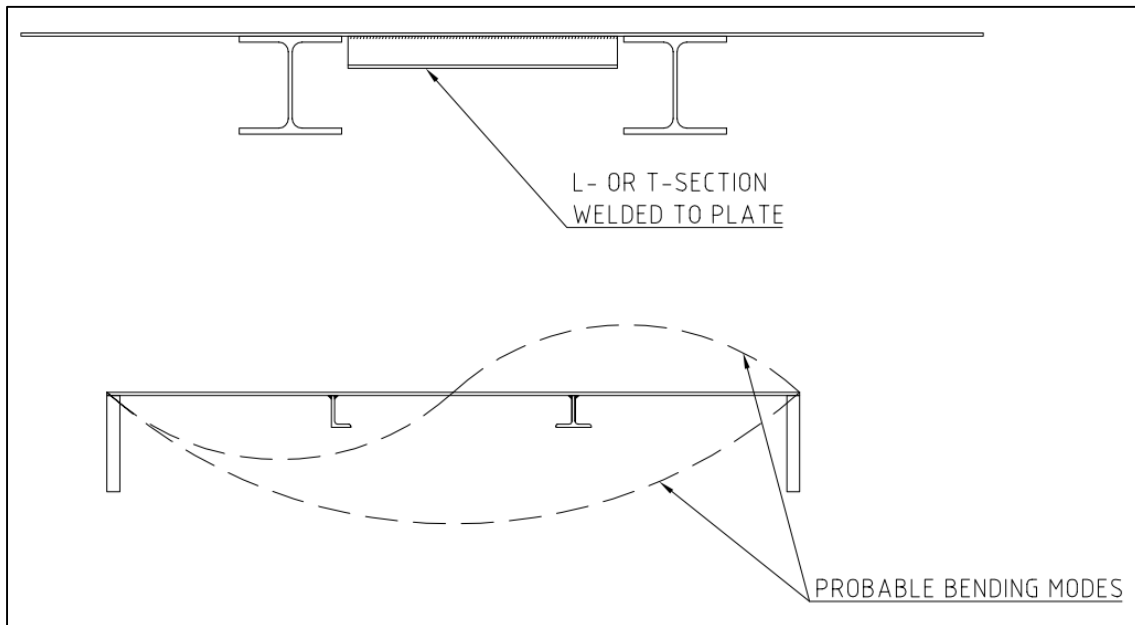


Figure 6.7. Sections with steel stiffeners obstructing probable plate motion.

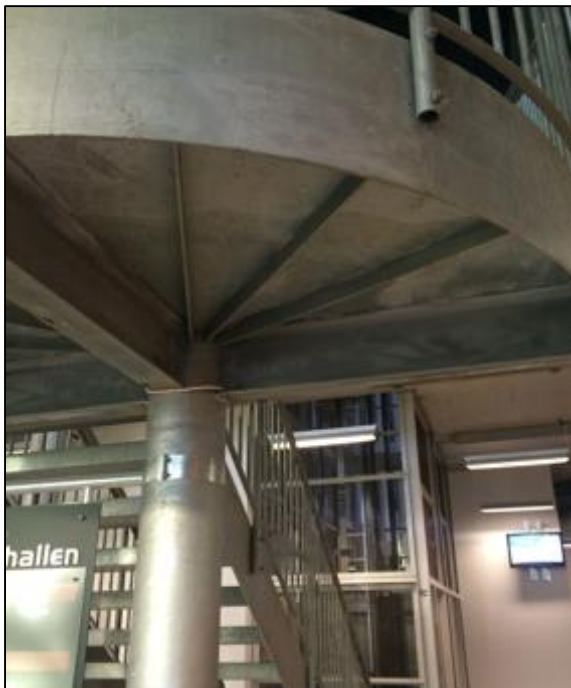


Figure 6.8. Stiffening plates under landing at Ubåtshallen in Malmö.

A rather technical solution would be to place tuned mass dampers under each tread to cancel out specific frequencies, see Figure 6.9. For example if the largest vibrations in the treads occurred at 290 Hz, this frequency could be reduced by applying a mass with a spring and viscous damper where

$$\sqrt{\frac{k}{M}} = \frac{290}{2\pi} \text{ Hz} \quad (\text{Eq. 2-10})$$

where

k is the spring stiffness

M is the mass

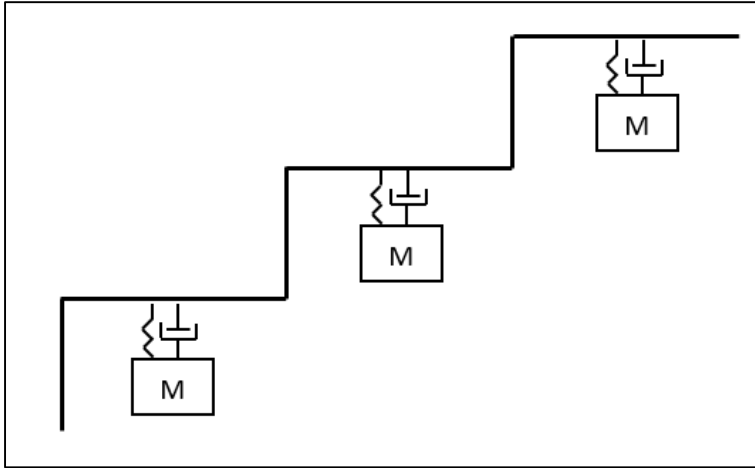


Figure 6.9. Example of tuned mass dampers on treads.

Attaching a TMD to every tread could be a costly and complicated way of solving the vibration problem. A more straight forward method could be to attach a mass under each tread, see Figure 6.10. This adjustment would result in less acceleration in the treads. By studying Newton's second law as in chapter 2.1.5 it can be seen that by doubling the mass in motion the acceleration will be halved, since the load is unchanged.

$$F = m \cdot a \quad (\text{Eq. 2-9})$$

By adopting (Odqvist, 1948) approximation that a third of the tread is in motion due to a centric point load it can be evaluated that to decrease the acceleration to halve its amplitude the added mass, M , should be

$$M = \frac{L \cdot W \cdot t \cdot \rho}{3} \approx 4 \text{ kg}$$

where

L, W and t are the dimensions of a tread as stated in Table 3.1.

ρ is the density as stated in the same table.

6. Case study discussions and conclusions

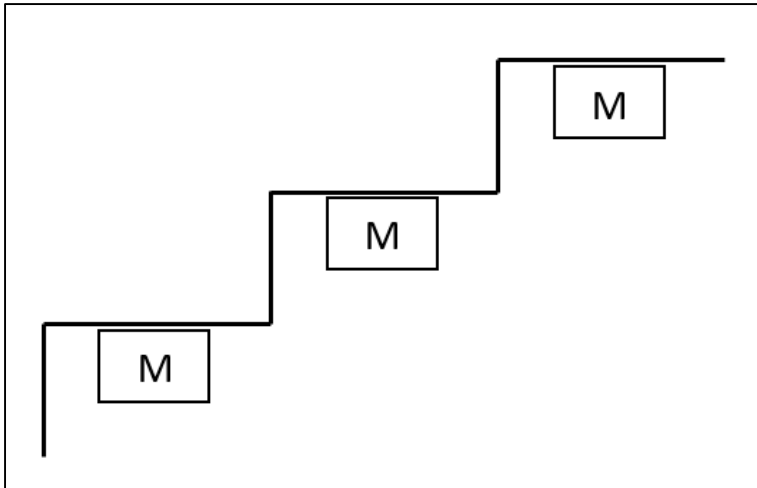


Figure 6.10. Example of added mass on treads.

A common way to design treads is with the use of infill, often stone or concrete. These are typical ways of adding mass to the tread, see Figure 6.11.



Figure 6.11. Treads with infill at Ubåtshallen and Malmö Högskola Orkanen in Malmö.

For structural solutions the FE-model will be used to show how an adjustment will affect the structural response. Adding a steel plate under each tread could be modeled either as an added mass to each tread or as an actual plate. Modeling it as a mass will show the mass effect alone and not regard the stiffening capacity of the plate. If the plate is welded properly it is likely that it will affect the stiffness of the tread. The responses in one of the treads are shown in Figure 6.12 with no alterations done to the treads, with the added plate modeled as a mass and modeled as a plate with both mass and stiffness.

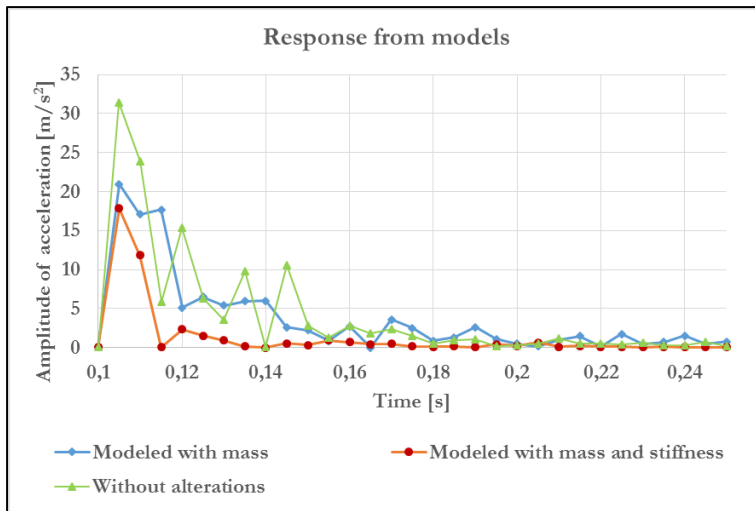


Figure 6.12. Response from modeling of alteration on tread.

It can be seen in the figure that adding the plate both will affect the amplitude of the motion and the decay, where the decay is dependent on the modeling of stiffness. It is likely that the response from this measure is somewhere between the mass model and the mass and stiffness model since the plate would not be fully integrated in the structure. If this measure was incorporated in the design to begin with, it is more likely to function with its full stiffness and mass. The results from the measure regarding acceleration amplitudes are presented in Table 6.3.

Table 6.3. Modeling of measure on tread.

Modeling of measure on tread	Acceleration amplitude [m/s ²]	Ratio of initial amplitude [%]
No measures	31,4	100
Plate modeled with mass	20,9	67
Plate modeled with mass and stiffness	17,8	57

From a bending moment point of view the adding of a structural material in the middle part of the tread very well corresponds to the moment diagram which suggest an effective use of material, see Figure 6.13.

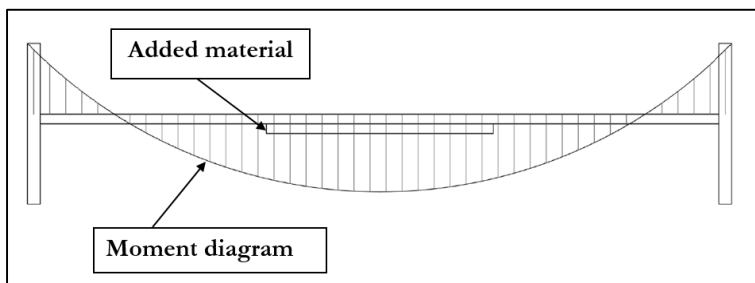


Figure 6.13. Bending moment corresponding to material placement.

6. Case study discussions and conclusions

6.3.2. Acoustical alterations

Although adjustments have been made since the problem was discovered in the staircase other alterations could be made in order to make the surrounding sound climate better in the office. Absorbents were already placed locally below the treads and landings which have been discussed in chapter 3.2. These absorbents have a very small effect on the overall reverberation in the room as seen in the early simulations in *CATT*, see Figure 5.9. The measurements showed that there was an increased reverberation time in the lower frequencies below 250 Hz. These frequencies also were the ones that had the highest sound pressure levels from the measurements of sound emittance while walking and running in the staircase, see chapter 4.1. This means that the noise from the staircase will take a longer time to be damped out and therefore more present for the people that uses the area around the staircase. This can be prevented by adding extra absorbents placed throughout the room.

The floors above the entry floor have extra absorbents in the form of cubicle screens surrounding each office space which do not exist in the investigated area. The proposed solution is therefore movable cubicle screens with absorbents with good absorption in the frequencies below 250 Hz.

A simple analysis was done by fitting the modeled reverberation time to the measured reverberation time, see chapter 5.4, and then adding absorbents with a probable surface area and then calculate the new reverberation in *CATT* with the same source and receiver positions as in chapter 5.2. The two strictest demands for reverberation time are 0,4 s (Class A) and 0,5 s (Class B) in offices for less than 20 people (Swedish Standards Institute, 2007). Three steps were investigated where the amount of alterations increased in each step. After the reverberation analysis an audibility investigation was carried out so that a comparison of the improved sound pressure level could be applied to an existing noise problem and a possible office area.

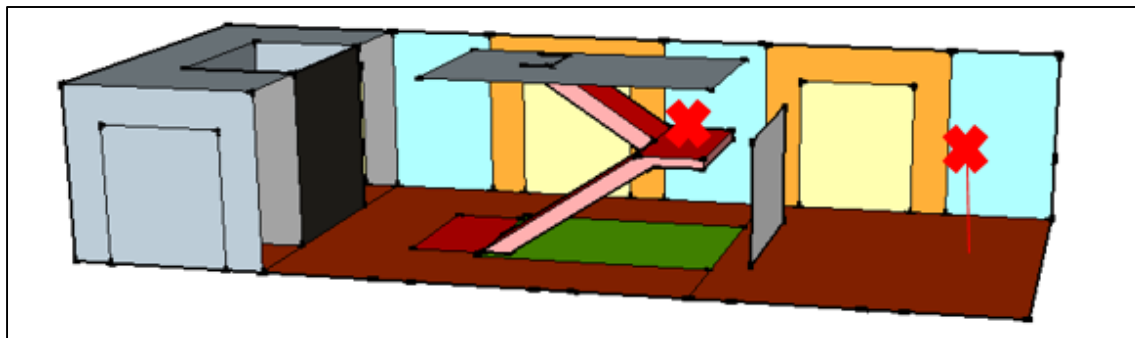


Figure 6.14. Overview of the room with its alterations. The figure shows the source position (in staircase) and the receiver position (in the office area) marked with a red X. The screens placement and absorbents on wall (dark yellow area) are shown and the missing ceiling is where the extra bass was applied.

The first step was done by adding 100 mm of the product *Ecophon Extra Bass* in the ceiling with properties according to (Ecophon Saint-Gobain, 2015). This improved absorption in the lower frequencies, 250 Hz and below. The ceiling area with *Extra Bass* was 54 m².

The second step was done by adding a screen, in addition to the alterations done in step one, with the area of 2,8 x 1,9 m². The product used was a storage screen named *Sabine* with properties

according to (Glimakra of Sweden, 2015). Except only decreasing the reverberation this alteration would also hinder the noise from the staircase reaching the suggested office area.

The third step was carried out by adding extra wall absorbents on the free walls in the room, this was also done in addition to step one and two.

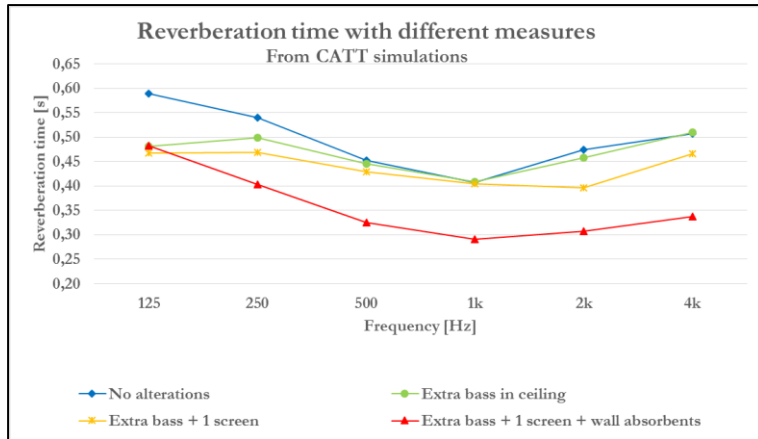


Figure 6.15. Comparison of the simulated reverberation time with different alterations.

In Figure 6.16 the audibility results are shown with the different alterations. The modeled sound level was performed for a person sitting down in the end of the suggested open office area and it shows only the receiver level. Figure 6.17 shows the improvement in the receiver position after each alteration.

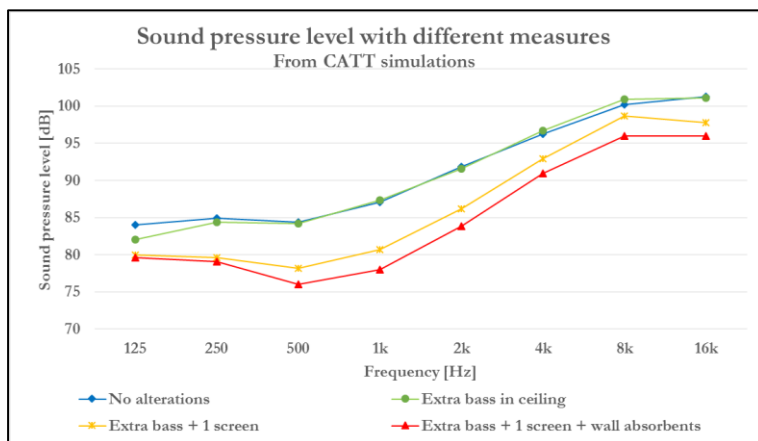


Figure 6.16. Modeled sound pressure level in the office area with a sound source placed on the upper landing, see Appendix D2.

6. Case study discussions and conclusions

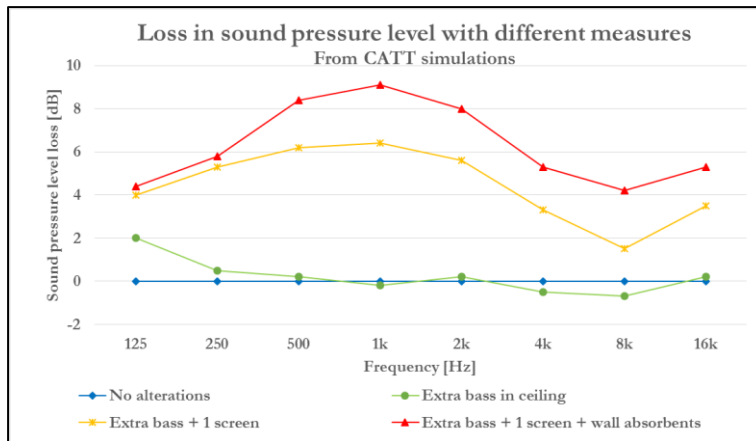


Figure 6.17. The sound pressure loss in the receiver position compared to when no alteration have been done.

The results showed that the alterations made in step three gave the best overall properties and reached Class A for reverberation. The audibility was also good in this alternative. Although step three was good step two, with no extra absorptents on the wall, showed very small difference in the frequencies that were problematic in our case study. Therefore step two was a more likely solution since it is not as extensive as step three. With this solution it is possible to decrease the sound pressure level with around 5 dB, see Figure 6.17. According to the measured A-weighted sound pressure levels while walking and running, see values for the whole measurement sequence Table 4.2, the new values can be estimated to 41 dBA for walking and 50 dBA for running.

Another alternative is to use a dense railing on the staircase so that sound created from the footstep is hindered to propagate into the surrounding room. This has not been investigated.

7. General conclusions and discussions

This chapter contains general conclusions, recommendations and discussions regarding steel staircase design. Note that the general conclusions are based on the findings in the case study.

7.1. General strategies in design

In this thesis the dynamic behavior of steel staircases were studied, but the obtained knowledge might as well be applied to other similar structures. It is possible to use these analyses for all slender structures affected by walking loads, for example entresol slabs, decks and walking bridges. Depending on the structure, and the setting of the structure, different analyses can be of importance. For example when it comes to propagation the sensitivity of the structure and the adjacent elements determine the importance of the propagation analysis.

7.1.1. Structural recommendations

Regarding the FE-modeling, boundary conditions have been dealt with in some different ways. Totally rigid connections have been avoided as much as possible since they do not describe any actual connection that well. Instead, springs were used to model the rigidity of adjacent elements. The spring stiffness of the springs were estimated by considering the strength of assumed stabilizing elements in the building. The estimation was not exact but still described the connection better than an infinitely rigid connection. In other cases expanded modeling was used as a way of dealing with boundaries in the studied part of the staircase. Instead of getting improper results at the boundary of the studied part the model was expanded keeping the boundaries further away from the studied part. By disregarding any local motion at the boundaries and only considering motion occurring in the studied part the model can be considered rather realistic. By using springs and expanded modeling proper results from FE-modeling can be achieved.

For slender structures probable mode shapes needs to be considered. Making the global system stiff to fulfill the criteria posed in the Eurocode is crucial, but no guarantee for a well-functioning staircase. Local plate motion can easily be excited from walking, which can generate both noise and vibration related problems. It is common to use infill on treads and landings, as displayed in Figure 6.11 above. These staircases usually do not suffer from vibration issues since their mass is too large to be excited from walking alone. As a rule of thumb it can therefore be said that to avoid issues from local plate motion either stiffness or mass should be added to bare plate areas, i.e. areas without infill or direct stiffeners, subjected to immediate impact from walking. Note that Newton's second law is applicable for rigid body motions and an increased mass does not lower the acceleration in all cases. To avoid issues from added mass these should be modeled before applied to the structure.

For bare plate treads, we suggest that an extra plate with one third of the length is welded on underneath the tread, increasing its weight. For example a tread designed with a 5 mm plate for load bearing capacity and serviceability an extra 5 mm plate should be added in the middle third of the tread.

For bare plate landings we suggest that a stiffening steel profile, such as L- or T-section, is added. By studying the probable plate motion in the landings, for example with a simple natural frequency analysis, suitable placements for the stiffener can be determined.

7. General conclusions and discussions

7.1.2. Acoustical recommendations

When designing a slender structure pertaining recommendations on vibrations are given in a frequency spectra up to 100 Hz, see chapter 2.2.1. This case study on the other hand showed that it is vital that not only the lower frequencies are studied. As seen from the measurements noise problems can occur if this is not taken in consideration. A rule of thumb should be that higher frequencies, at least up to 400 Hz according to this case study, are taken into considerations in these stiffer complex lightweight structures if noise problems are to be avoided.

If the staircase is placed in a sensitive environment there should be some kind of damping surface on top of the stepping plates, not only for the structural vibrations but for the direct impact noise created from walking in the staircase.

Screens are a usable tool to decrease the propagated sound and they can be incorporated early on when designing a staircase. For example a dense railing that has a secondary function to prevent walking sound spread into the surrounding area can be used.

A model is a very good tool to use and it gives a direct and relatively accurate result. Some simplifications can be made without affecting the results too much and in combination with the operative standards this becomes an effective tool, both when investigating the reverberation and the sound propagation.

7.2. Overall pros and cons of the analysis

The sound pressure level measurements show good results but there are a lot of disturbances that need to be taken into consideration. A discussion regarding background noise and sound from impact rather than vibrations are crucial to get a just result.

The natural frequency measurements are good in the sense that they portray the motion of the actual structure. The downside of this analysis is that it is time-consuming and sensitive to impact positions and settings in the software. For larger structures, such as the staircase in the case study, a large amount of DOFs are required to get clear motion patterns.

The vibration analysis with walking is a rather good analysis since it investigates the actual vibrations from common usage. The downside of the analysis is the difference between conditions in the performed tests due to different test persons, shoes etc.

The upside of vibration analysis with impact hammer is that the applied force is accurately recorded. The downside in the analysis is that the load is not necessarily that similar to an actual footprint and the response can therefore vary in terms of frequencies and duration.

The propagation analysis in the case study was performed with a simple test showing a method of investigating the effect the vibrations have on adjacent structures. In the chosen case study propagation was not much of an issue but in some cases it may be crucial to investigate. More demanding structures could for example be structures with adjacent highly sensitive equipment or fragile objects such as glass or cladding.

The reverberation time measurements give a good understanding of the sound properties of the surrounding area. It is easy and quick to perform and if there are potential for enhancement there

are many possible solutions. The downside of this analysis is that it does not consider the sound source.

The natural frequency modeling is rather straight forward to perform, given that the boundary conditions and geometry are well-defined. An obvious upside to modeling in general is that it can be done in the design phase and can be altered to visualize different options. A downside of the analysis is that it is hard to verify complex structures without performing measurements.

The reverberation time simulation is easy to perform, but requires detailed information regarding material parameters. Details such as furniture can be hard to take into consideration in the modeling giving room for some error sources.

7.3. Further studies

Analytical comparison methods, such as MAC-values, can be evaluated further. For example an increased number of DOFs during measurement might be more suitable for these types of comparisons.

The same type of structure could be analyzed using OMA technique. By using OMA techniques, actual walking loads and variance in these is used rather than an impact hammer.

More detailed studies on propagation analysis could be performed on a case with high requirements, for example a staircase closer to sensitive equipment. In this thesis propagation analysis was dealt with but there is much more to be done. It would be interesting to investigate this further with a case study demanding a more detailed analysis.

8. References

- Adhikari, S. (2000). *Damping Models for Structural Vibration*. Cambridge: Cambridge University Engineering Department.
- Alipour, A., & Zareian, F. (2008). Study Rayleigh Damping in Structures; Uncertainties and Treatments. *World Conference on Earthquake Engineering*. Beijing: International Association for Earthquake Engineering.
- Allemang, R. J. (2003). The Modal Assurance Criterion - Twenty Years of Use and Abuse. *Sound & Vibration*.
- Alten, K., Friedl, H., & Flesch, R. (2010). Calculating Ground-Borne Noise From Ground-Borne Vibration. *ISMA 2010* (ss. 3431-3440). Heverlee: ISMA International Conference on Noise and Vibration Engineering.
- Brandt, A. (2011). *Noise and Vibration Analysis*. Chichester: John Wiley and Sons, Ltd.
- Chevret, P., & Chatillon, J. (October 2015). Acoustic Discomfort for Tertiary-Sector Employees: Issues and Means of Action for Prevention. *Acoustics in Practice*.
- Chopra, A. K. (1995). *Dynamics of Structures*. New Jersey: Prentice Hall.
- Cremer, L., & Müller, H. A. (1982). *Principles and Applications of Room Acoustics*. Barking : Applied Science Publishers LTD.
- Ecophon Saint-Gobain. (2015, November 17). *Master Rigid A*. Retrieved from Ecophon Saint-Gobain: <http://www.ecophon.com/sv/produkter/Akustiktak/Master/Master--Rigid-A/>
- Fastl, H., & Zwicker, E. (2007). *Psychoacoustics*. Berlin Heidelberg: Springer-Verlag.
- Glimakra of Sweden. (2015, November 17). *Sabine*. Retrieved from Glimakra of Sweden: <http://www.glimakra.com/Sabine.htm>
- Howard, D. M., & Angus, J. (2009). *Acoustics and Psychoacoustics*. Oxford: Elsevier Ltd.
- Imamovic, N. (1998). *Validation of Large Structural Dynamic Models Using Modal Test Data*. London: University of London.
- Johansson, P. (2009). *Vibration of Hollow Core Concrete Elements Induced by Walking*. Lund: Media-Tryck LU.
- Kerr, S. (1998). *Human Induced Loading on Staircases*. London: University of London.
- Kristensson, T. (2014). *Modal Testing and Structural Identification*. Lund: Media-Tryck LU.
- Meriam, J. L., & Kraige, L. G. (2008). *Engineering Mechanics Dynamics*. Danvers: John Wiley & Sons, Inc.

8. References

- Miller, C. W. (1993). *Optimization of modal analysis and crossorthogonality techniques to insure finite element model correlation to test data*. Rochester: Rochester Institute of Technology.
- Murray, T. (2001, March). Tips for Avoiding Office Building Floor Vibrations. *Modern Steel Construction*.
- Murray, T. M., Allen, D. E., & Ungar, E. E. (1997). *Floor Vibrations Due to Human Activity*. American Institute of Steel Construction, Inc.
- Nilsson, E., Johansson, A.-C., Brunskog, J., Sjökvist, L.-G., & Holmberg, D. (2002). *Grundläggande Akustik*. Lund: Teknisk Akustik, LTH.
- Odqvist, F. K. (1948). *Hållfasthetslära*. Stockholm: Bokförlaget Natur och Kultur.
- Rao, S. S. (2011). *Mechanical Vibrations*. Upper Saddle River: Pearson Education Inc.
- Rayleigh, J. (1877). *The Theory of Sound*. London: MacMillan and Co.
- Saar, O. S. (2006). *Dynamics in the Practice of Structural Design*. Southampton: WIT Press.
- Sciulli, D. (1997). *Dynamics and Control for Vibration Isolation Design*. Blacksburg: Virginia Polytechnic Institute and State.
- Smith, J. W., & Kappos, A. (2001). *Dynamic Loading and Design of Structures*. London: Spon Press.
- Swedish Standards Institute. (2002). *Eurocode: Basis of structural design*. Stockholm: SIS Förlag AB.
- Swedish Standards Institute. (2004a). *Eurocode 5: Design of timber structures*. Stockholm: SIS Förlag AB.
- Swedish Standards Institute. (2004b). *Vibration and Shock - Measurement and Guidelines for Evaluation of Comfort in Buildings*. Stockholm: SIS Förlag AB.
- Swedish Standards Institute. (2007). *Acoustics - Sound Classification of Spaces in Buildings - Healthcare Premises, Rooms for Education, Preschools and Leisure-time Centres, Rooms for Office Work, Hotels and Restaurants*. Stockholm: SIS Förlag AB.
- Thorby, D. (2008). *Structural Dynamics and Vibration in Practice*. Oxford: Elsevier Ltd.
- Vigran, T. (2008). *Building Acoustics*. Abingdon: Taylor & Francis.
- Willford, M., & Young, P. (2006). *A Design Guide for Footfall Induced Vibration of Structures*. Trowbridge: Cromwell Press.

Appendix A1

Visual identification of motion in natural frequencies from FE-model.

Natural frequency [Hz]	Type of motion
23,449	First bending of landing as cantilevered from flight.
30,018	First bending of landing as cantilevered from flight.
34,626	Torsion in landing as cantilevered from flight.
38,354	Torsion and bending of landing as cantilevered from flight.
42,120	Torsion in landing as cantilevered from flight.
46,007	Torsion in flight and landing as cantilevered from flight.
46,507	Torsion in landing as cantilevered from flight.
51,687	Torsion in landing as cantilevered from flight. Bending in flight.
54,750	Disregarded - No motion in landing or flight.
54,813	Disregarded - No motion in landing or flight.
55,791	Torsion in landing as cantilevered from flight.
57,729	Torsion in landing as cantilevered from flight.
62,952	Torsion in landing as cantilevered from flight. Bending in flight.
71,329	Bending in flight. First bending mode in lower landing plate.
83,012	First bending mode in lower landing plate.
86,538	First bending mode in lower landing plate.
87,709	First bending mode in lower landing plate.
88,495	First bending mode in lower landing plate.
88,816	First bending mode in lower landing plate.
89,684	First bending mode in lower landing plate.
92,821	First bending mode in lower landing plate and torsion in flight.
93,984	First bending mode in lower landing plate and torsion in flight.
94,944	First bending mode in lower landing plate and torsion in flight.
96,080	First bending mode in lower landing plate and torsion in flight.
98,328	Disregarded - No motion in landing or flight.
98,448	Disregarded - No motion in landing or flight.
103,52	First bending mode in lower landing plate and torsion in flight.
104,34	First bending mode in lower landing plate and torsion in flight.
105,57	Disregarded - No motion in landing or flight.
110,68	Second bending mode in lower landing plate.
114,71	Second bending mode in lower landing plate.
116,47	Second bending mode in lower landing plate.
119,55	Second bending mode in lower landing plate. Torsion in flight.
120,15	Second bending mode in lower landing plate.
121,49	First and second bending mode in lower landing plate.
122,65	Second bending mode in landing plate.
126,47	Second bending mode in landing plate.
127,82	Second bending mode in landing plate.
129,24	First and second bending mode in landing plate. Torsion in flight.
131,30	First bending mode in upper landing plate.
132,83	First bending mode in upper landing plate.
133,16	First bending mode in upper landing plate.
134,25	First and second bending mode in landing plate.
134,54	Second bending mode in lower landing plate, first bending mode in lower landing, torsion in flight.
138,74	First bending mode in lower landing plate, torsion in flight, first bending mode in treads.
140,35	Second bending mode in lower landing plate, first bending mode in lower landing, torsion in flight, first bending mode in treads.
140,85	First bending mode in lower landing plate, torsion in flight, first bending mode in treads.
148,66	Second bending mode in landing plate.

151,95	Second bending mode in landing plate. First bending mode in treads.
152,62	Second bending mode in landing plate. First bending mode in treads.
160,26	Third bending mode in lower landing plate, torsion in flight, first bending mode in treads.
161,75	Second bending mode in landing plate. First bending mode in treads.
165,31	Disregarded - No motion in landing or flight.
166,15	Disregarded - No motion in landing or flight.
167,58	Second bending mode in landing plate. First bending mode in treads.
172,06	Third bending mode in lower landing plate, first bending mode in tread.
172,82	Third bending mode in lower landing plate, first bending mode in tread.
175,32	Second bending mode in landing plate. First bending mode in treads.
180,95	Third bending mode in landing and first bending mode in tread.
181,09	Third bending mode in landing and first bending mode in tread.
182,45	Third bending mode in landing and first bending mode in tread.
183,59	Second and third bending mode in landing, first bending mode in tread.
186,96	Second and third bending mode in landing, first bending mode in tread.
189,21	Third bending mode in landing, first bending mode in tread.
190,00	Second bending in landing, first bending in treads.
190,93	Third bending mode in lower landing plate, first bending mode in treads, second bending mode in upper landing.
192,01	Third bending mode in lower landing plate, first bending mode in treads, second bending mode in upper landing.
194,85	Third bending mode in lower landing plate, first bending mode in treads, second bending mode in upper landing.
199,30	Second bending in landing, first bending in treads.
201,34	Third bending mode in lower landing plate, first bending mode in treads.
203,54	Third bending mode in lower landing plate, first and second bending mode in treads.
206,34	Third bending mode in lower landing plate, first and third bending mode in treads.
209,48	Third bending mode in lower landing plate, first and second bending mode in treads.
209,99	First and second bending mode in treads.
211,21	Second bending in landing, first bending in treads.
211,87	Second bending in landing, first bending in treads.
213,25	Second bending in landing, first bending in treads.
216,41	Third bending mode in lower landing plate, first bending mode in treads.
218,90	First bending in treads.
219,63	First and second bending in treads and landing.
220,81	Second bending short direction landing, first bending treads
221,73	Third bending mode in landing plate, first and second bending mode in treads.
223,57	Second bending mode in landing plate, first and second bending mode in treads.
225,20	Second bending mode in landing plate, first and second bending mode in treads.
225,73	Second bending short direction landing, first bending mode treads.
227,82	Second bending short direction landing, first bending mode treads.
229,99	Second bending short direction landing, first bending mode treads.
231,97	Second bending short direction landing, first bending mode treads.
232,91	Second bending landing, first bending mode treads.
234,88	Bending short direction landing, first bending mode treads.
235,96	Bending short direction landing, first bending mode treads.
238,05	Bending short direction landing, first bending mode treads and risers.
239,59	Bending short direction landing, second bending mode treads.
239,99	Third bending mode landing, first bending mode treads.
242,70	Third bending mode landing, first bending mode treads.
243,14	Third bending mode landing, second bending mode treads.
244,09	Third bending mode landing, second bending mode treads.
245,84	Bending short direction landing, first bending mode treads.
248,07	Bending short direction landing, second bending mode in treads.
248,54	Bending short direction landing, second bending mode in treads.
250,07	Bending short direction landing, second bending mode in treads.

250,76	Bending short direction landing, second bending mode in treads.
251,95	Bending short direction landing, second bending mode in treads.
252,08	Bending short direction landing, first bending mode in treads.
252,62	Second bending mode in treads.
252,94	Bending short direction landing, second bending mode in treads.
253,07	Second bending mode in treads.
253,97	Bending short direction landing, second bending mode in treads.
254,47	Bending short direction landing, second bending mode in treads.
255,57	Bending short direction landing, second bending mode in treads and risers.
257,04	Bending short direction landing, second bending mode in treads.
258,52	Bending short direction landing, second bending mode in treads and risers.
259,60	Bending short direction landing, first bending mode in treads.
260,26	Disregarded - No motion in landing or flight.
260,47	First and second bending mode in treads.
260,84	Disregarded - No motion in landing or flight.
262,13	Bending short direction landing, second bending mode in treads and risers.
264,10	Bending short direction landing, second bending mode in treads and risers.
264,28	Bending short direction landing, second bending mode in treads and risers.
264,67	Bending short direction landing.
265,41	Bending short direction landing, second bending mode in treads.
265,65	Bending short direction landing, second bending mode in treads.
265,72	Bending short direction landing.
265,89	Bending short direction landing, second bending mode in treads and risers.
267,07	Third bending mode in landing plate and risers. First bending mode in treads.
267,33	Third bending mode in landing plate and risers. First bending mode in treads.
269,29	Bending short direction landing.
269,70	Disregarded - No motion in landing or flight.
271,03	Bending short direction landing, second bending mode in treads and risers.
273,32	Fourth and second bending mode in landing plate, second bending mode in treads.
273,96	Fourth and second bending mode in landing plate, second bending mode in treads and risers.
275,00	Fourth and first bending mode in landing plate, second bending mode in treads.
275,77	Fourth and third bending mode in landing plate, second bending mode in treads.
276,28	Disregarded - No motion in landing or flight.
278,01	Disregarded - No motion in landing or flight.
278,60	Bending short direction landing, second bending mode in treads.
279,75	Bending short direction landing, second bending mode in treads.
281,19	Bending short direction landing, second bending mode in treads.
283,03	Second bending mode in treads and risers.
285,21	Bending short direction landing, third bending mode in treads.
287,29	Disregarded - No motion in landing or flight.
287,54	Disregarded - No motion in landing or flight.
288,51	Bending short direction landing, second bending mode in treads.
289,68	Disregarded - No motion in landing or flight.
290,50	Bending short direction landing, second bending mode in treads.
290,98	Second bending mode in treads and risers.
291,75	Disregarded - No motion in landing or flight.
292,27	Bending short direction landing, second bending mode in treads and risers.
294,49	Fourth bending mode in landing plate, second bending mode in treads.
295,48	Third bending mode in landing plate and treads.
296,17	Disregarded - No motion in landing or flight.
296,54	Second bending mode in treads and risers.
298,91	Bending short direction landing, third bending mode in treads.
300,12	Bending short direction landing, third bending mode in treads.
301,18	Bending short direction landing, third bending mode in treads.
302,46	Bending short direction landing, third bending mode in treads and risers.
303,82	Bending short direction landing, third bending mode in treads and risers.
304,72	Second bending mode in landing plate, third bending mode in treads and risers.
308,60	Bending short direction landing, third bending mode in treads and risers.

310,51	Bending short direction landing, third bending mode in treads and risers.
311,09	Third bending mode in treads and risers.
312,44	Bending short direction landing, third bending mode in treads and risers.
312,79	Third bending mode in treads and risers.
314,08	Third bending mode in treads and risers.
315,16	Third bending mode in treads and risers.
318,43	Fourth bending mode in landing plate.
318,95	Fourth bending mode in landing plate, third bending mode in treads, torsion in beams under landing.
321,11	Bending short direction landing, third bending mode in treads.
321,31	Bending short direction landing, third bending mode in treads.
321,59	Bending short direction landing, third bending mode in treads.
321,81	Bending short direction landing, third bending mode in treads.
322,58	Bending short direction landing, third bending mode in treads and risers, torsion in beams under landing.
323,49	Bending short direction and fourth bending mode in landing, third bending mode in treads.
325,54	Fourth bending mode in landing plate, third bending mode in treads.
326,73	Fourth bending mode in landing plate, third bending mode in treads.
327,76	Fourth bending mode in landing plate, third bending mode in treads, torsion in beams under landing.
328,37	Disregarded - No motion in landing or flight.
328,42	Third bending mode in treads, torsion in beams under landing.
329,22	Third bending mode in treads and risers.
330,20	Fourth bending mode in landing plate, third bending mode in treads.
331,28	Disregarded - No motion in landing or flight.
334,32	Bending short direction landing, third bending mode in treads and risers, torsion in beams under landing.
335,58	Bending short direction landing, third bending mode in treads and risers, torsion in beams under landing.
336,43	Third bending mode in treads and risers.
336,54	Disregarded - No motion in landing or flight.
336,63	Third bending mode in treads and risers.
337,01	Bending short direction landing, third bending mode in treads, torsion in beams under landing.
337,45	Disregarded - No motion in landing or flight.
339,17	Bending short direction landing, third bending mode in treads, torsion in beams under landing.
339,80	Third bending mode in treads, torsion in beams under landing.
340,56	Bending short direction landing, third bending mode in treads, torsion in beams under landing.
341,05	Third bending mode in landing plate, torsion in beams under landing.
342,60	Third bending mode in treads and risers, torsion in beams under landing.
343,15	Third bending mode in treads and risers, torsion in beams under landing.
343,51	Bending short direction landing, third bending mode in treads, torsion in beams under landing.
344,54	Fourth bending mode in landing plate, second bending mode in treads, torsion in beams under landing.
345,57	Fourth bending mode in landing plate, second bending mode in treads, torsion in beams under landing.
346,88	Disregarded - No motion in landing or flight.
346,96	Third bending mode in treads and risers.
347,07	Disregarded - No motion in landing or flight.
347,65	Fourth bending mode in landing plate, second bending mode in treads, torsion in beams under landing.
348,36	Fourth bending mode and bending in short direction landing plate.
348,57	Fourth bending mode and bending in short direction landing plate.
349,05	Fourth and third bending mode and bending in short direction landing plate, torsion in beams under landing.
349,38	Fourth bending mode in landing plate and treads.

350,13	Fourth and third bending mode in landing plate, second bending mode in treads and risers.
351,41	Fourth and third bending mode in landing plate.
351,91	Fourth and third bending mode in landing plate, torsion in beams under landing.
354,83	Fourth bending mode in landing plate, torsion in beams under landing.
358,97	Bending short direction landing, fourth bending mode in treads, torsion in beams under landing.
360,85	Bending short direction landing, third bending mode in treads, torsion in beams under landing.
364,74	Bending short direction landing, second bending mode in treads.
365,73	Fourth bending mode in landing plate, third bending mode in treads.
366,85	Fourth bending mode in landing plate, third bending mode in treads and risers, torsion in beams under landing.
370,31	Fourth bending mode in landing plate, third bending mode in treads and risers, torsion in beams under landing.
371,63	Bending short direction landing, second bending mode in treads.
372,21	Bending short direction landing, third bending mode in treads, torsion in beams under landing.
374,77	Disregarded - No motion in landing or flight.
377,72	Fourth bending mode in landing plate, third bending mode in treads and risers.
380,07	Fourth bending mode in landing plate, third bending mode in treads and risers.
382,95	Disregarded - No motion in landing or flight.
384,28	Disregarded - No motion in landing or flight.
386,85	Fifth bending mode and bending short direction landing, third bending mode in treads, torsion in beams under landing.
387,77	Bending short direction landing, third bending mode in treads.
389,66	Bending short direction landing, fourth bending mode in treads.
390,46	Bending short direction landing, fourth bending mode in treads and risers, torsion in beams under landing.
391,18	Third bending mode in treads and risers, twisting of stringers.
392,33	Third bending mode in treads and risers, twisting of stringers.
395,29	Fourth bending mode in landing plate, treads and risers, twisting of stringers.
396,04	Fourth bending mode in landing plate.
397,10	Fourth bending mode in treads and risers.
397,77	Fourth bending mode in landing plate, treads and risers.
398,60	Fourth bending mode in landing plate, treads and risers.
398,72	Fourth bending mode in landing plate.
399,48	Bending short direction landing, fourth bending mode in treads and risers.

Appendix A2

Visual identification of motion in natural frequencies from measurements.

Setup 1			
Mode	Frequency [Hz]	Type of motion	Damping [%]
1	47,333	Global motion in landings and treads.	13,37
2	56,041	Weak global motion, highest in landings.	4,67
3	58,926	Some motions in landings.	14,18
4	60,566	Weak global motion, highest in landings.	2,88
5	66,091	Weak global motion, highest in landings.	11,31
6	68,759	Global motion, highest in landings.	3,73
7	74,661	Global motion, highest in landings.	3,96
8	86,523	Global motion in landings.	8,33
9	91,911	Plate motion in landing.	4,76
10	112,541	Plate motion in landings and treads.	2,06
11	123,376	Plate motion in landings.	4,56
12	123,954	Plate motion in landings, treads and riser.	2,49
13	129,16	Plate motion in landings, second bending mode.	4,24
14	147,704	Plate motion in landings and vague torsion in landings and treads.	1,67
15	153,812	Plate motion in landings and treads.	3,48
16	179,565	Plate motion in landings and treads.	1,90
17	186,794	Plate motion, mainly in landings.	1,44
18	189,461	Plate motion, mainly in landings.	6,00
19	190,887	Plate motion in landings and treads.	1,28
20	192,675	Plate motion in landings and treads.	1,52
21	192,843	Plate motion, mainly in landings.	3,73
22	203,76	Plate motion in landings and treads.	3,28
23	204,156	Plate motion in landings and treads.	3,66
24	219,795	Plate motion in landings and treads.	1,83
25	221,93	Plate motion, mainly in landings.	3,12
26	229,034	Plate motion in landings and treads.	2,97
27	231,107	Plate motion in landings and treads. Possibly second bending mode in treads.	2,94
28	232,433	Plate motion in landings and treads.	1,99
29	247,505	Complex plate motion in landings. Possibly second bending mode in treads.	2,38
30	258,302	Complex plate motion in landings. Possibly third bending mode in treads.	1,71
31	273,47	Plate motion, mainly in landings.	1,46
32	279,476	Plate motion, mainly in landings.	2,12
33	279,489	Plate motion, mainly in landings.	2,05
34	284,797	Complex plate motion in landings. Possibly second bending mode in treads.	1,67
35	290,568	Complex plate motion in landings. Possibly second bending mode in treads.	1,95
36	299,638	Complex plate motion in landings. Possibly second bending mode in treads.	1,54

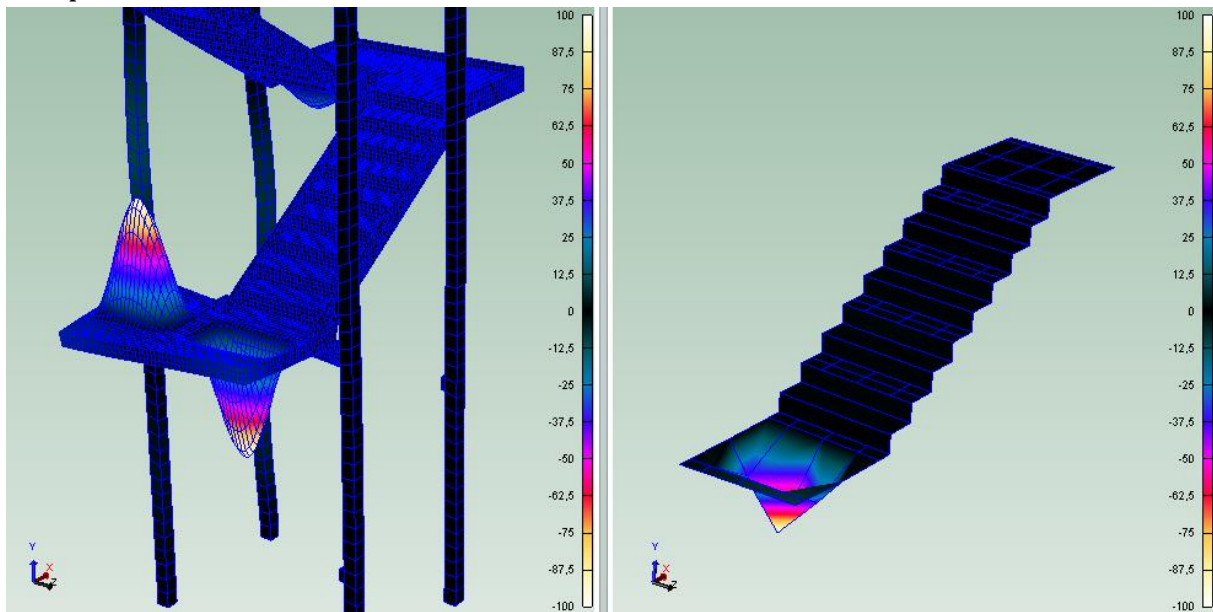
37	305,698	Complex plate motion in landings. Possibly third bending mode in treads.	1,77
38	308,134	Complex plate motion in landings. Possibly third bending mode in treads.	2,61
39	319,798	Complex plate motion in landings. Possibly second bending mode in treads.	3,18
40	320,861	Complex plate motion in landings. Possibly second bending mode in treads.	2,94
41	338,387	Complex plate motion in landings and treads.	0,68
42	344,088	Complex plate motion in landings and treads.	1,27
43	344,236	Complex plate motion, mainly in landings.	2,17
44	350,921	Complex plate motion in landings and treads.	1,11
45	353,951	Complex plate motion in landings and treads.	1,81
46	358,444	Complex plate motion in landings and treads.	0,90
47	361,01	Complex plate motion in landings and treads.	1,48
48	361,976	Complex plate motion, mainly in landings.	2,52
49	369,886	Complex plate motion in landings and treads.	1,75
50	374,165	Complex plate motion in landings and treads.	1,97
51	374,531	Complex plate motion in landings and treads.	1,48

Setup 2		
Mode	Frequency [Hz]	Type of motion
1	50,092	Complex motion, possibly global.
2	55,907	Global motion.
3	66,832	Complex motion, possibly global.
4	82,308	Complex motion, possibly global.
5	87,927	Complex motion, possibly global.
6	89,6	Plate motion.
7	91,602	Plate motion, possibly global.
8	124,708	Second bending mode.
9	128,719	Complex motion, possibly global. First bending mode in plate close to flight.
10	187,746	Complex motion, first bending mode in plate close to flight.
11	187,849	Plate motion, possibly global.
12	230,861	Complex motion.
13	264,812	Complex motion, second bending mode in plate close to flight.
14	265,088	Complex motion, second bending mode in plate close to flight.
15	269,308	Complex motion, second bending mode in plate close to flight.
16	275,512	Complex motion, second bending mode in plate close to flight.
17	280,004	Complex motion, second bending mode in plate close to flight.
18	301,861	Complex motion, second bending mode in plate close to flight.
19	306,779	Complex motion, second bending mode in plate close to flight.
20	317,188	Complex motion, second bending mode in plate close to flight.
21	341,368	Complex motion, second bending mode in plate close to flight.
22	363,174	Complex motion, second bending mode in plate close to flight.
23	366,952	Complex motion, second bending mode in plate close to flight.
24	377,024	Complex motion, second bending mode in plate close to flight.
Hard to distinguish modes due to too few measurement points.		

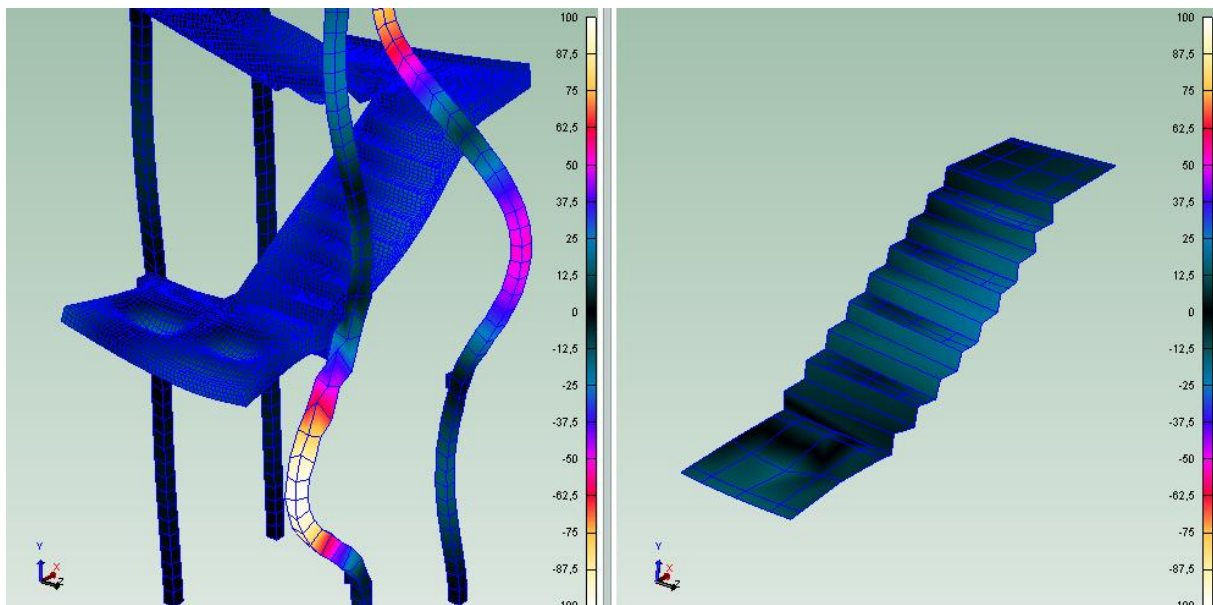
Setup 3		
Mode	Frequency [Hz]	Type of motion
1	50,0482	Plate motion in tread and riser. First bending mode.
2	68,4193	Plate motion in tread and riser. First bending mode.
3	78,5991	Plate motion in tread and riser. First bending mode.
4	124,812	Plate motion in tread and riser. First bending mode.
5	136,177	Plate motion in tread and riser. First bending mode.
6	139,480	Plate motion in tread and riser. First bending mode.
7	186,487	Plate motion in tread and riser. First bending mode.
8	189,519	Plate motion in tread and riser. First bending mode.
9	192,998	Plate motion in tread and riser. First bending mode.
10	210,958	Plate motion in tread and riser. First bending mode.
11	213,610	Plate motion in tread and riser. Second bending mode.
12	230,660	Plate motion in tread and riser. Second bending mode.
13	259,099	Plate motion in tread and riser. Second bending mode.
14	279,093	Plate motion in tread and riser. Second bending mode.
15	285,927	Plate motion in tread and riser. Possibly third bending mode.
16	303,849	Plate motion in tread and riser. Possibly third bending mode.
17	353,101	Plate motion in tread and riser. Possibly third bending mode.
18	370,454	Plate motion in tread and riser. Possibly third bending mode.
19	374,149	Plate motion in tread and riser. Possibly third bending mode.
20	375,587	Plate motion in tread and riser. Possibly third bending mode.
Hard to distinguish modes and unable to identify global motions due to too few measurement points.		

Appendix A3

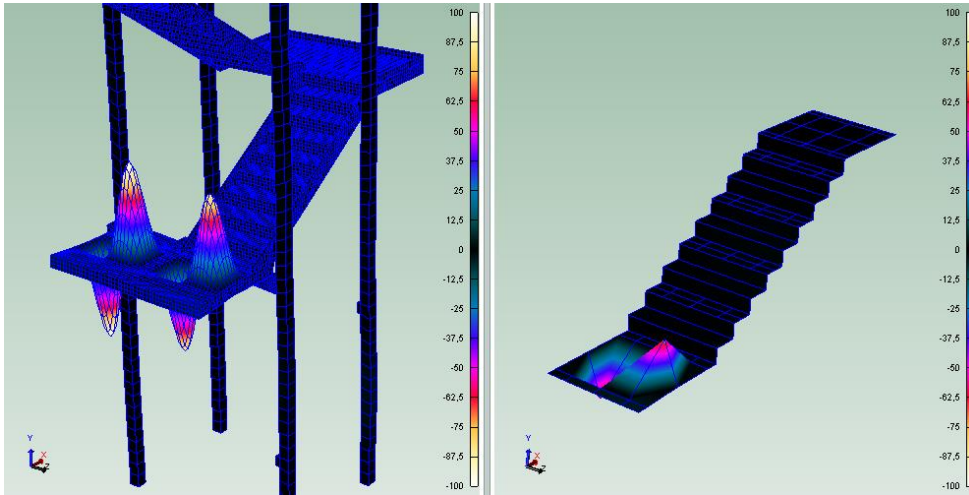
Comparison initial decimated model and FE-model.



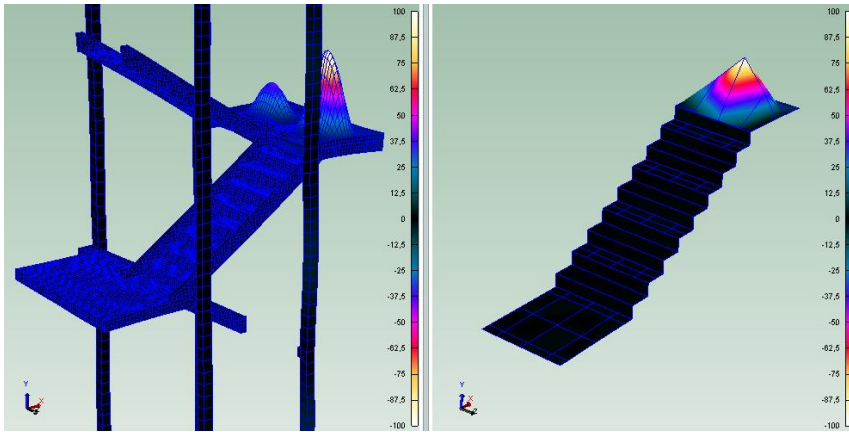
88,49 Hz. First bending mode in the landing (mode 4)



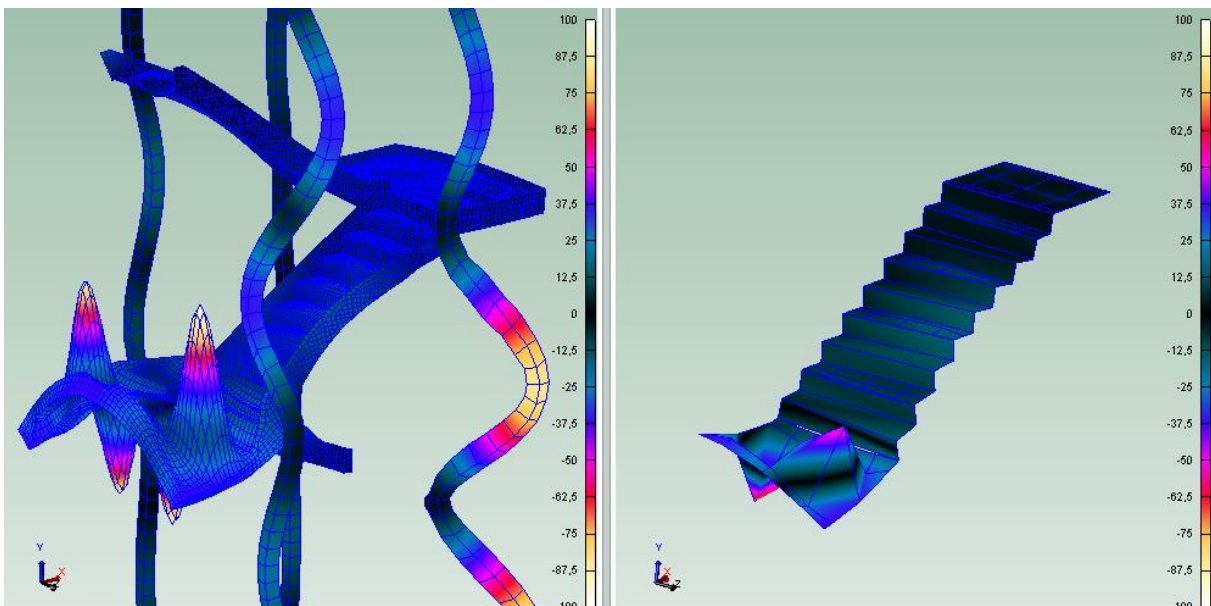
92,821 Hz (mode 7). First bending mode in the landing with torsion over the whole flight



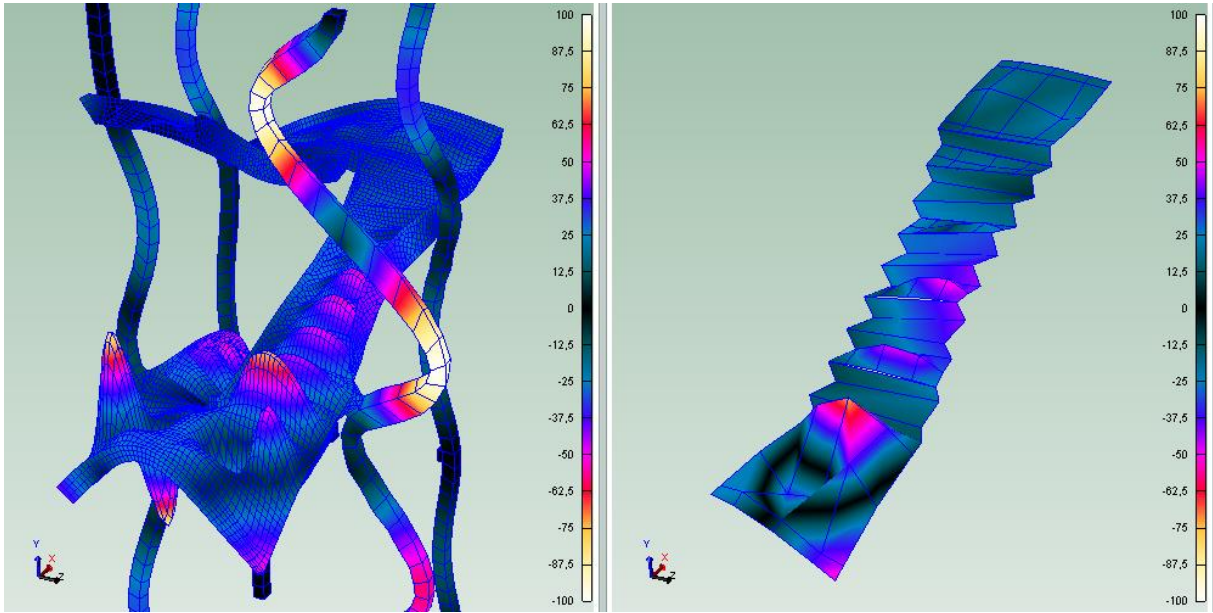
122,65 Hz (mode 22). Second bending mode in the landing



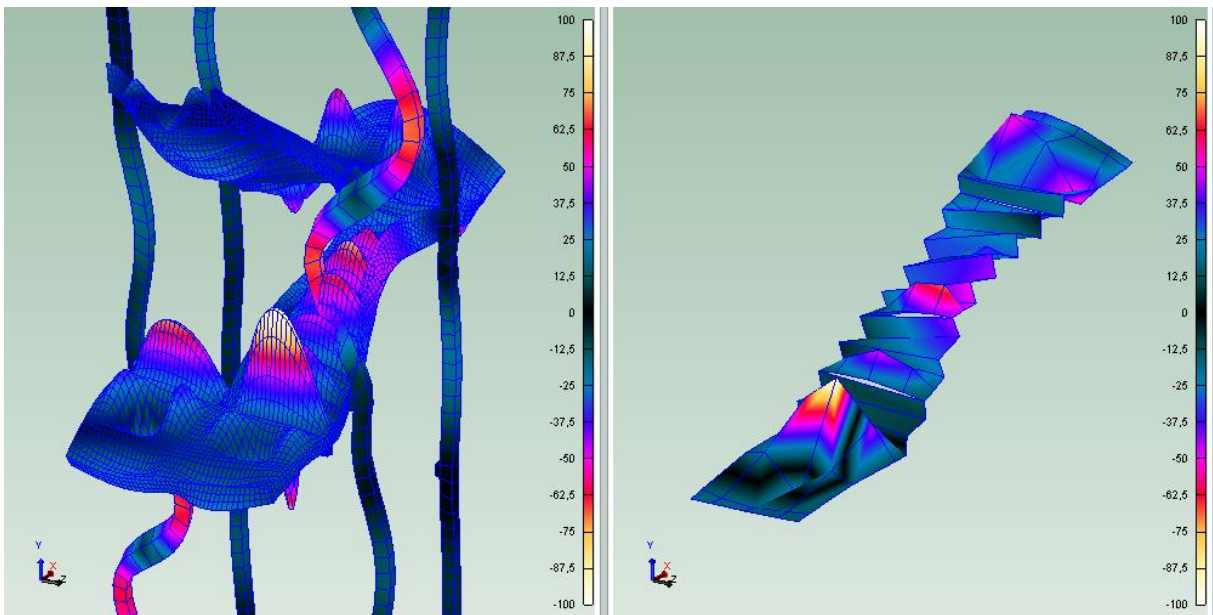
133,16 Hz (mode 27). First bending mode in the upper landing



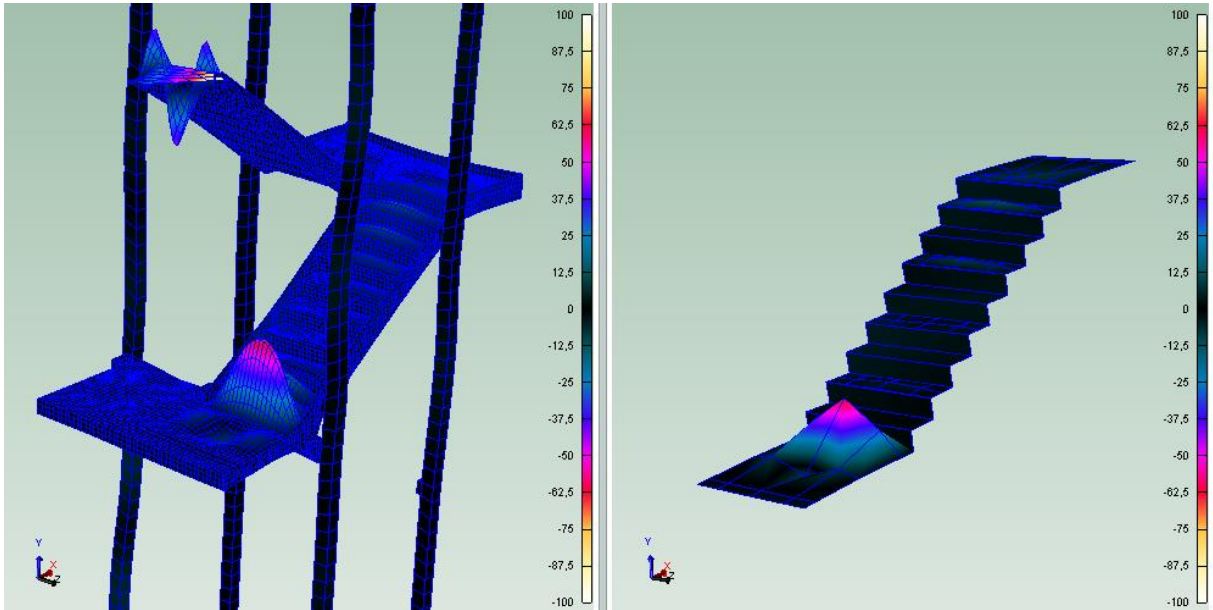
134,54 Hz (mode 29). Second bending mode in the landing and torsion mode over the flight.



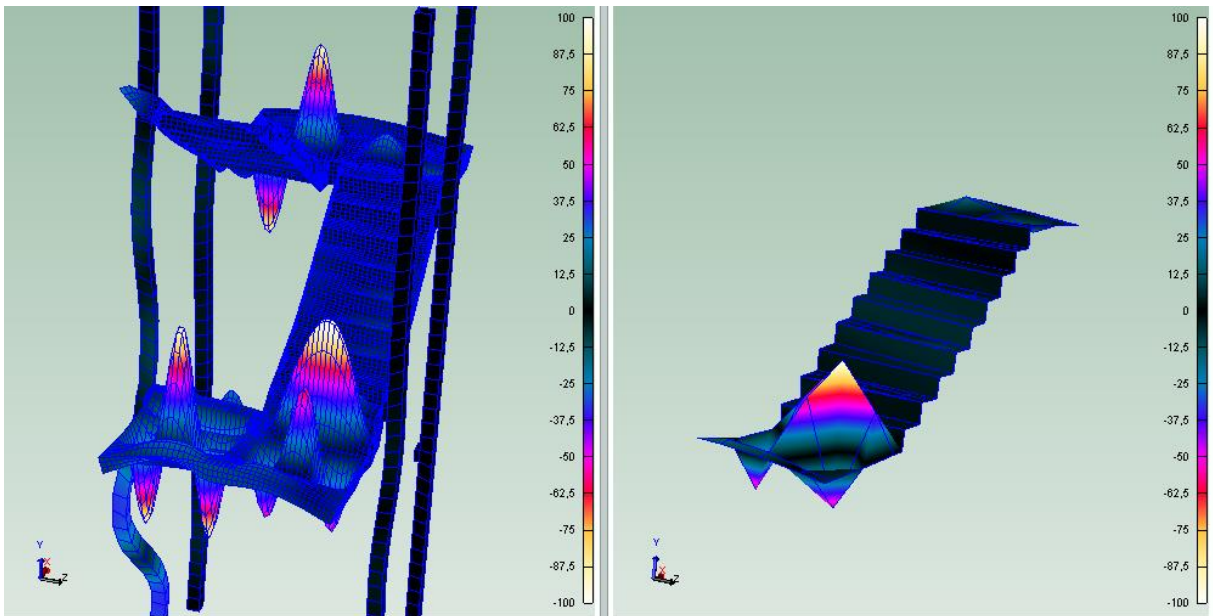
140,35 Hz (mode 31). The Decimated model fails to recognize the difference between the second mode in the landing and the first bending mode in the first tread



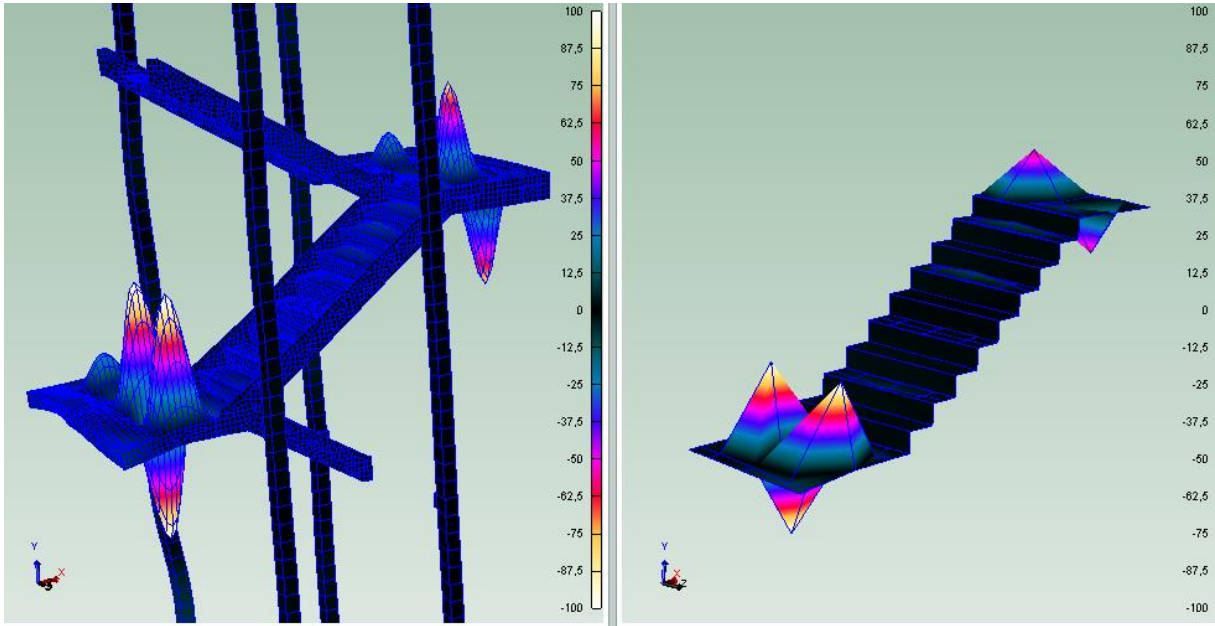
160,26 Hz (Mode 36). The decimated model fails to recognize the third bending mode in the landing because of the strong first bending mode in the first step. In the rest of the flight it looks good.



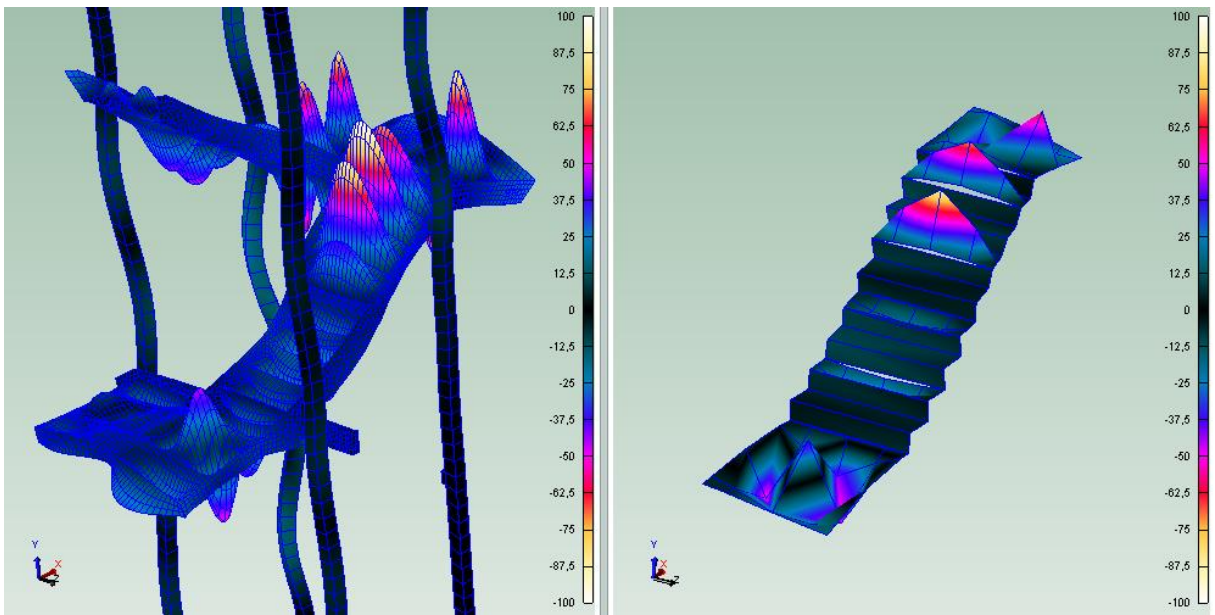
172,82 Hz (mode 42). Same problem as in the two mode forms above.



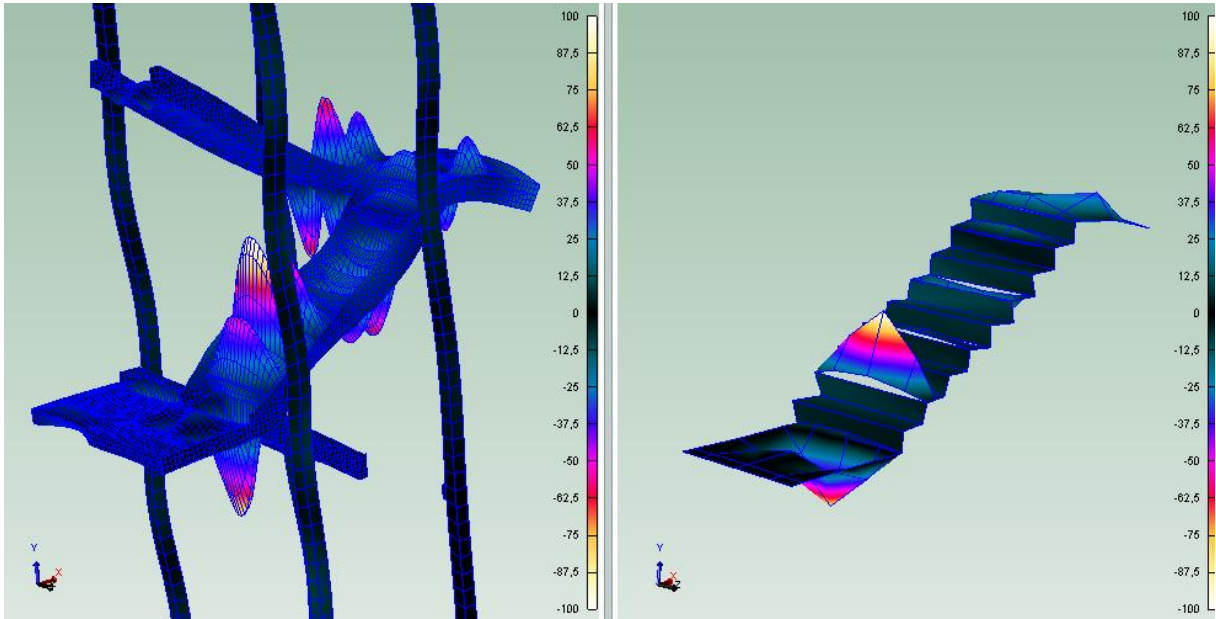
180,95 Hz (mode 44). The same problem as the three mode forms above.



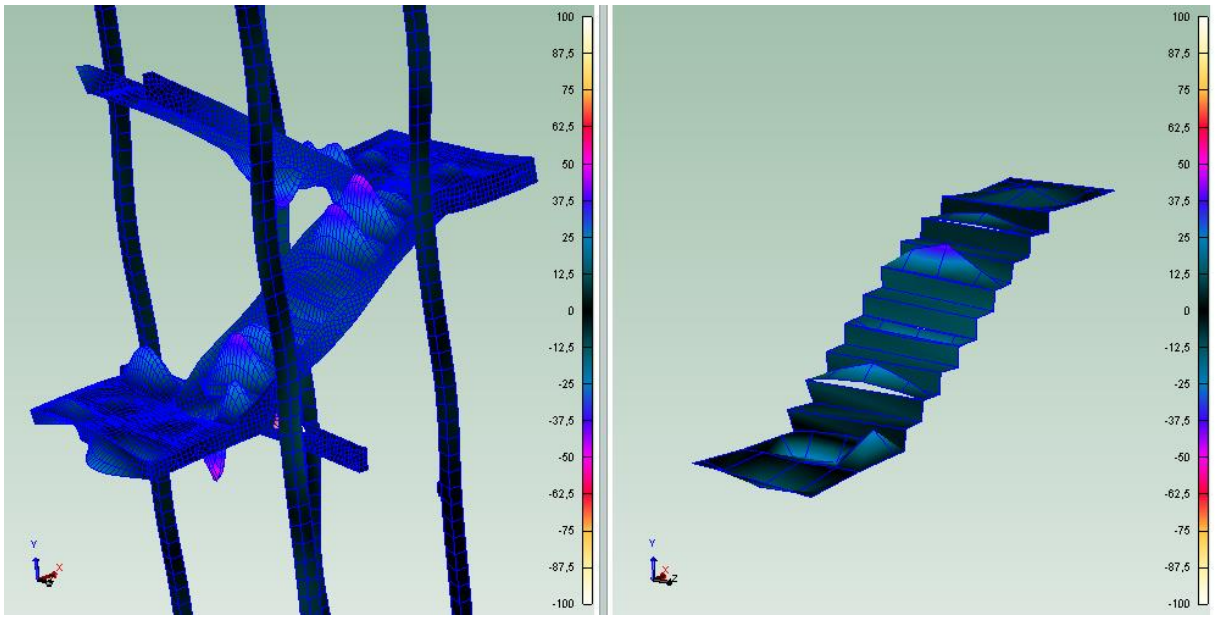
183,59 Hz (mode 47).



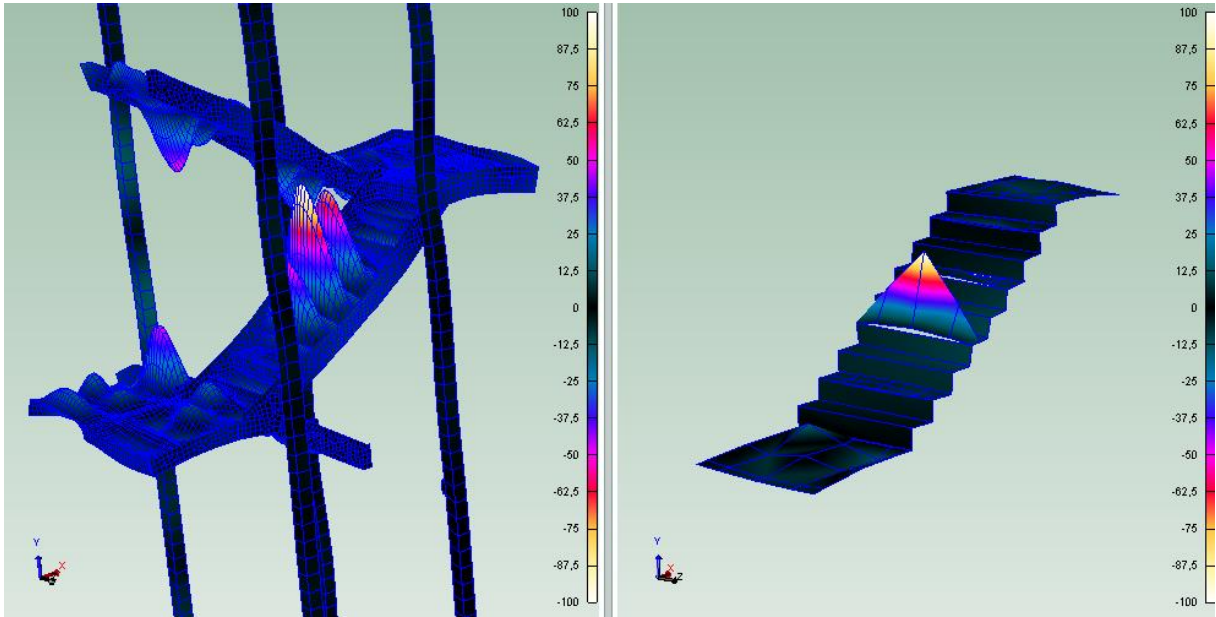
190,93 Hz (mode 51)



194,85 Hz (mode 53)



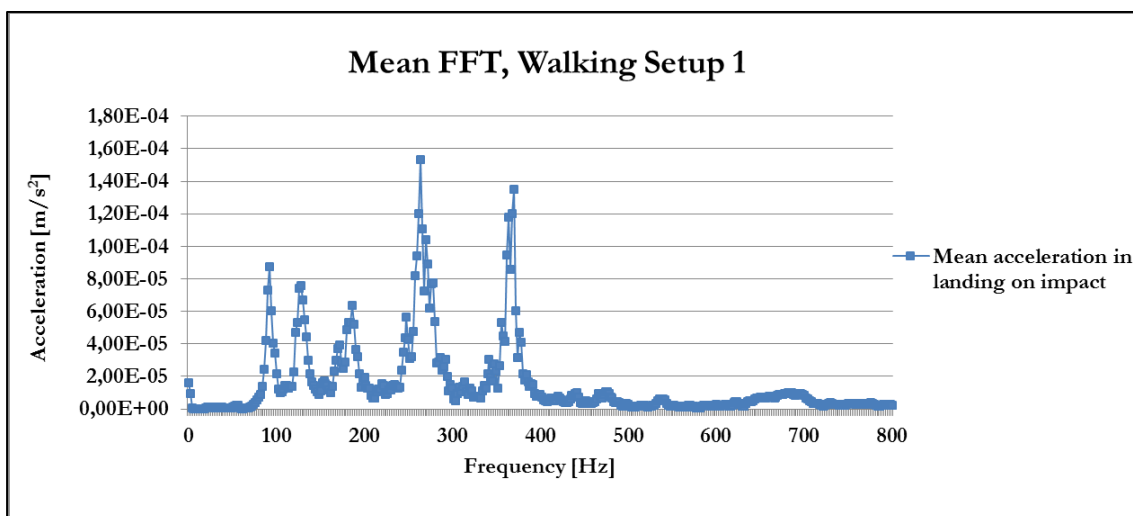
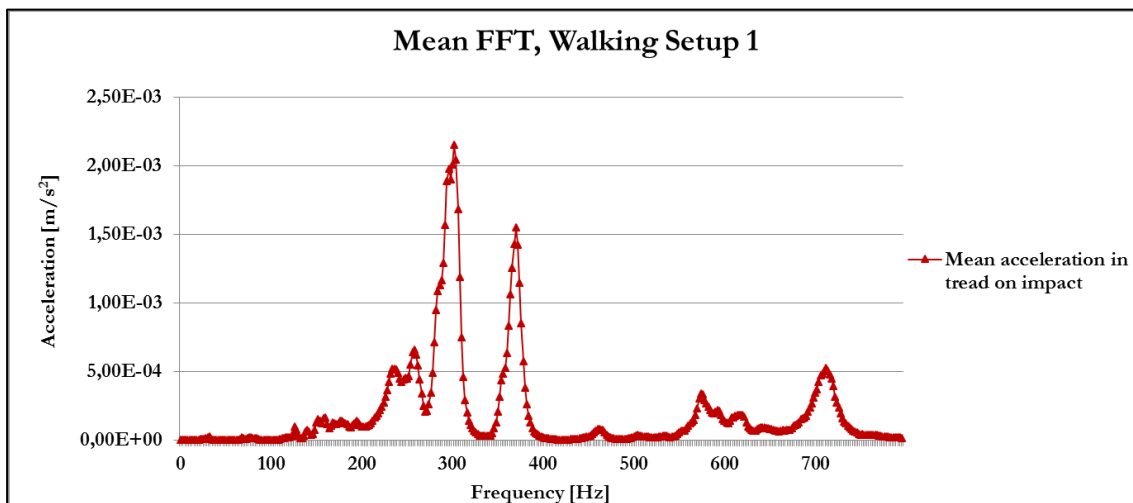
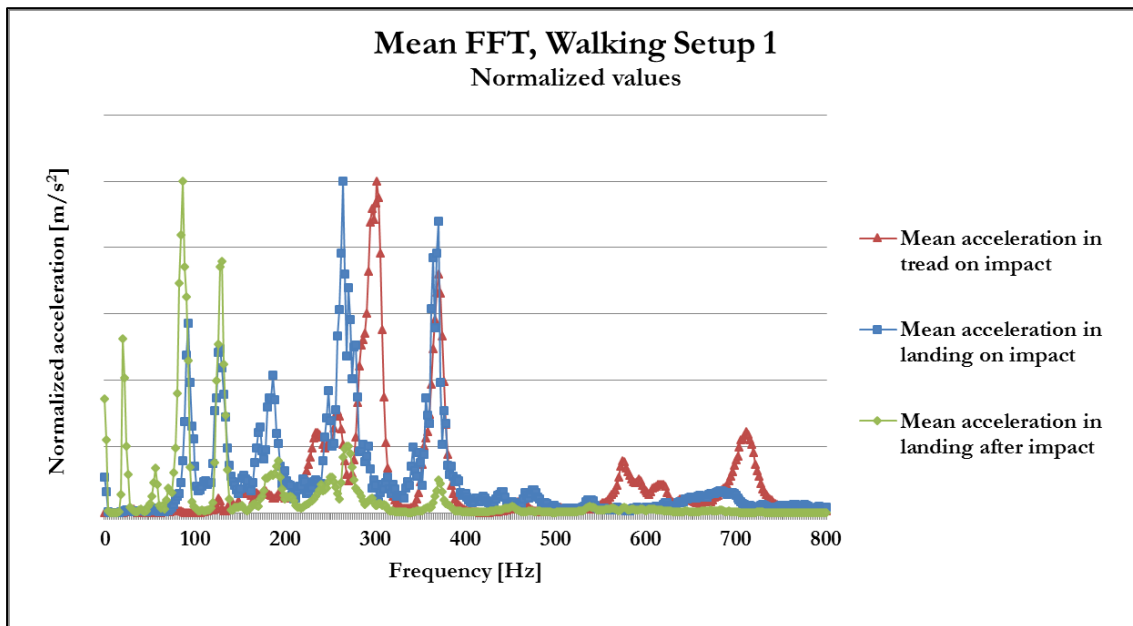
206,34 Hz (mode 57).

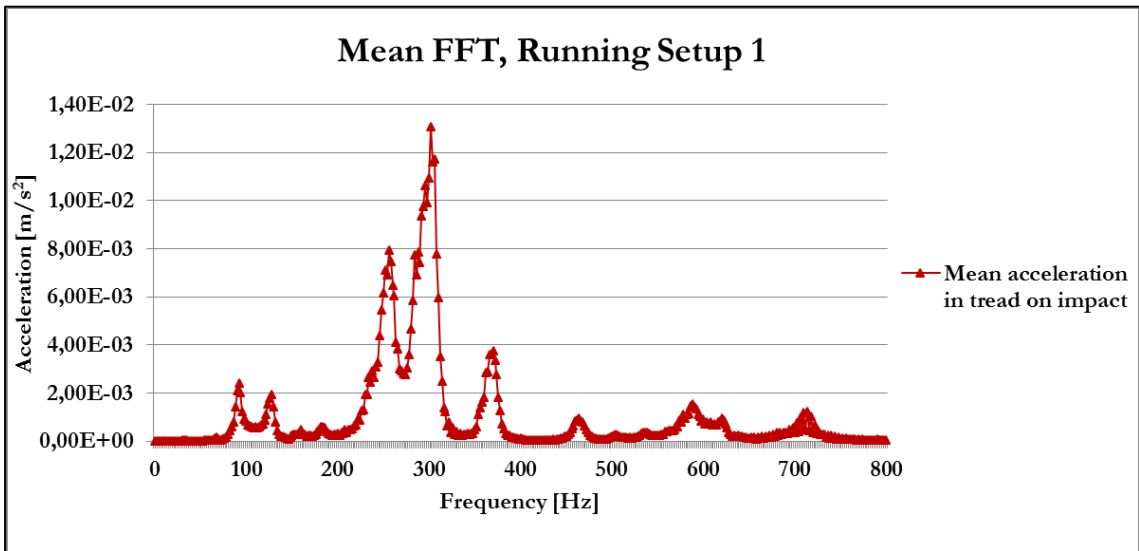
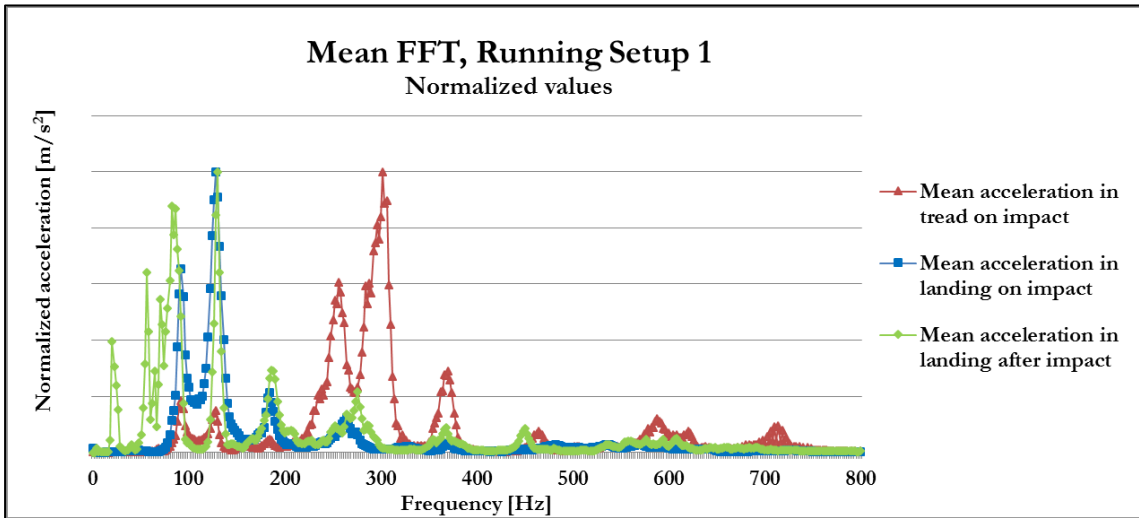
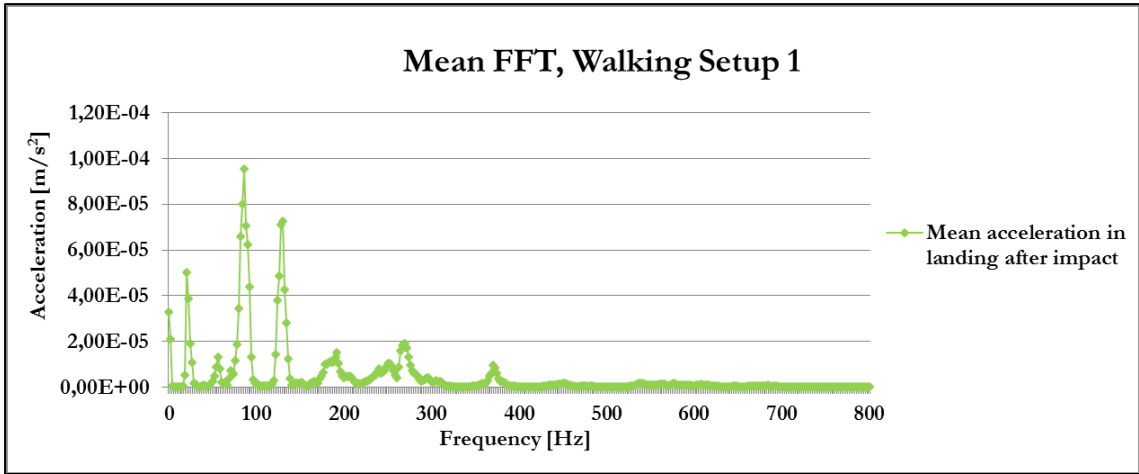


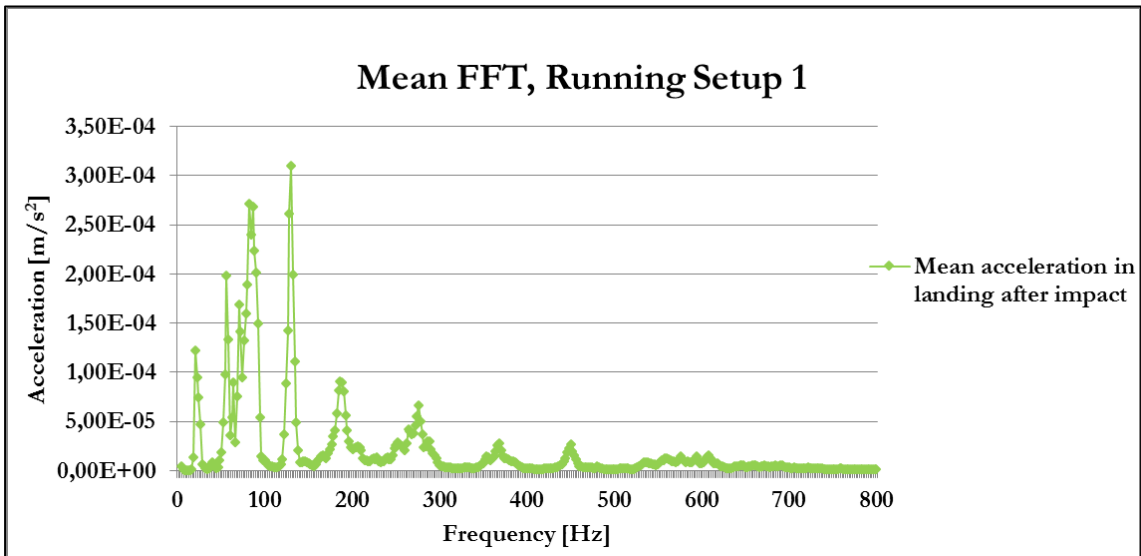
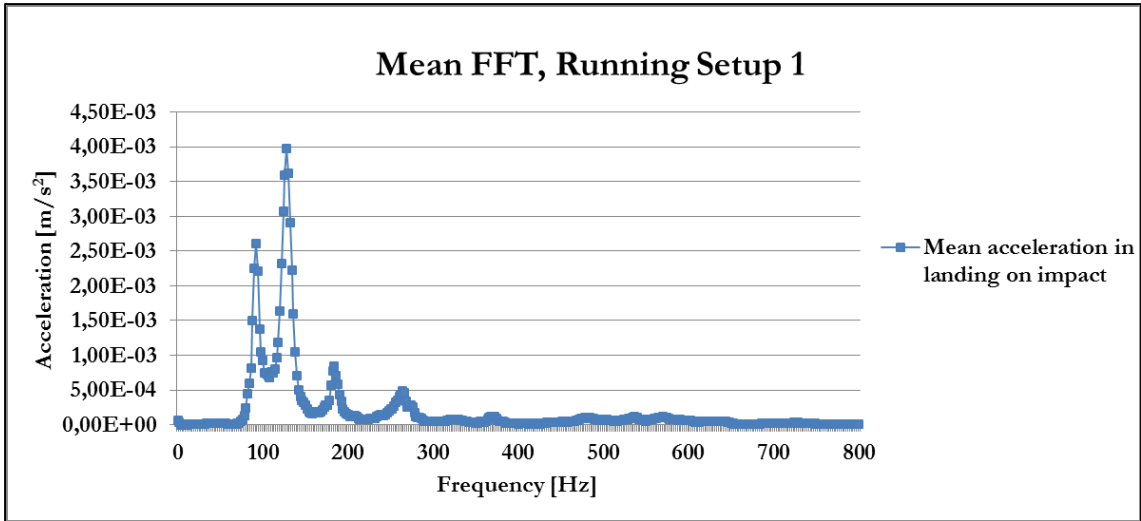
216,41 Hz (mode 63)

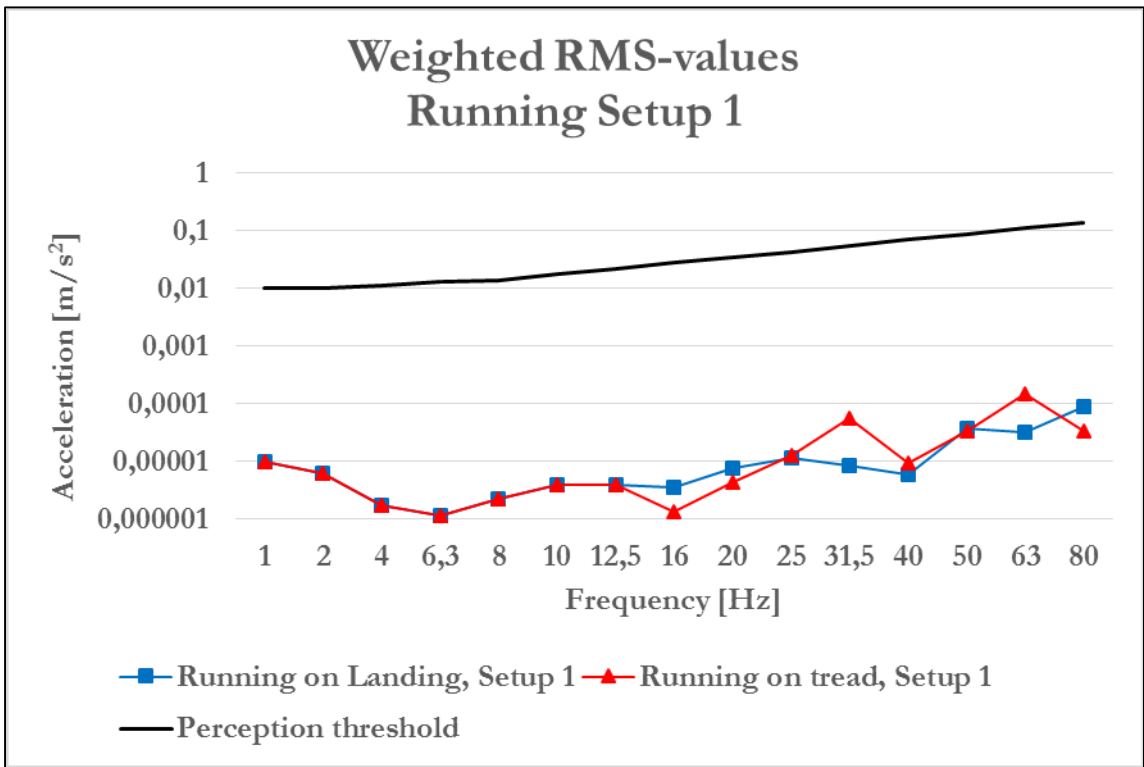
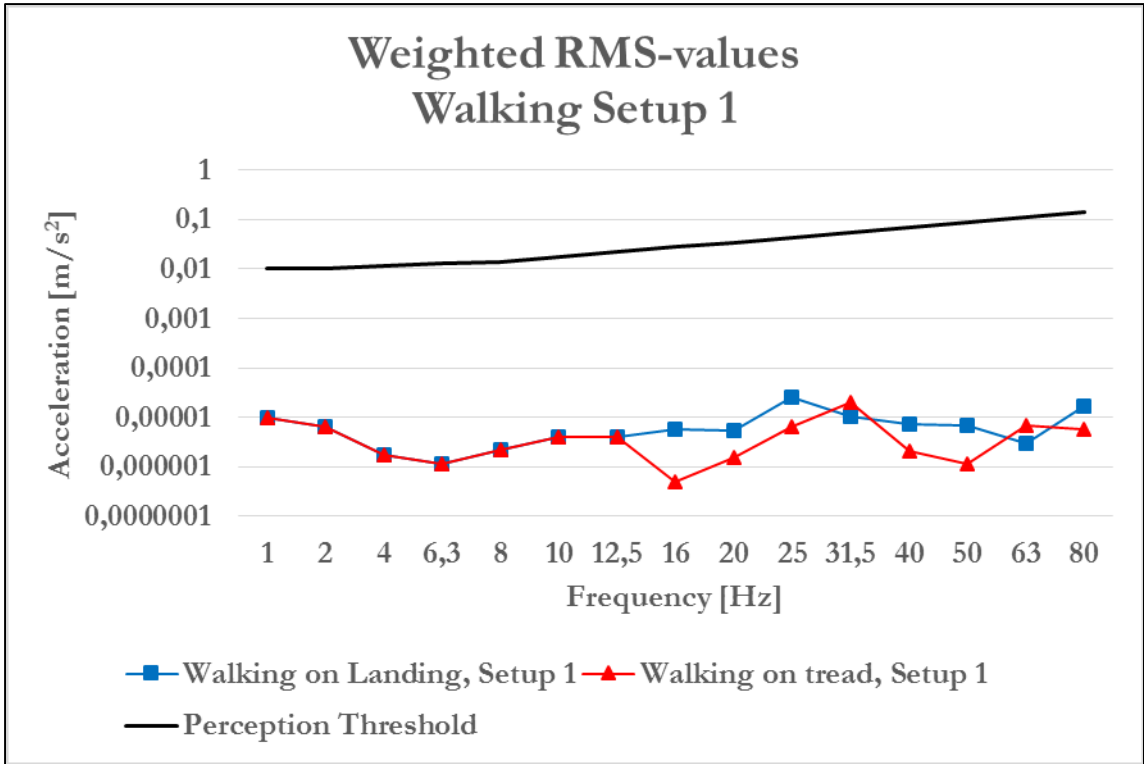
Appendix B1

Measurement data vibration from walking and running setup 1.



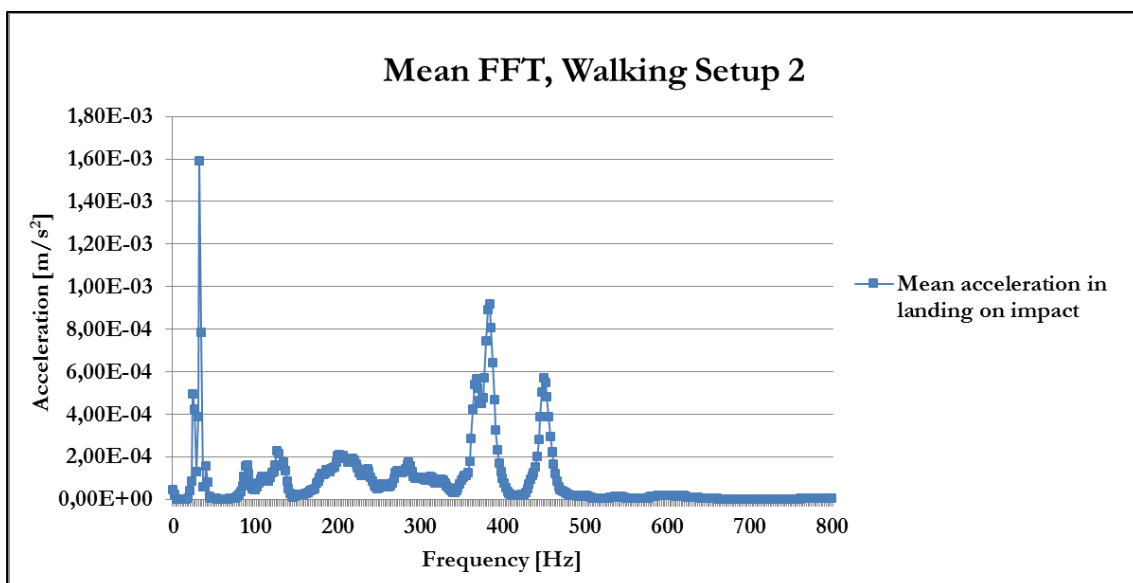
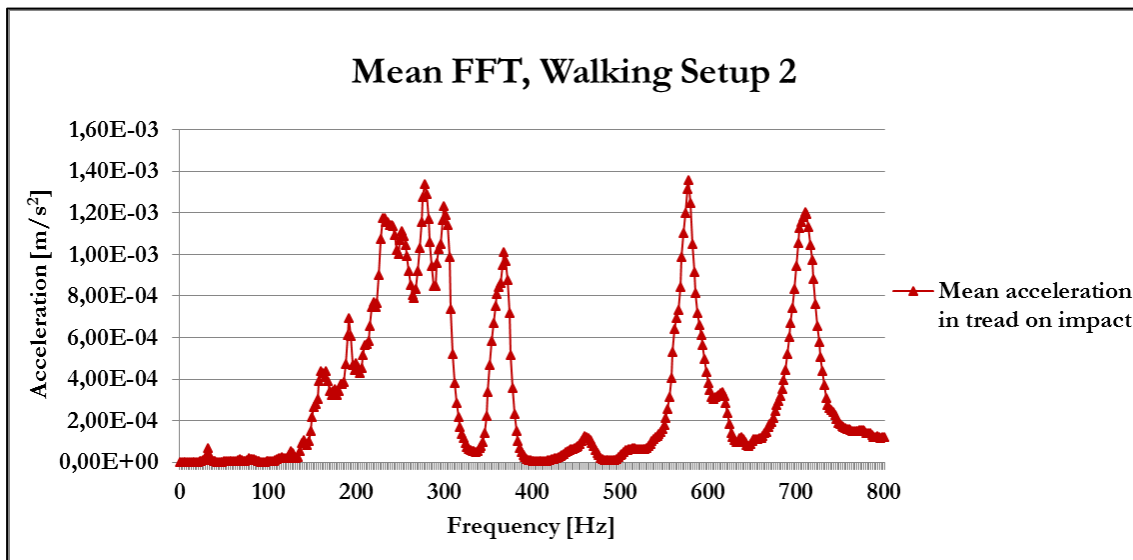
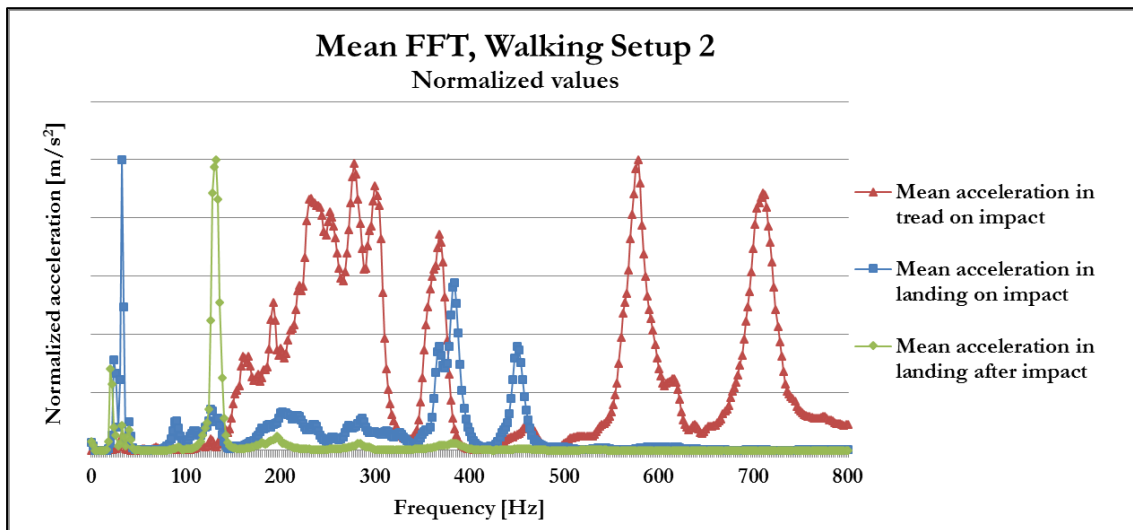


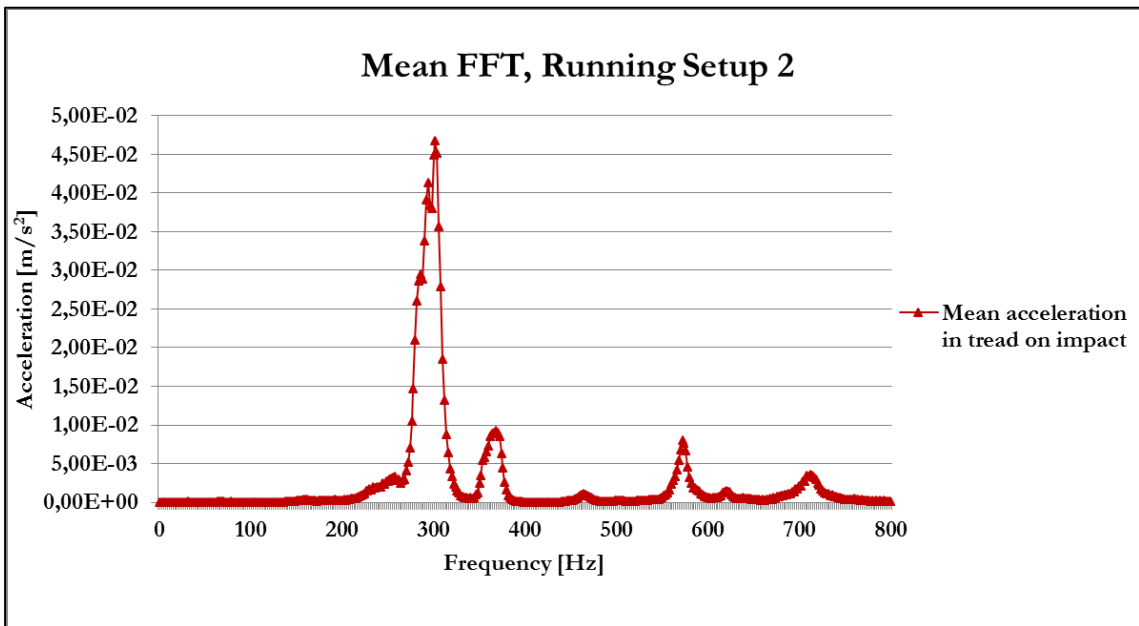
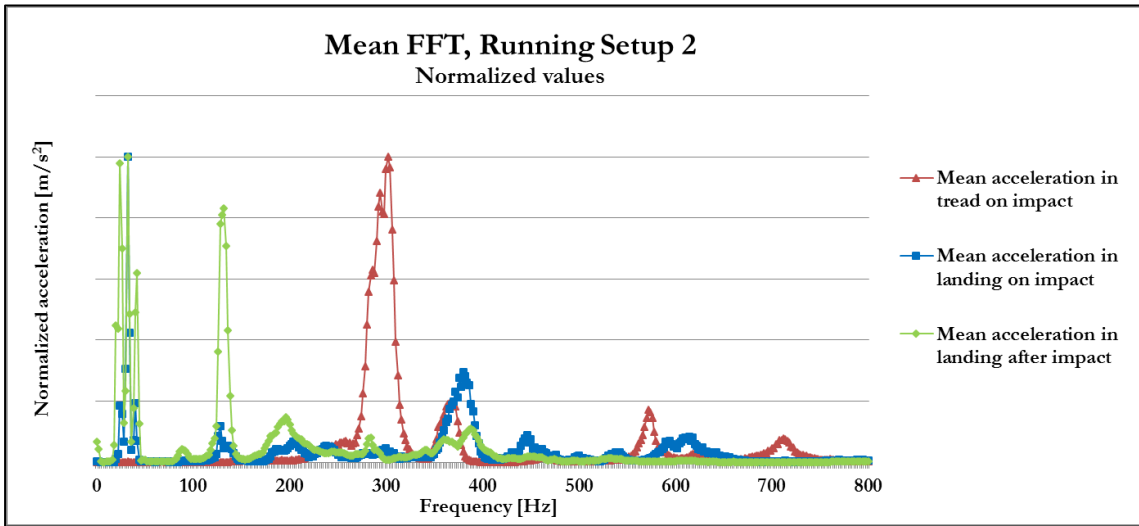
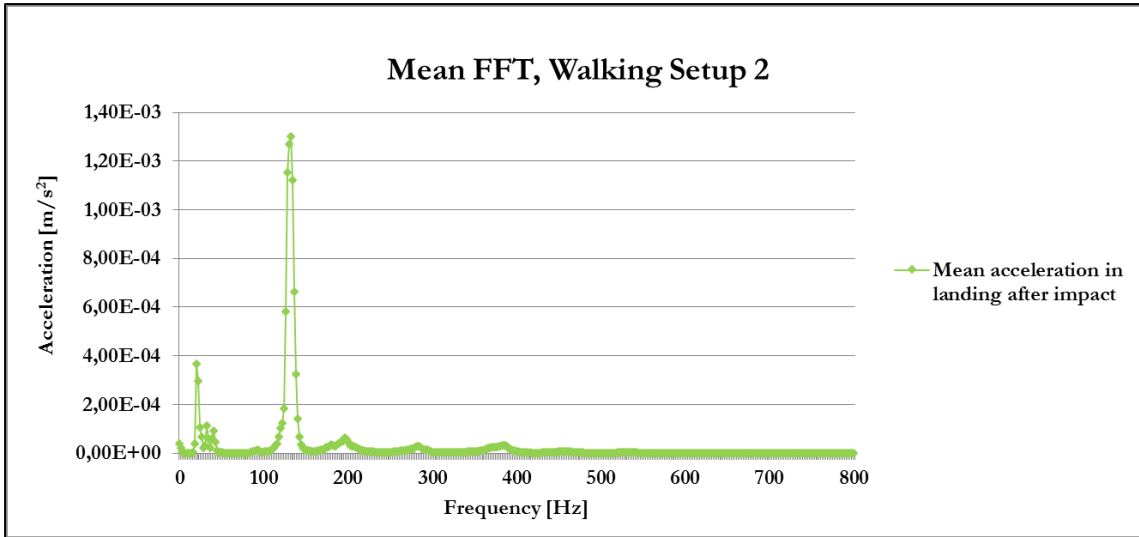


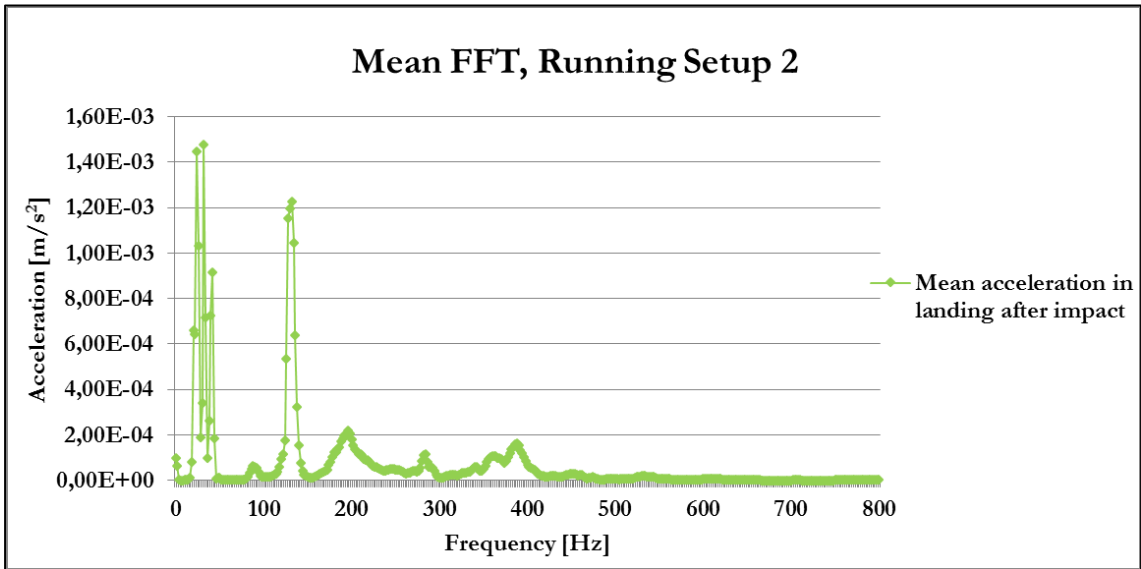
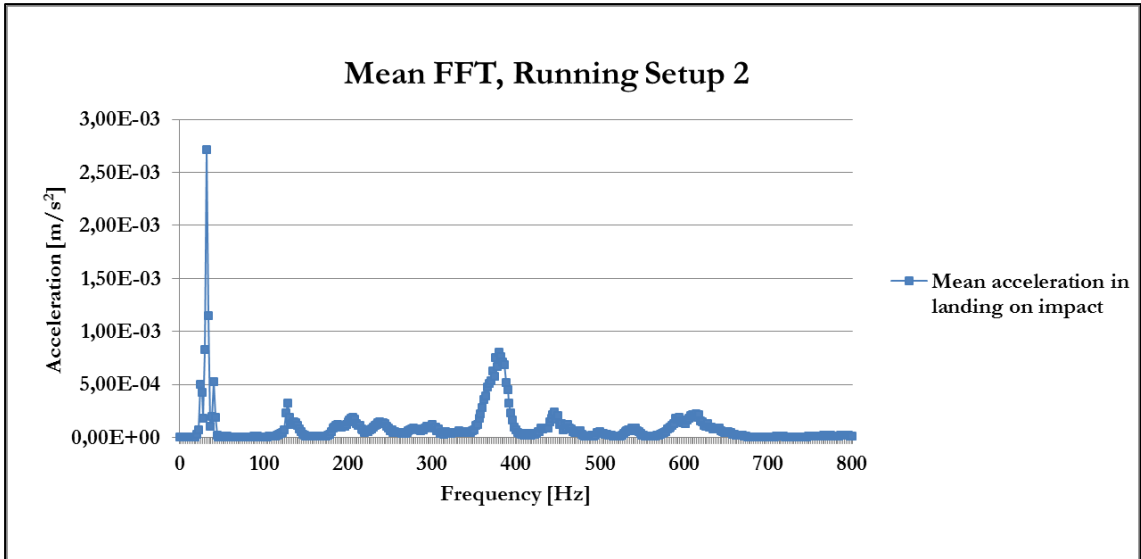


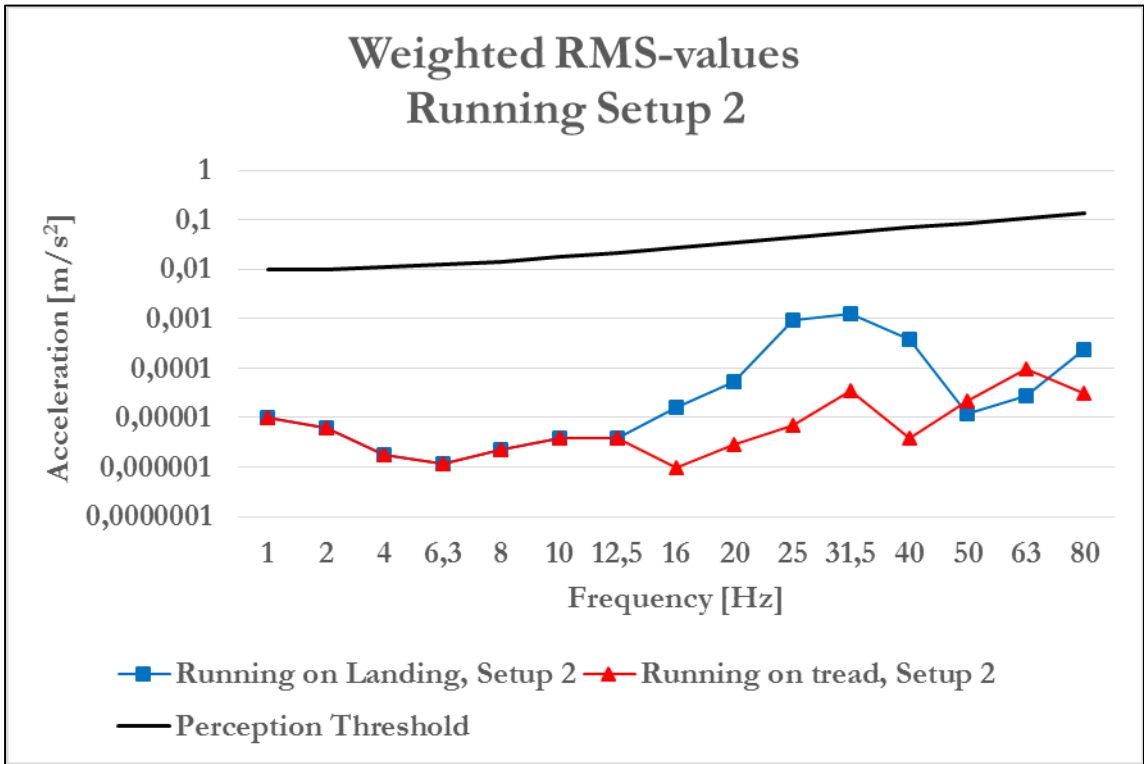
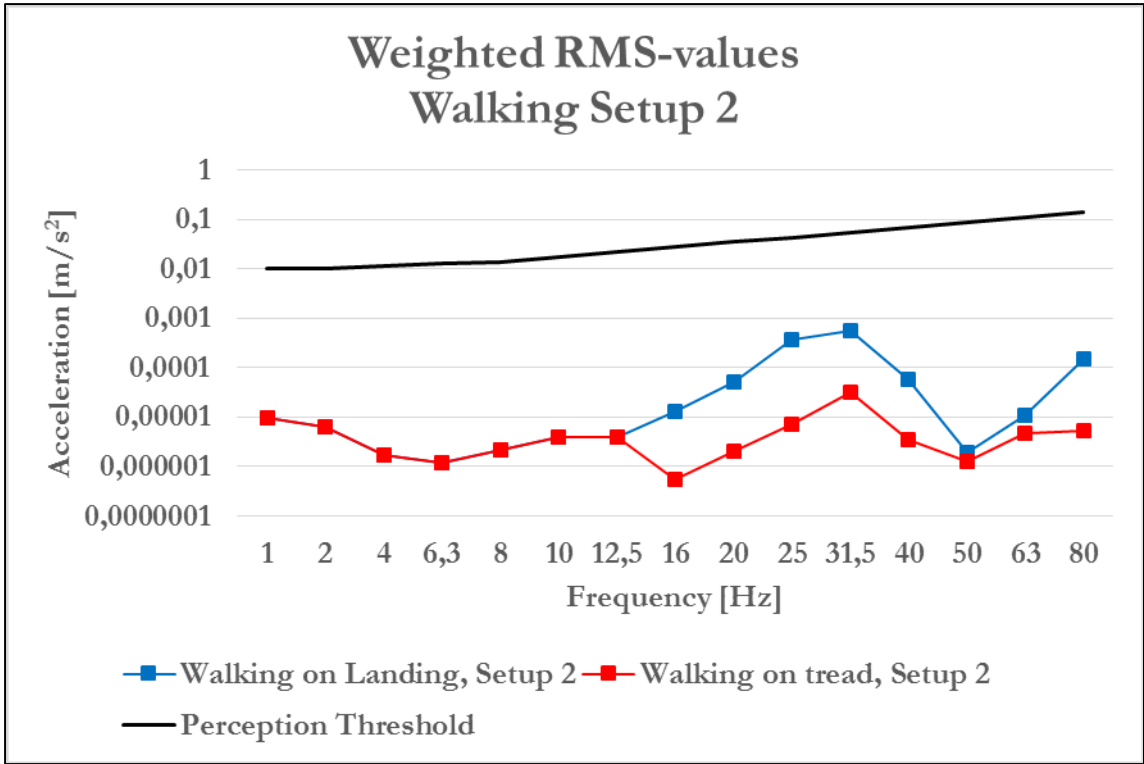
Appendix B2

Measurement data vibration from walking and running setup 2.









Appendix C1

Visual comparison for validation and AutoMAC of mode shapes in setup 1.

Modes from measurements [Hz]	Good resemblance with [Hz] (Orthogonality)	Some resemblance with [Hz] (Orthogonality)
47,333	None	46,507 (0,931)
56,041	None	55,791 (-28,167) 110,68 (0,969)
58,926	None	None
60,566	None	57,729 (25,324)
66,091	62,952 (41,185)	None
68,759	71,329 (-43,05)	None
74,661	None	71,329 (-6,172)
86,523	86,538 (462,808)	None
91,911	None	103,52 (0,676)
112,541	None	None
123,376	122,65 (-6,599)	None
123,954	None	122,65 (-0,876) 140,85 (-1,514)
129,16	129,24 (20,293)	None
147,704	148,66 (-14,513) 140,85 (-1,082)	160,21 (-1,379)
153,812	152,62 (-2,158)	138,74 (-0,96)
179,565	None	161,75 (1,343)
186,794	None	186,96 (11,006)
189,461	None	None
190,887	None	190,83 (-9,659)
192,675	None	192,01 (-12,642)
192,843	None	192,01 (-22,541)
203,76	None	203,54 (-89,992)
204,156	None	203,54 (-89,992) 209,48 (1,868)
219,795	219,63 (48,583)	None
221,93	None	220,81 (27,1) 213,25 (1,312)
229,034	None	None
231,107	None	None
232,433	None	232,91 (-44,992)
247,505	248,07 (3,197) 248,54 (-0,826)	252,94 (0,802)
258,302	258,52 (1,199)	None
273,47	None	273,32 (19,707) 265,65 (0,884)
279,476	None	279,75 (120,926)
279,489	None	279,75 (132,866)
284,797	285,21 (-7,898)	283,03 (-1,934)
290,568	None	290,5 (19,748)
299,638	300,12 (-10,791) 303,82 (-0,927)	294,49 (0,763)
305,698	304,72 (8,231)	None

308,134	None	308,6 (2,538)
319,798	None	321,59 (-0,804)
320,861	None	321,11 (-15,201) 231,81 (0,956) 334,32 (0,833)
338,387	339,17 (-2,563)	330,2 (0,893) 334,32 (1,001)
344,088'	None	344,54 (1,279) 346,96 (-0,782)
344,236'	None	346,88 (-0,88) 337,01 (0,663)
350,921'	None	None
353,951'	None	None
358,444'	None	358,97 (5,38)
361,01'	None	360,85 (70,98)
361,976'	None	None
369,886'	None	None
374,165'	None	374,77 (15,222)
374,531'	None	None
' Higher bending modes	Higher bending modes in landing were hard to distinguish due to low detailing in measurement model.	

AutoMAC Setup 1

	47,333	56,041	58,926	60,566	66,091	68,759	74,661	86,523	91,911
47,333	1	0,669	0,71	0,654	0,735	0,647	0,554	0,568	0,579
56,041	0,669	1	0,893	0,937	0,936	0,886	0,747	0,701	0,783
58,926	0,71	0,893	1	0,9	0,866	0,884	0,742	0,601	0,634
60,566	0,654	0,937	0,9	1	0,963	0,907	0,728	0,778	0,766
66,091	0,735	0,936	0,866	0,963	1	0,933	0,785	0,799	0,863
68,759	0,647	0,886	0,884	0,907	0,933	1	0,872	0,651	0,811
74,661	0,554	0,747	0,742	0,728	0,785	0,872	1	0,391	0,833
86,523	0,568	0,701	0,601	0,778	0,799	0,651	0,391	1	0,669
91,911	0,579	0,783	0,634	0,766	0,863	0,811	0,833	0,669	1

	112,541	123,376	123,954	129,16	147,704	153,812	179,565	186,794	189,461
112,541	1	0,022	0,056	0,072	0,133	0,253	0,041	0,102	0,059
123,376	0,022	1	0,009	0,076	0,375	0,062	0,28	0,008	0,251
123,954	0,056	0,009	1	0,114	0,094	0,019	0,095	0,171	0,102
129,16	0,072	0,076	0,114	1	0,009	0,183	0,197	0,604	0,532
147,704	0,133	0,375	0,094	0,009	1	0,597	0,445	0,144	0,265
153,812	0,253	0,062	0,019	0,183	0,597	1	0,309	0,317	0,349
179,565	0,041	0,28	0,095	0,197	0,445	0,309	1	0,451	0,737
186,794	0,102	0,008	0,171	0,604	0,144	0,317	0,451	1	0,563
189,461	0,059	0,251	0,102	0,532	0,265	0,349	0,737	0,563	1

	190,887	192,675	192,843	203,76	204,156	219,795	221,93	229,034	231,107
190,887	1	0,601	0,348	0,68	0,621	0,121	0,625	0,631	0,555
192,675	0,601	1	0,61	0,597	0,566	0,407	0,727	0,372	0,427
192,843	0,348	0,61	1	0,632	0,673	0,595	0,742	0,374	0,361
203,76	0,68	0,597	0,632	1	0,982	0,305	0,844	0,667	0,641
204,156	0,621	0,566	0,673	0,982	1	0,356	0,823	0,619	0,594
219,795	0,121	0,407	0,595	0,305	0,356	1	0,474	0,121	0,197
221,93	0,625	0,727	0,742	0,844	0,823	0,474	1	0,722	0,73
229,034	0,631	0,372	0,374	0,667	0,619	0,121	0,722	1	0,898
231,107	0,555	0,427	0,361	0,641	0,594	0,197	0,73	0,898	1

	232,433	247,505	258,302	273,47	279,476	279,489	284,797	290,568	299,638
232,433	1	0,011	0,029	0,462	0,248	0,229	0,132	0,024	0,032
247,505	0,011	1	0,025	0,049	0,019	0,023	0,022	0,039	0,001
258,302	0,029	0,025	1	0,046	0,051	0,052	0,011	0,03	0,014
273,47	0,462	0,049	0,046	1	0,436	0,409	0,239	0,033	0,024
279,476	0,248	0,019	0,051	0,436	1	0,985	0,22	0,019	0,021
279,489	0,229	0,023	0,052	0,409	0,985	1	0,199	0,021	0,025
284,797	0,132	0,022	0,011	0,239	0,22	0,199	1	0,275	0,08
290,568	0,024	0,039	0,03	0,033	0,019	0,021	0,275	1	0,248
299,638	0,032	0,001	0,014	0,024	0,021	0,025	0,08	0,248	1

	305,698	308,134	319,798	320,861	338,387	344,088	344,236	350,921	353,951
305,698	1	0,031	0,001	0,003	0,005	0,071	0,005	0,022	0,054
308,134	0,031	1	0,124	0,079	0,327	0,15	0,008	0,197	0,114
319,798	0,001	0,124	1	0,822	0,122	0,264	0,01	0,05	0,039
320,861	0,003	0,079	0,822	1	0,114	0,245	0,003	0,095	0,075
338,387	0,005	0,327	0,122	0,114	1	0,2	0,01	0,257	0,375
344,088	0,071	0,15	0,264	0,245	0,2	1	0,044	0,058	0,04
344,236	0,005	0,008	0,01	0,003	0,01	0,044	1	0,251	0,124
350,921	0,022	0,197	0,05	0,095	0,257	0,058	0,251	1	0,509
353,951	0,054	0,114	0,039	0,075	0,375	0,04	0,124	0,509	1

	358,444	361,01	361,976	369,886	374,165	374,531
358,444	1	0,608	0,143	0	0,024	0,512
361,01	0,608	1	0,262	0,048	0,005	0,244
361,976	0,143	0,262	1	0,047	0,163	0,038
369,886	0	0,048	0,047	1	0,055	0,006
374,165	0,024	0,005	0,163	0,055	1	0,037
374,531	0,512	0,244	0,038	0,006	0,037	1

Appendix C2

Visual comparison for validation and AutoMAC of mode shapes in setup 2.

Modes from measurements [Hz]	Good resemblance with [Hz] (MAC-value)	Some resemblance with [Hz] (MAC-value)
50,092	None	None
55,907	55,791 (0,339)	None
66,832	None	None
82,308	None	83,012 (0,533)
87,927	None	87,709 (0,195)
89,6 ‘	89,684 (0,61) 88,816 (0,638) 88,495 (0,614)	None
91,602 ‘	92,821 (0,226) 89,684 (0,645) 88,816 (0,649) 93,984 (0,673)	None
124,708 “	126,47 (0,789) 122,65 (0,892) 120,15 (0,891) 119,55 (0,891)	None
128,719 “	None	129,24 (0,217)
187,746 ””	None	186,96 (0,364) 189,21 (0,243)
187,849 ””	None	186,96 (0,247) 192,01 (0,506)
230,861	229,99 (0,675) 231,97 (0,844) 223,57 (0,842)	None
264,812	None	264,67 (0,1)
265,088	None	264,67 (0,198)
269,308 ”””	None	269,29 (0,066)
275,512 ”””	None	275,77 (0,052) 267,33 (0,579)
280,004	279,75 (0,014)	None
301,861	None	301,18 (0,262) 302,46 (0,251)
306,779	None	None
317,188	315,16 (0,532)	318,43 (0,104) 311,09 (0,774) 321,81 (0,877)
341,368	None	321,81 (0,958) 329,22 (0,893) 336,43 (0,814) 341,05 (0,012)
363,174	None	None
366,952	None	None
377,024	None	377,72 (0,081)
‘ First bending mode ””” Fourth bending mode	” Second bending mode Natural frequencies in beams above 350 Hz.	”” Third bending mode
Higher bending modes were hard to distinguish due to low detailing in measurement model.		

AutoMAC Setup 2

	50,092	55,907	66,832	82,308	87,927	89,6	91,602	124,708	128,719
50,092	1	0,101	0,059	0,048	0,055	0,027	0,137	0,07	0,007
55,907	0,101	1	0,008	0,158	0,007	0,033	0,116	0,002	0,022
66,832	0,059	0,008	1	0,465	0,487	0,37	0,117	0,481	0,481
82,308	0,048	0,158	0,465	1	0,565	0,531	0,066	0,416	0,245
87,927	0,055	0,007	0,487	0,565	1	0,785	0,412	0,494	0,473
89,6	0,027	0,033	0,37	0,531	0,785	1	0,628	0,288	0,496
91,602	0,137	0,116	0,117	0,066	0,412	0,628	1	0,102	0,284
124,708	0,07	0,002	0,481	0,416	0,494	0,288	0,102	1	0,158
128,719	0,007	0,022	0,481	0,245	0,473	0,496	0,284	0,158	1

	187,746	187,849	230,861	264,812	265,088	269,308	275,512	280,004
187,746	1	0,967	0,178	0,162	0,287	0,016	0,062	0,342
187,849	0,967	1	0,222	0,199	0,33	0,01	0,04	0,335
230,861	0,178	0,222	1	0,159	0,332	0,074	0,097	0,411
264,812	0,162	0,199	0,159	1	0,795	0,373	0,038	0,342
265,088	0,287	0,33	0,332	0,795	1	0,354	0,014	0,376
269,308	0,016	0,01	0,074	0,373	0,354	1	0,372	0,061
275,512	0,062	0,04	0,097	0,038	0,014	0,372	1	0,606
280,004	0,342	0,335	0,411	0,342	0,376	0,061	0,606	1

	301,861	306,779	317,188	341,368	363,174	366,952	377,024
301,861	1	0,643	0,267	0,235	0,034	0,358	0,17
306,779	0,643	1	0,468	0,404	0,131	0,262	0,278
317,188	0,267	0,468	1	0,877	0,23	0,664	0,695
341,368	0,235	0,404	0,877	1	0,334	0,621	0,676
363,174	0,034	0,131	0,23	0,334	1	0,374	0,351
366,952	0,358	0,262	0,664	0,621	0,374	1	0,734
377,024	0,17	0,278	0,695	0,676	0,351	0,734	1

Appendix C3

Visual comparison for validation and AutoMAC of mode shapes in setup 3.

Modes from measurements [Hz]	Good resemblance with [Hz] (MAC-value)	Some resemblance with [Hz] (MAC-value)
50,048	None	None
68,419	71,329 (0,92)	62,952 (0,916)
78,599	71,329 (0,917)	89,684 (0,928) 62,952 (0,923)
124,812	None	140,35 (0,855) 138,74 (0,816)
136,177 ‘	140,35 (0,855)	138,74(0,659)
139,480 ‘	140,35 (0,635)	None
186,487 ‘	186,96 (0,9)	183,5 (0,872) 189,21 (0,864)
189,519 ‘	None	186,96 (0,634) 183,5 (0,568)
192,998 “	190 (0,901) 203,54 (0,88) 192,01 (0,779)	201,34 (0,89)
210,958 “	211,21 (0,963) 225,73 (0,949) 225,2 (0,938)	None
213,610 “	213,25 (0,345) 209,48 (0,665)	None
230,660 “	229,99 (0,09) 248,07 (0,602)	None
259,099 “	258,52 (0,986) 252,94 (0,982) 264,1 (0,98)	None
279,093 “	271,03 (0,964)	295,48 (0,93) 278,6 (0,684)
285,927 ””	None	285,21 (0,003) 271,03 (0,971) 273,32 (0,88)
303,849 ””	None	303,82 (0,078) 312,79 (0,972) 321,59 (0,978)
353,101 ””	None	354,83 (0,032) 335,58 (0,761) 347,65 (0,716)
370,454 ””	None	370,31 (0,213)
374,149 ””	None	392,33 (0,812) 374,77 (0,715) 372,21 (0,611)
375,587 ””	None	374,77 (0,345)
‘ First bending mode ” Second bending mode ”” Third bending mode	Hard to distinguish third bending mode in measurement model due to few DOFs.	

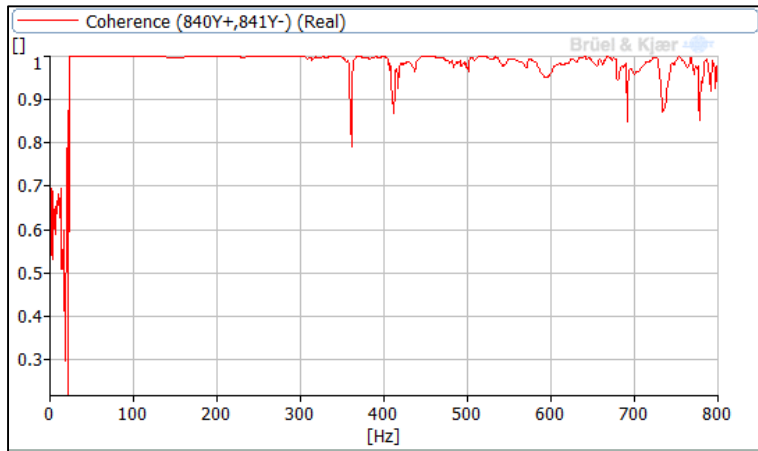
AutoMAC Setup 3

	50,048	68,419	78,599	124,812	136,177	139,48	186,487	189,519	192,998	210,958
50,048	1	0,057	0,039	0,024	0,031	0,059	0,08	0,149	0,096	0,041
68,419	0,057	1	0,878	0,614	0,363	0,424	0,228	0,463	0,256	0,506
78,599	0,039	0,878	1	0,328	0,104	0,149	0,044	0,225	0,044	0,38
124,812	0,024	0,614	0,328	1	0,904	0,75	0,67	0,599	0,798	0,76
136,177	0,031	0,363	0,104	0,904	1	0,886	0,886	0,712	0,94	0,687
139,48	0,059	0,424	0,149	0,75	0,886	1	0,939	0,894	0,818	0,428
186,487	0,08	0,228	0,044	0,67	0,886	0,939	1	0,869	0,89	0,392
189,519	0,149	0,463	0,225	0,599	0,712	0,894	0,869	1	0,753	0,267
192,998	0,096	0,256	0,044	0,798	0,94	0,818	0,89	0,753	1	0,643
210,958	0,041	0,506	0,38	0,76	0,687	0,428	0,392	0,267	0,643	1

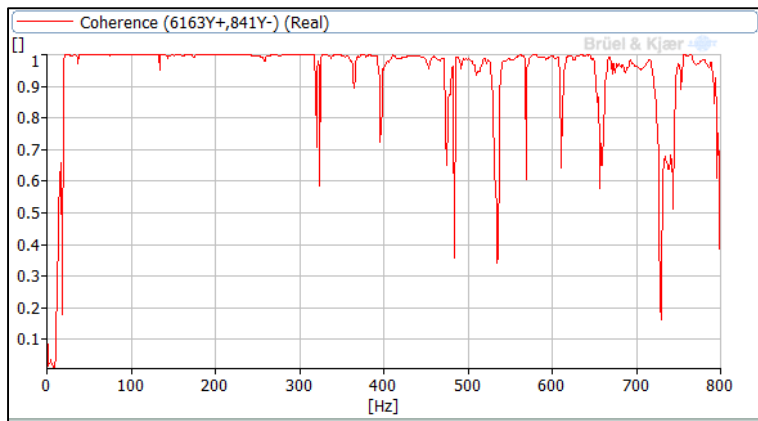
	213,61	230,66	259,099	279,093	285,927	303,849	353,101	370,454	374,149	375,587
213,61	1	0,599	0,764	0,391	0,39	0,314	0,83	0,367	0,694	0,432
230,66	0,599	1	0,808	0,952	0,939	0,891	0,707	0,776	0,268	0,599
259,099	0,764	0,808	1	0,682	0,708	0,577	0,96	0,627	0,532	0,288
279,093	0,391	0,952	0,682	1	0,973	0,963	0,556	0,851	0,114	0,59
285,927	0,39	0,939	0,708	0,973	1	0,975	0,613	0,759	0,169	0,587
303,849	0,314	0,891	0,577	0,963	0,975	1	0,488	0,756	0,132	0,677
353,101	0,83	0,707	0,96	0,556	0,613	0,488	1	0,491	0,657	0,34
370,454	0,367	0,776	0,627	0,851	0,759	0,756	0,491	1	0,033	0,443
374,149	0,694	0,268	0,532	0,114	0,169	0,132	0,657	0,033	1	0,479
375,587	0,432	0,599	0,288	0,59	0,587	0,677	0,34	0,443	0,479	1

Appendix D1

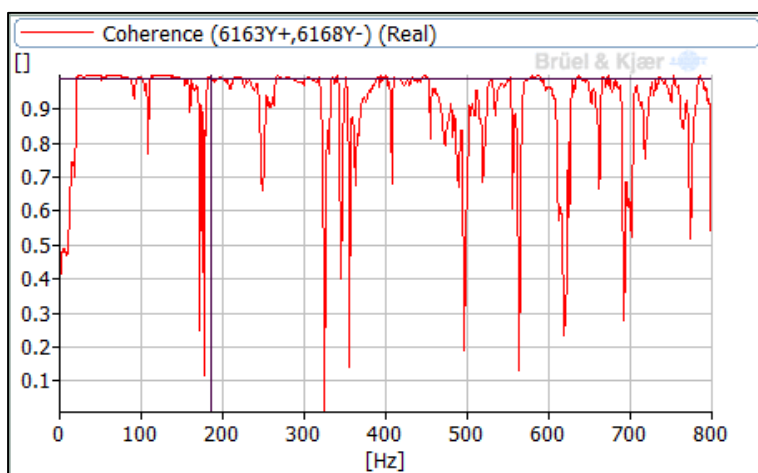
Coherence data for vibration measurements with hammer impact.



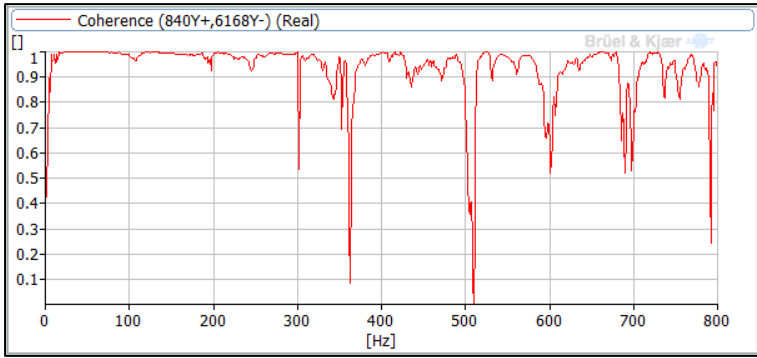
Coherence in tread with impact on tread.



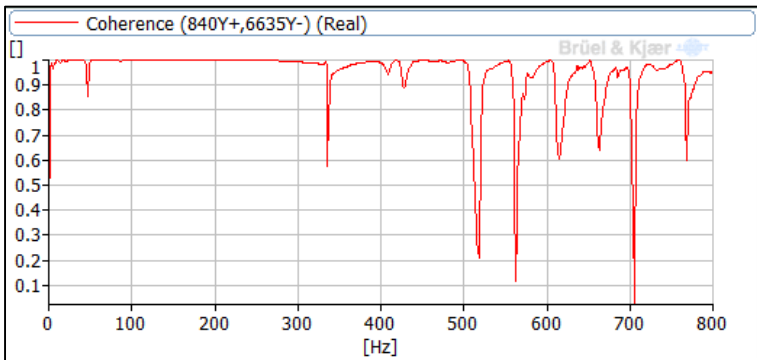
Coherence in landing with impact on tread.



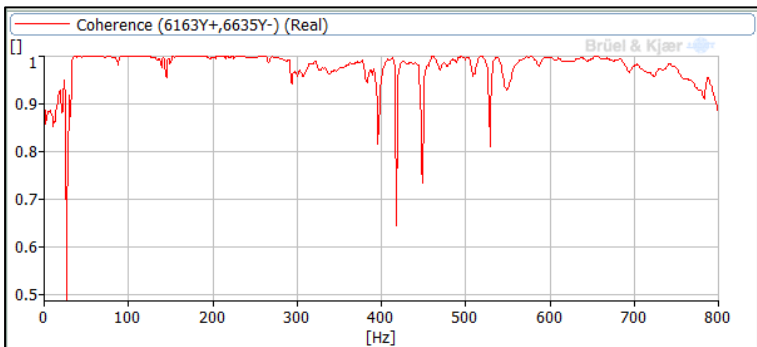
Coherence in landing with impact on mid-span landing.



Coherence in tread with impact on mid-span landing.



Coherence in tread with impact above beam in landing.

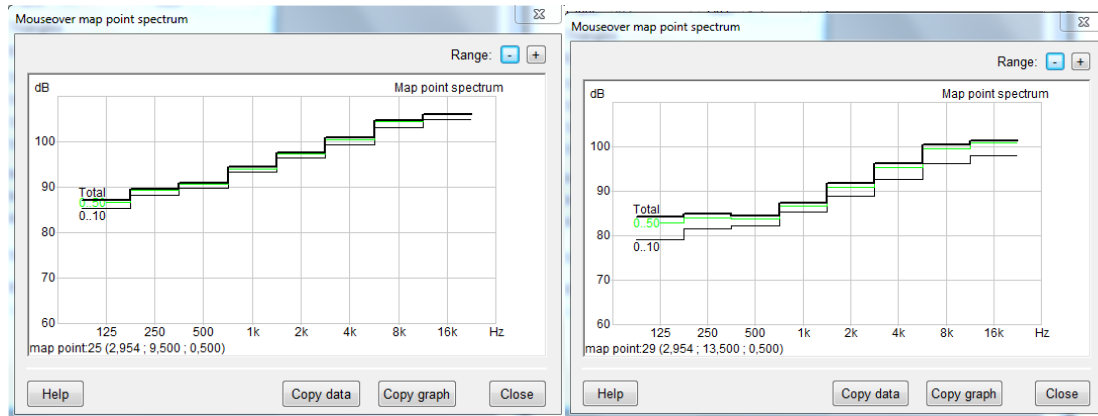


Coherence in landing with impact above beam in landing.

Appendix D2

Audibility investigation in different positions and adjustments.

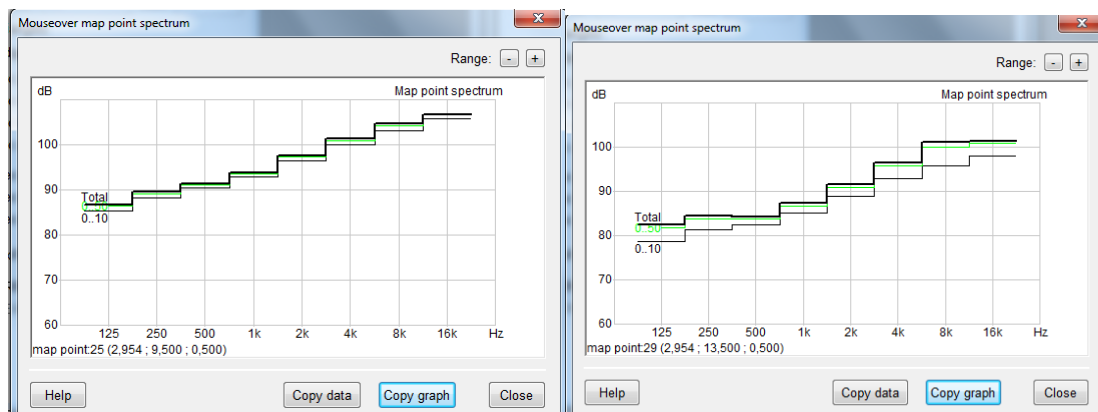
No adjustments



Source position

Receiver position

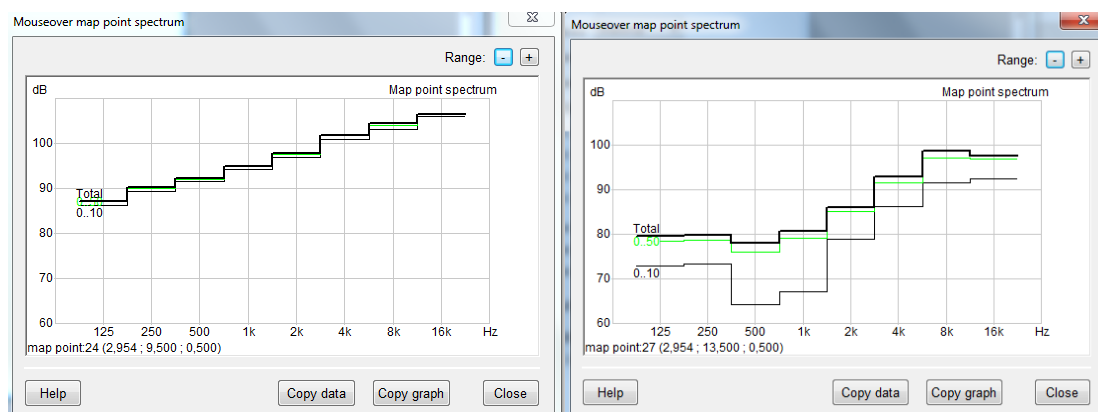
Extra Bass in Ceiling



Source position

Receiver position

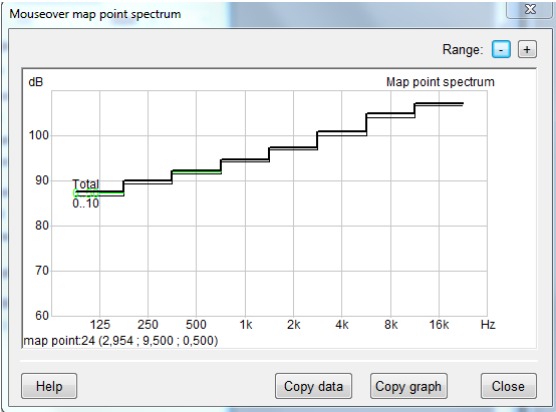
Extra bass and a screen



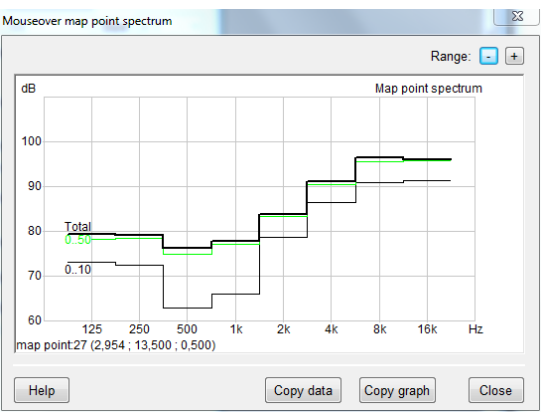
Source position

Receiver position

Extra bass, one screen and wall absorbents



Source position



Receiver position

Appendix E1

Theoretical background

Theories handling structural dynamics and acoustics have many similarities because of its common origin.

Structural dynamics

Structural mechanics can generally be divided into two groups: Statics and Dynamics. Statics is what structural engineers deal with on a daily basis, namely load effects on structural elements at rest. In most cases it is enough to consider the structural elements to actually be at rest but in reality few structural elements are completely at rest when carrying loads. Dynamics deal with loads that vary over time, causing the structural elements to vibrate either periodically or randomly. (Thorby, 2008)

General dynamics

In this chapter the general dynamic phenomena and properties will be presented.

Dynamic and static response

Dynamic loading, as opposed to static loading, is a situation where the load varies over time. In the static case the effect of loading is a certain deflection in the structure while the deflection in the dynamic case depends on the properties of the amplitude and duration of the loading and of the structural system. For example a static load case of a certain amplitude and point of action can result in a deflection much lower than one of a short dynamic loading of the same size and point of action. This phenomenon, called dynamic magnification, is the result of applying loads at different speed and is time-dependent. The relation between the static and dynamic deflections can be described as

$$\delta_d(t) = \delta_{st} \cdot DMF(t) \quad (\text{Eq. E1-1})$$

where

$\delta_d(t)$ is the dynamic deflection at time t

δ_{st} is the static deflection

$DMF(t)$ is the Dynamic Magnification Factor at time t

The size of the dynamic magnification factor depends on two different relations: the relation between the mass and the stiffness of the system and the relation between the duration of the load application and the natural time period of the system. The static loading and the dead weight of the structure determine the mass and the stiffness depends on the properties of the structural members and the connection between them. The natural time period is the time it takes for the structure to complete a certain periodic motion. It is possible to consider the motion as part of either a natural frequency, motions performed in one second, or angular frequency, the portion of the periodic motion performed during the natural time period when considering the full motion as a circular motion of 360 degrees or 2π . The formulas can be written as

$$f = \frac{1}{T} \text{ and } \omega = \frac{2\pi}{T} \quad (\text{Eq. E1-2})$$

where

f is the number of cycles performed in 1 s [Hz]

T is the natural time period [s]

ω is the angular frequency [rad/s]

(Saar, 2006)

Vibration modes

When a structure vibrates it will move in a combination of different vibration modes. Each mode has a corresponding natural time period and therefore also a corresponding frequency. These typical modes for the structure are usually ordered from lowest frequency, the first mode, to higher modes. (Saar, 2006) For simple structures it is also visible that the complexity of the vibration increases with the mode number, see Figure E1. 1. With increasing complexity in the modes a pattern of nodes, areas that are not excited by the vibration, arises. (Saar, 2006) For a simple system, with only one mass and one stiffness value, called SDOF-system or single degree of freedom system an equation can be formulated as

$$m \cdot \ddot{u}(t) + k \cdot u(t) = 0 \quad (\text{Eq. E1-3})$$

called the equation of motion where

m is the mass

$\ddot{u}(t)$ is the velocity at time t

k is the stiffness

$u(t)$ is the deflection at time t

A trial solution for the system is adopted so that

$$u(t) = u_0 \sin(\omega_n t) \quad (\text{Eq. E1-4})$$

where

ω_n is the natural angular frequency

so

$$\ddot{u}(t) = -\omega^2 u_0 \sin(\omega_n t) \quad (\text{Eq. E1-5})$$

Inserted to Eq. E1-3

$$m \cdot (-\omega^2 u_0 \sin(\omega t)) + k \cdot u_0 \sin(\omega t) = 0 \leftrightarrow (k - \omega^2 m) \cdot u_0 = 0$$

(Eq. E1-6)

To solve the equation the following must hold

$$k - \omega^2 m = 0 \leftrightarrow \omega = \sqrt{\frac{k}{m}} \quad (\text{Eq. E1-7})$$

which is the first natural angular frequency for a SDOF-system.

This shows the relation between the natural frequency, the mass and the stiffness of the system. If a mass in the system is decreased and the stiffness is constant the system will get a lower natural angular frequency. In the same way a decrease in stiffness will lower the natural angular frequency. When using the word *natural* this is a way to describe that these frequencies are properties of the system and will appear when the system is moving in free vibration, without external forces. (Chopra, 1995)

Consider for example a simply supported beam, see Figure E1. 1. With increasing mode number both the complexity of the vibration and the number of nodes increases. Each mode has its own natural frequency and time period.

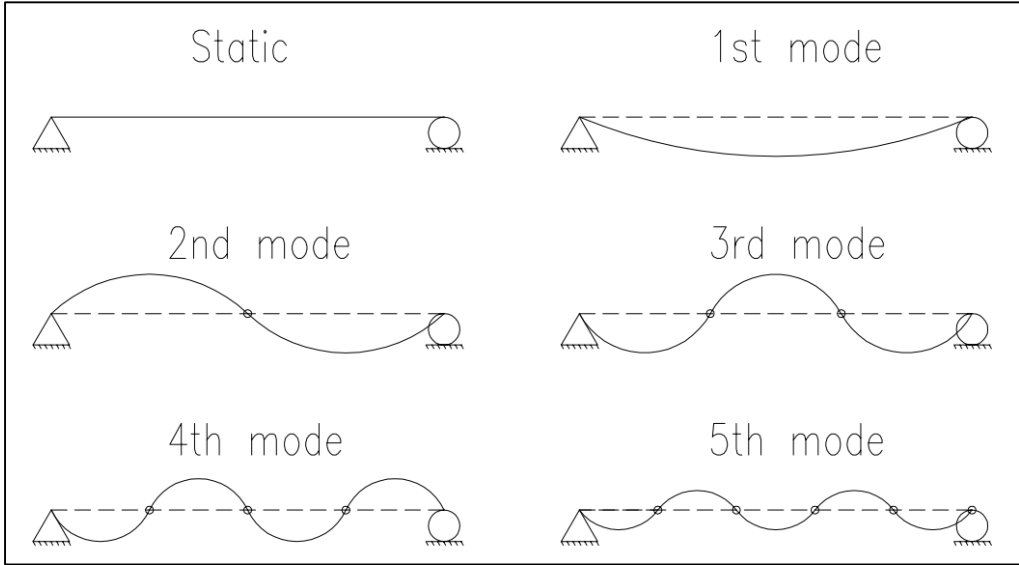


Figure E1. 1 Mode shapes from simply supported beam.

Damping

When a structure is set into motion it eventually stops, provided that there are no external forces. The phenomenon is called damping and happens due to internal energy consumption in the structure, since each vibrating motion requires energy. The damping can originate from different parts of the system such as connections between different parts, external forces and deflections in the structure. Considering the damping is one of the most important factors in dynamic analyses of structures but it is also one of the hardest things to do correctly. (Saar, 2006) Since there are so many different components and combinations of these that can create damping in a structure it is really difficult to determine the damping mathematically with any good precision. (Chopra, 1995) It is therefore fitting to use damping values from experiments on existing structures in the design stage to get an adequate approximation of the behavior of the structure. (Saar, 2006) Since damping is energy consuming and the higher modes use more energy it is probable that vibrations in the higher modes result in faster damping. The damping force, f_d , depends on the velocity of the motion and can be formulated as

$$f_d = c\dot{u}(t) \tag{Eq. E1-8}$$

where

c is the damping coefficient

$\dot{u}(t)$ is the velocity at time t (Chopra, 1995)

The considering of damping force as dependent on a damping coefficient and velocity being a strictly mathematical convenience due to the fact that the damping phenomena is too unexplored and complex to be able to correctly state in mathematical terms. The true physical situation is yet to be completely mapped and therefore there are a lot of uncertainties in the damping behavior of structures. (Adhikari, 2000) By expressing the damping as solely dependent on the velocity and the damping coefficient an assumption is being made that the damping is entirely viscous, i.e. behaves as a body moving in a thick fluid. (Odqvist, 1948)

By considering the damping in the equation of motion it can now be formulated as

$$m \cdot \ddot{u}(t) + c \cdot \dot{u}(t) + k \cdot u(t) = 0 \quad (\text{Eq. E1-9})$$

Dividing by the mass gives

$$\ddot{u}(t) + \frac{c}{m} \cdot \dot{u}(t) + \frac{k}{m} \cdot u(t) = 0 \leftrightarrow \ddot{u}(t) + 2\zeta\omega_n \cdot \dot{u}(t) + \omega_n^2 \cdot u(t) = 0$$

$$(\text{Eq. E1-10})$$

where

$\zeta = \frac{c}{2m\omega_n}$ is the damping ratio or fraction of critical damping

$\omega_n = \sqrt{\frac{k}{m}}$ as described earlier

The damping ratio is a measurement of the structure's reaction when released from a deflected state. If the damping ration is below one the system will oscillate before coming to a full stop, called underdamped system, and if the damping ratio greater than one it won't oscillate after release, called overdamped system. If the damping ratio is exactly one the system is critically damped, meaning that the system is on the verge of starting to oscillate when released.

(Chopra, 1995)

Damping is generally quite difficult to determine, especially in more complex structures where different materials are interconnected. Therefore experimental methods are often necessary to be with some certainty able to determine the damping ratio. To determine the damping in a specific structure experimentally the structure can be set into motion, either by applying a force or an initial deflection. Generally the decaying amplitude of deflection in a structure vibrating in a natural frequency can be expressed as

$$u(t) = C e^{-\zeta\omega_n t} \quad (\text{Eq. E1-11})$$

By measuring the displacements in the same point of sequential vibration cycles and also determining the time period, see Figure E1. 2, an expression can be formulated as

$$\frac{u_1}{u_2} = \frac{C e^{-\zeta \omega_n t_1}}{C e^{-\zeta \omega_n (t_1 + \tau_d)}} = e^{\zeta \omega_n \tau_d} \quad (\text{Eq. E1-12})$$

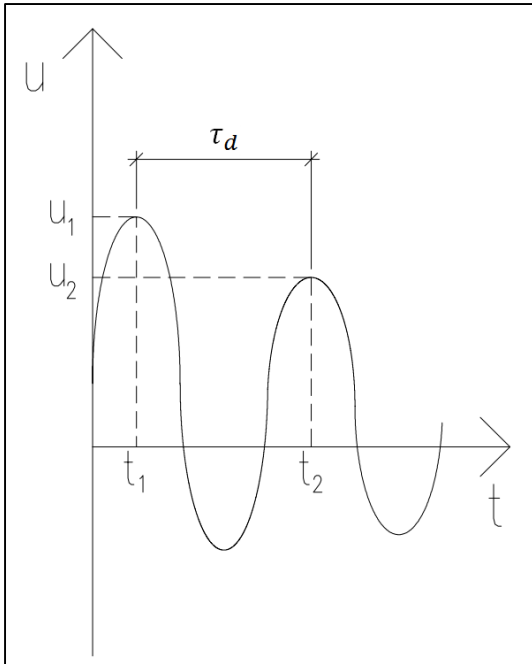


Figure E1. 2. Determining damping ratio.

So the damping ratio for each natural frequency can be determined as

$$\zeta = \frac{\ln\left(\frac{u_1}{u_2}\right)}{\sqrt{(2\pi)^2 + \ln\left(\frac{u_1}{u_2}\right)^2}} \quad (\text{Eq. E1-13})$$

(Meriam & Kraige, 2008)

Typical damping ratio for welded steel structures during normal working stress is about 2-3 %, but approaches 5-7 % as the stress level approaches the yield point in the material. For bolted steel structures the damping ratio is 5-7 % during working stress and 10-15 % closer to the yield point. (Chopra, 1995)

Periodic loading, resonance and harmonics

When a structure is set into motion by a periodical dynamic load, see Figure E1. 3, at a certain angular frequency, Ω , the system will after some initial deviance move almost exclusively with the same angular frequency as the load. This motion will repeat itself as long as the periodic load is constant and is called the steady-state response of the structure. (Saar, 2006) In the equation of motion this can be derived as

$$m \cdot \ddot{u}(t) + c \cdot \dot{u}(t) + k \cdot u(t) = P_0 \sin(\Omega t) \quad (\text{Eq. E1-14})$$

Inserting initial conditions at $t=0$ as

$$u(t) = u(0) \text{ and } \dot{u}(t) = \dot{u}(0)$$

leading to a solution with one part being the steady state solution namely

$$u_s(t) = \frac{p_0}{k} \frac{1}{\left(1 - \frac{\Omega}{\omega_n}\right)^2} \cdot \sin(\Omega t) \text{ where } \Omega \neq \omega_n$$

(Eq. E1-15)

and the other part being the transient solution, written as

$$u_t(t) = u(0) \cos(\omega_n t) + \left[\frac{\dot{u}(0)}{\omega_n} - \frac{p_0}{k} \frac{\frac{\Omega}{\omega_n}}{\left(1 - \frac{\Omega}{\omega_n}\right)^2} \right] \cdot \sin(\omega_n t)$$

(Eq. E1-16)

(Chopra, 1995)

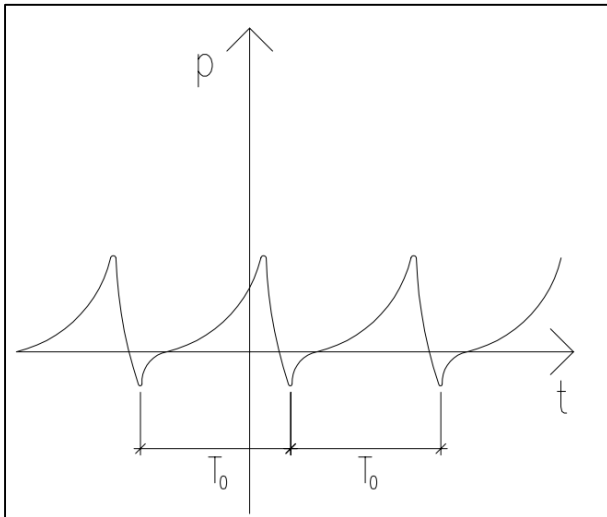


Figure E1. 3. Periodic loading.

As earlier described the response in the structure can be calculated as the static response times the DMF, where the DMF is dependent on the mass and stiffness of the system. The relation between the mass and the stiffness determine the natural angular frequency of the structure, ω_n , and if Ω approaches ω_n the DMF will increase causing large vibrations, in theory reaching infinity. This phenomenon is called resonance. In real structures the theory does not hold when the DMF approaches infinity, since the structures starts to behave nonlinearly and the material start to yield. (Saar, 2006) If the ratio between the frequencies, Ω/ω_n , is much smaller than one the DMF is marginally bigger than one. Thus leading to the approximation of the deflection being

$$\delta_d(t) \approx \delta_{st} = \frac{P_0}{k} \quad (\text{Eq. E1-17})$$

In this case the DMF is almost independent of the damping in the system; ergo the DMF is controlled by the stiffness in the structure. If the ratio much larger than one, i.e. the frequency of the load is much higher than the natural frequency of the structure, the DMF will approach zero. (Chopra, 1995)

So it has now been established that the response factor, and therefore the deflection, approaches infinity when the ratio between the forcing frequency and the natural frequency approaches one. However, if you turn the ratio around i.e. ω_n/Ω instead of Ω/ω_n , there may very well be other forcing frequencies than the natural frequencies causing the deflections to increase tremendously. If the natural frequency, ω , is a multiple of the forcing frequencies also have a tendency of causing large response factors in the structure. The higher multiples causing resonance are called the harmonics of the forcing frequency. The harmonics will cause resonance in the system but in a much slower pace. (Willford & Young, 2006) Compare setting a swing into motion, giving it a push in every pendulum motion compared to in every second or third.

Impulse loading, forced and free vibration

Forces acting during a short time period are called impulsive forces, or impulses. A sequence of impulses of very short duration can in a good way represent arbitrary time-varying forces, or transients see Figure E1. 4. (Chopra, 1995) Impulses can either be regular or non-regular, meaning that they either arise in a certain pattern or at random. If the impulse is regular the interval or time period between the repeating impulses is of big importance when investigating the risk of resonance in impulse loading. (Saar, 2006) The response from a transient load can be described as a super positioning of the response of a sequence of impulses describing the arbitrary transient.¹ When applying an impulse loading to a structure it will behave in different ways during the application and after the application. During the application of the impulse loading the response will be forced into a vibration depending on the impulse. After the impulse the structure will enter a free vibration phase. Looking at the equation of motion for the two cases

$$m \cdot \ddot{u}(t) + c \cdot \dot{u}(t) + k \cdot u(t) = \begin{cases} p(t) & \text{During the impulse} \\ 0 & \text{After the impulse} \end{cases}$$

(Eq. E1-18)

(Chopra, 1995)

¹ Per-Erik Austrell. Prof. Department of Structural Mechanics, Faculty of Engineering LTH at Lund University. Lecture Spring 2015, Lund.

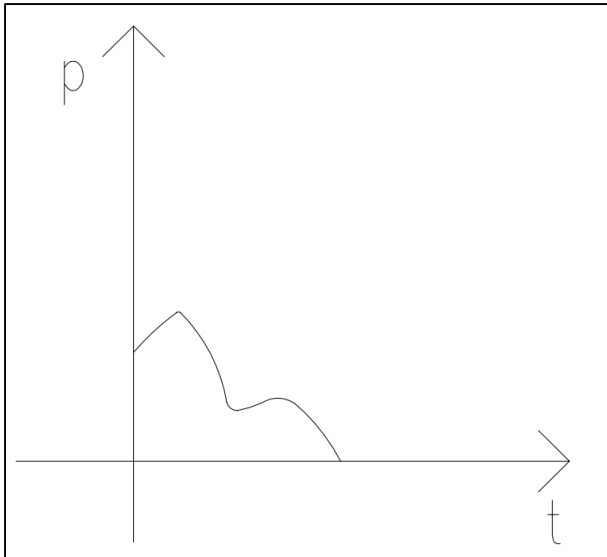


Figure E1. 4. Transient loading.

Applying a force with duration longer than the natural time period for the motion the response in the structure will be counteracted by the applied force. However, if the duration is shorter than the natural time period the response will only be accelerated into motion with some delay. Having duration with the approximate equal length to the natural time period will result in a slowly increasing response with its maximum deflection just after the impulse has started to decrease. (Rayleigh, 1877)

Dynamics in structural design and modeling

When considering dynamics in structural design the most important thing is to recognize the different dynamic events that may occur. Typical dynamic events can be earthquakes, wind load accidental loads. The dynamic loads can be defined as time-varying loads but more often than not a slow varying load can be considered a static load, for example in quasi-static serviceability limit state. (Saar, 2006)

Dynamic loads

Another typical dynamic load apart from the periodic load is the impulse load. The impulse load is characterized by a short pulse load, for example a hammer hitting the structure. When impulse loading is being applied in a regular pattern it can create the same response as a periodic loading, which can lead to resonance in the structure. This can occur if the time period of the pattern for the impulse loading is shorter than the time needed for the structure to decay its motion, i.e. if the damping can't terminate the motion before the next impulse is being applied. (Saar, 2006) Human activity can cause these type of impulse loading through activities like walking, running, dancing etcetera. The frequency range for human walking or running is usually somewhere between 1.5 and 5 Hz. For slender elements, especially made out of steel, it's quite common for walking and running to cause dynamic magnification, or resonance, in the response of the structure. The magnitude and pattern of the impulse load depend on the number of people, and their weight, that are walking on the structure and the tempo they are walking or running in. (Saar, 2006)

The human step is characterized by two peaks, the “heel strike” and the “toe off”, and is a typical transient load, see Figure E1. 5. The amplitude of the peaks increases with the walking speed and which of the two that dominates depends on the walking pattern. In staircases people more often than not tend to run up and down causing the “heel strike” to be dominant. This can typically cause vibration problems in slender lightweight staircases. (Smith & Kappos, 2001). Energetic walking or running in a staircase can cause the dynamic load to be well over four times the static load. This means that structural dynamics is vitally important in these kinds of structures. (Smith & Kappos, 2001)

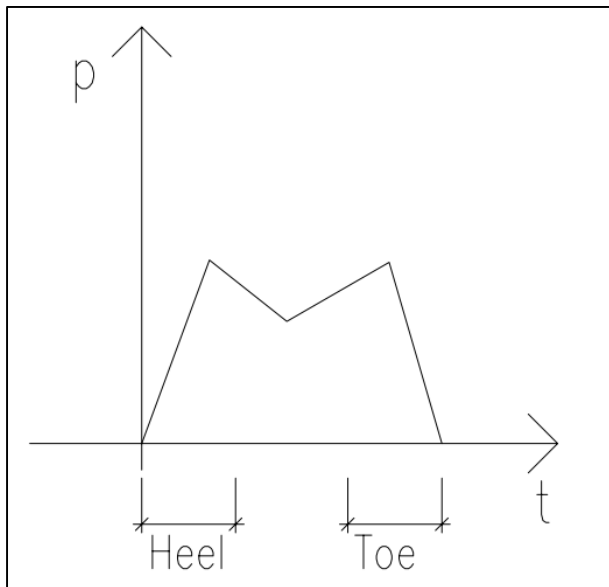


Figure E1. 5. Load from human step.

In his article on tips to prevent floor vibrations in office buildings Murray describes how you as a structural engineer should avoid not only having the typical walking frequency as a natural frequency, but also multiples of this. Murray recommends that the natural frequency shouldn't be able to occur in any of the first three harmonics, i.e. that if the forcing frequency is 2 Hz the floor should be checked for natural frequencies around 2, 4 and 6 Hz. (Murray T. , 2001)

The main difference between impact from walking on a flat slab and descending or ascending a staircase is in what part of the step the force is applied. It has also been shown that the geometry of the staircase has a great impact on the footfall. Unlike a slab where the user is free to alter the stride length the geometry of the staircase provides a finite possibility, such as making the user choose between stepping on every or every other tread. These conditions force the user to change the frequency in the steps rather than increasing or decreasing the stride length to adjust the walking speed. (Kerr, 1998)

Vibrations

Basically a dynamic event is a vibrating load and can for example be caused by human activity like running or dancing, vibrating machines or traffic. The dynamic effects on a structure from such loads are mainly overstressing, fatigue of the material or vibrations. (Saar, 2006)

Modern structures have a tendency of being lighter, stronger and more slender than older structures. The combination was demanded but it also led to increasing issues with vibrations. The vibrations may lead to discomfort of the users or tenants of the structures or even cause structural damages such as cracks or fatigue. In lightweight structures it is common for humans to be discomforted by the vibrations rather than the vibrations to cause structural damage, since the human sensitivity level is lower than the vibration level that causes structural damage. A typical example for this is lightweight footbridges that are easily put in to motion by human activity that usually doesn't produce any physical damage. (Saar, 2006)

From a collection of different staircase measurements performed by Kerr it is stated that any staircase with natural frequencies lower than 10 Hz are probable to cause vibrations of unacceptable levels. (Kerr, 1998)

Damping

Modeling damping for a structure can be done in a number of different ways. Looking at the equation of motion, as described earlier, the C represents a damping matrix containing information about the damping for each vibration mode. Assuming that the damping is frequency dependent and viscous, i.e. velocity dependent, the damping matrix can be described using Rayleigh damping as

$$C = \alpha M + \beta K \tag{Eq. E1-19}$$

The Rayleigh damping is described as a linear combination of the mass and stiffness matrix. Since the response in the equation of motion is linear the Rayleigh damping may have lack of accuracy in nonlinear behavior, such as yielding of steel. For each vibration mode the damping ratio can be described as

$$\zeta_i = \frac{\alpha}{2} \frac{1}{\omega_{n,i}} + \frac{\beta}{2} \omega_{n,i} \tag{Eq. E1-20}$$

(Alipour & Zareian, 2008)

The typical appearance of damping ratio as a function of frequency is presented in Figure E1. 6.

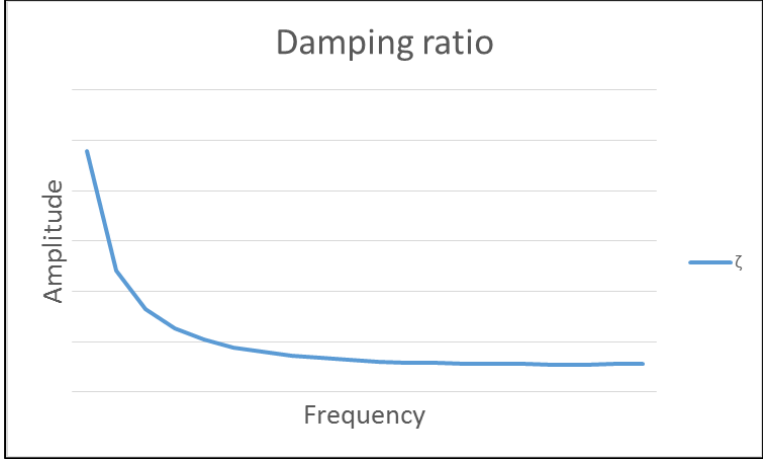


Figure E1. 6. Typical appearance of damping ratio.

To be able to determine α and β an approximation using the half power bandwidth can be used. It can be shown that the damping factor can be approximated from the width of the peak at resonance when performing a frequency sweep so that

$$\frac{\omega_b - \omega_a}{\omega_n} = 2\zeta_i \quad (\text{Eq. E1-21})$$

where ω_a and ω_b describe the width at half power. (Adhikari, 2000) Inserting this into Eq. E1-20 leads to

$$\begin{bmatrix} \frac{1}{2\omega_1} & \frac{\omega_1}{2} \\ \vdots & \vdots \\ \frac{1}{2\omega_i} & \frac{\omega_i}{2} \end{bmatrix} \begin{bmatrix} \alpha \\ \beta \end{bmatrix} = \begin{bmatrix} \zeta_1 \\ \vdots \\ \zeta_i \end{bmatrix} \quad (\text{Eq. E1-22})$$

(Alipour & Zareian, 2008)

Simplified modeling

In structural design it is often not possible to create a full-sized FE-model, taking surroundings and full geometry into account, due to time and cost restrictions. For these situations it is sometimes better to analyze a simplified model looking at some smaller parts of the structure in a two dimensional model. In this way critical areas can be analyzed in a more time-effective manner.

Rayleigh's method for a vibrating system with one degree of freedom can be used to determine the natural frequency of the system. The first mode for the beam is when the midpoint is moving in a harmonic motion. Looking at the effective mass and stiffness in the structure in comparison to a simple mass on a spring will give a simple approximation of the behavior of the system. (Odqvist, 1948)

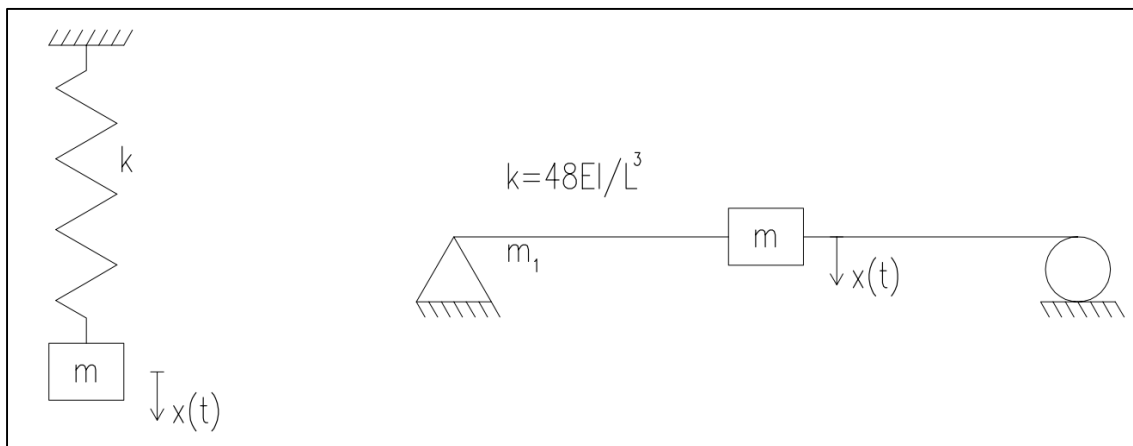


Figure E1. 7. Approximation of system with simply supported beam.

In the spring system with stiffness k the mass m is vibrating in the direction of the arrow, see Figure E1. 7. For a simply supported beam the equivalent effective stiffness is

$$k_{eff} = \frac{48EI}{L^3} \quad (\text{Eq. E1-23})$$

For the simply supported case m_1 is the mass of the beam whilst m is a mass at midpoint. It is reasonable to approximate that one third of the beam's mass is active during the vibration, provided that the mass is evenly distributed along the beam. By applying this approximation the effective mass can be determined as

$$m_{eff} = m + \frac{m_1}{3} \quad (\text{Eq. E1-24})$$

For the spring system this can be derived from the energy criterion and neglecting effect of damping, which earlier is said not to affect the natural frequencies. In the equilibrium position, $x = 0$, the elastic potential energy, W , is zero and the kinetic energy, T , is at its maximum value of

$$T = \frac{m_{eff}}{2} a^2 \omega_n^2 \text{ and } W = 0$$

where

a is the amplitude of the motion

ω_n is the angular frequency of the motion

When the spring is fully retracted, $x = \pm a$, the kinetic energy is zero and the elastic potential energy is at its maximum value, i.e.

$$W = \frac{k_{eff} a^2}{2} \text{ and } T = 0$$

Putting $T=W$ gives

$$\frac{m}{2} a^2 \omega_n^2 = \frac{k a^2}{2} \leftrightarrow \omega_n = \sqrt{\frac{k_{eff}}{m_{eff}}} \quad (\text{Eq. E1-25})$$

For the simply supported beam this means that an approximation of the first natural angular frequency is

$$\omega_n = \sqrt{\frac{\frac{48EI}{L^3}}{m + \frac{m_1}{3}}} \quad (\text{Eq. E1-26})$$

(Odqvist, 1948)

Acoustics

When describing the acoustics for a structure the same formulas as in structural dynamics can be applied in vibration analysis to model and describe how the structural system is going to behave. When looking at a structure from an acoustical standpoint it takes into consideration how the surrounding sound and vibration climate are affected when different loads are applied to the structure instead of only the durability and deflection of the structure. The discomfort or direct harm for people in or around the structure is of most importance as well as the functionality of different sensitive equipment.

Basic acoustics

Acoustics covers both sound and vibrations in air and different materials. Sound can be described as a wave that propagates in and between most materials. These waves are created when particles are set in motion like, for example, when a stone is thrown in still water and rings appear propagating on the water surface.

Wavelength

The wavelength (λ) describes length of the wave and relates to the frequency (f) and the speed of the wave (c) as following

$$\lambda = \frac{c}{f} \quad (\text{Eq. E1-27})$$

Frequency

Describes how many periods per second the wave oscillates with and it depends on the period time (T).

$$f = \frac{1}{T} \quad (\text{Eq. E1-28})$$

Sound pressure level

The strength or the amplitude in a wave is measured in pressure (Pa). But since the spectrum which humans perceive sound is vast this linear scale is unpractical and therefore transformed to a logarithmic scale instead.

$$L_p = 10 \log \frac{\tilde{p}^2}{p_0^2} \quad (\text{Eq. E1-29})$$

where \tilde{p} is the root-mean-square value of the wave which means the effective value of the pressure and is usually used to describe sound. The reference pressure p_0 is $2 \cdot 10^{-5}$ Pa since this is lowest pressure level that we humans can perceive at 1000 Hz. This logarithmic has the unit decibel (dB) with the values between 0-120 dB.

(Nilsson, Johansson, Brunskog, Sjökvist, & Holmberg, 2002)

Acoustics in design

In designing structures from an acoustic standpoint the sources where sound or vibrations radiates from must be determined i.e. which loads that affects the structure. This is necessary to be able to define the problems that may occur and prevent these. (Murray, Allen, & Ungar, 1997) Since this report mostly is about vibration and structural dynamics the following design steps handles dynamic loadings.

As said above determining the source is the first step in analyzing a structure. Dynamic loadings can be divided into four types: harmonic, periodic, transient and impulse loads. Harmonic loads are oscillating loads that behave like a sinusoidal curve when studied and are usually created by rotating machinery. Periodic loadings are created by human activities of a rhythmic structure such

as dancing or aerobics but can also occur in different machines. People in movement, walking or running, creates the third type called transient loads. For example a staircase in an office this is the most prominent type of load. The last type is impulse loads which occur from sudden impacts on the structure like someone jumping or drops something. When the type of loading is determined the frequency span of the load is analyzed, for human walking and running on floors it is between 1.5 Hz and 5 Hz. (Murray, Allen, & Ungar, 1997)

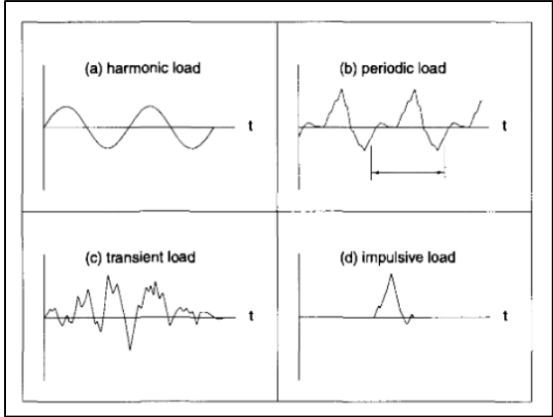


Figure E1. 8. Description of different dynamic loads. (Murray, Allen, & Ungar, 1997)

Next step is to determine the structures dynamic properties and find the structures natural frequency. If the natural frequencies are the same as frequencies of the loads correction must be made to the structure. This is to prevent resonance which means that when the loads frequency span overlaps some of the structures natural frequencies the effects are greater than if it wouldn't. Corrections are made to alter the natural frequency so that it is higher than the loads. (Murray, Allen, & Ungar, 1997)

The final step is to calculate the presumed behavior of the structure. That is done either by modeling the structure and analyzing it or by using simplified vibration criterion for the structure. For example a floor system excited by human walking can be analyzed by a simplified vibration criterion considering the weight of the structure. $\frac{a_p}{g}$ describes the ratio between the peak acceleration and the gravity with its limits $\frac{a_0}{g}$, Figure E1. 10.

$$\frac{a_p}{g} = P_0 \cdot \frac{\exp(-0,35 \cdot f_n)}{\beta \cdot W} \leq \frac{a_0}{g} \tag{Eq. E1-30}$$

P_0 = the excitation force

f_n = fundamental natural frequency of a beam, joist panel, girder panel or a combined panel

β = modal damping ratio

W =effective weight supported by the beam, joist panel, girder panel or the combined panel

Table 4.1 Recommended Values of Parameters in Equation (4.1) and a_o/g Limits			
	Constant Force P_o	Damping Ratio β	Acceleration Limit $a_o/g \times 100\%$
Offices, Residences, Churches	0.29 kN (65 lb)	0.02–0.05*	0.5%
Shopping Malls	0.29 kN (65 lb)	0.02	1.5%
Footbridges—Indoor	0.41 kN (92 lb)	0.01	1.5%
Footbridges—Outdoor	0.41 kN (92 lb)	0.01	5.0%

* 0.02 for floors with few non-structural components (ceilings, ducts, partitions, etc.) as can occur in open work areas and churches,
0.03 for floors with non-structural components and furnishings, but with only small demountable partitions, typical of many modular office areas,
0.05 for full height partitions between floors.

Figure E1. 9 Recommended values slabs and footbridges in simplified vibration criterion. (Murray, Allen, & Ungar, 1997)

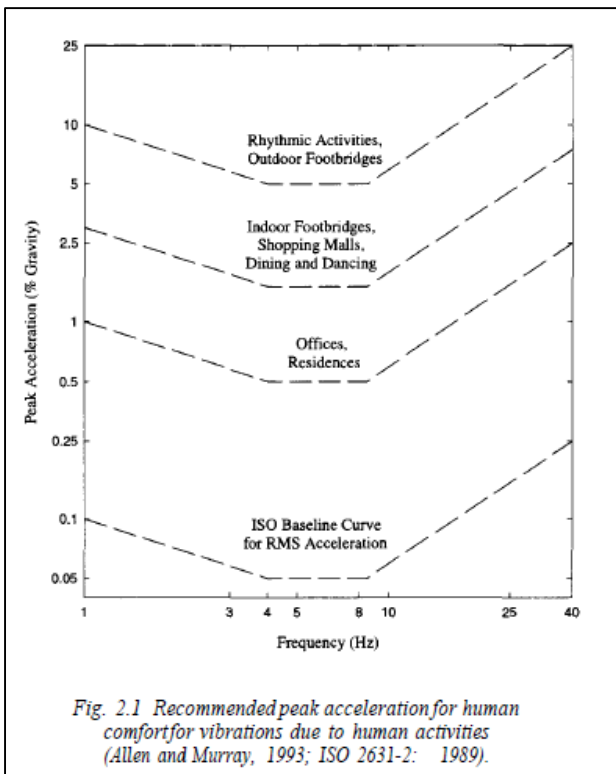


Figure E1. 10. Recommended peak acceleration for human comfort in simplified vibration criterion. (Murray, Allen, & Ungar, 1997)

Psychoacoustics

Psychoacoustics considers the sound experienced by the recipient rather than the measured sound pressure level. The experience is related to the level and type of the sound in question, the surrounding sound climate and the structure of the surrounding room. (Howard & Angus, 2009)

The experience also varies between different recipients, meaning that a certain sound can be disturbing to one person but not even noticeable for another. Personal references are also an

important factor to how a sound is experienced. If the given sound is in a surrounding with loud background noise the perception is different from a completely quiet surrounding. The kind of sound is also of great importance, for example bird song can be greatly soothing in the right surroundings whilst a train going by can be very uncomfortable. When two sound events happen at the same time it can be hard to hear one of the sounds because of the other, a phenomenon called masking. (Fastl & Zwicker, 2007) The general perception of sound in a certain environment is the base for all the operative standards in acoustics that are in use today.

How loud a sound is perceived depends on the frequencies since the ear is more sensitive to some frequencies than others. To compensate the measured sound level to how loud it is perceived different frequency-weightings are used, namely A- and C-weighting. These rescale the frequency levels so that they are more similar to how loud we perceive them and are therefore used in almost all airborne sound measurements to provide the right ratios. (Howard & Angus, 2009)

Verifying acoustic properties

For verifying that the structure is in good health and/or functions as it was intended to do measurements can be carried out. For measuring vibrations accelerometers connected to a computerized system which logs the vibration events. The results are given time weighted for each frequency or as a mean value and are to be given in either acceleration or velocity in three coordinate directions, two horizontal and one vertical. The measurements are carried out by either exciting the structure with a known force or in special cases when a special vibration event occurs. (Swedish Standards Institute, 2004b)

Converting the results to decibel

To express the measurement results in decibel following calculation applies. \bar{L}_{aV} and \bar{L}_{vV} is the weighted vibration acceleration or velocity over time expressed in decibel. The reference values a_0 and v_0 is set to 10^{-6} m/s² respective 10^{-9} m/s.

$$\bar{L}_{aV} = 20 \cdot \lg \frac{a_v}{a_0} \quad (\text{Eq. E1-31})$$

$$\bar{L}_{vV} = 20 \cdot \lg \frac{v_v}{v_0} \quad (\text{Eq. E1-32})$$

To calculate how much sound that radiates from the surface that vibrates over time following formulas is used.

Sound power level (L_W) at the surface:

$$L_W = \bar{L}_V + \left(10 \cdot \lg \frac{S}{S_0} + 10 \cdot \lg \sigma + 10 \cdot \lg \frac{\rho c}{(\rho c)_0} \right) \quad (\text{Eq. E1-33})$$

Sound pressure level (\bar{L}_P)

$$\bar{L}_P = L_W + \left(-10 \cdot \lg \frac{S}{S_0} + 10 \cdot \lg \frac{\rho c}{(\rho c)_0} \right) \quad (\text{Eq. E1-34})$$

or

$$\bar{L}_p = L_w + \left(10 \cdot \lg \sigma + 10 \cdot \lg \left(\frac{\rho c}{(\rho c)_0} \right)^2 \right)$$

(Eq. E1-35)

\bar{L}_v = average vibration velocity over time and plate area

S = surface area (m²)

S₀ = reference area 1 m²

σ = radiation efficiency of the plate

c = speed of sound in air (m/s)

ρ = air density (kg/m³)

(ρc)₀ = characteristic acoustic impedance of air (420 Ns/m³ at 20°C)

(Alten, Friedl, & Flesch, 2010)

These equations can be used to get further understanding in the surrounding climate of the sound source and for understanding the structures problems or weaknesses.